Estimation of the Early Cs-137 Intake of Evacuees from Areas Affected by the 2011 Fukushima Daiichi Nuclear Power Plant Accident Based on Personal Behavioral Data and the Latest Atmospheric Transport and Dispersion Model Simulation

ESTIMATION OF THE EARLY ^{137}CS INTAKE OF EVACUEES FROM AREAS AFFECTED BY THE 2011 FUKUSHIMA DAIICHI NUCLEAR POWER PLANT ACCIDENT BASED ON PERSONAL BEHAVIORAL DATA AND THE LATEST ATMOSPHERIC TRANSPORT AND DISPERSION MODEL SIMULATION

Eunjoo Kim,* Yu Igarashi,*,[†] Shozo Hashimoto,* Kotaro Tani,*

Tetsuo Ishikawa,[§] Munehiko Kowatari,* and Osamu Kurihara*

*National Institutes for Quantum and Radiological Science and Technology, 4-9-1 Anagawa, Inage-ku, Chiba-city, Chiba, Japan

[†]The University of Tokyo, 5-1-5 Kashiwanoha, Kashiwa-city, Chiba, Japan

[§]Fukushima Medical University, 1-Hikarigaoka, Fukushima-city, Fukushima, Japan

The authors declare no conflicts of interest.

1 **Corresponding author:** Dr. Osamu Kurihara, Department of Radiation Measurement and

2 Dose Assessment, Center for Advanced Radiation Emergency Medicine, Quantum Medical

3 Science Directorate, National Institutes for Quantum and Radiological Science and Technology,

4 4-9-1 Anagawa, Inage-ku, Chiba-city, Chiba 263-8555, Japan.

5

6 Tel.: +81-43-206-4734, Fax: +81-43-284-1769. Email: kurihara.osamu@qst.go.jp

7

8

1 **ABSTRACT**

2 More than nine years have passed since the 2011 nuclear disaster in Fukushima Prefecture,

3 Japan. During this period, much effort has been made on the dose reconstruction for Fukushima

4 residents; however, the estimation of the internal dose due to the potential intake of the short-

5 lived radionuclides (mainly, ^{131}I) has been challenging because of the lack of direct human

6 measurements at the early phase of the accident. Our previous study revealed that the residual

7 cesium body contents observed in delayed whole-body counter (WBC) measurements of

8 residents from Namie-town, one of the most affected municipalities), varied greatly with the

9 timepoint of their evacuations on 12 March 2011 when the first explosive event occurred at the

10 accident site; i.e., the late evacuees had much higher residual Cs body contents compared to the

11 prompt evacuees. The present study thus aimed to clarify this finding by reproducing the

12 exposure situation based on the evacuees' personal behavioral data in combination with the

13 latest atmospheric transport and dispersion model (ATDM) simulation for 356 selected subjects

14 in adult and 15-year (13–17 yrs) age groups. The results demonstrated that the ATDM

15 simulation-based method could reasonably reproduce the subjects' exposure situation,

16 supporting the previous finding. However, the residual ^{137}Cs body contents calculated by this

17 method were only 10%–20% of those in the subjects' WBC measurements. This large

18 discrepancy was considered to be caused by both the present method's underestimation and the

19 overestimation of the subjects' early intake in the WBC measurements due to a conservative

20 intake scenario not assuming potential additional intake. Additional studies are needed to

21 further clarify the reasons for the discrepancy and to evaluate the magnitude of the inhalation

22 dose in the accident.

23

24 **Key words:** Fukushima; early internal dose; ^{137}Cs; ATDM

25

1 **INTRODUCTION**

2 More than nine years have passed since the Tokyo Electric Power Company's (TEPCO's)

3 Fukushima Daiichi Nuclear Power Plant (FDNPP) accident that was triggered by the Great East

4 Japan Earthquake and subsequent massive tsunami on 11 March 2011. During this period, much

5 effort has been made to determine the dose assessment of the residents of Fukushima Prefecture

6 regarding their additional radiation exposure from the accident (Ishikawa 2017). The results of

7 the research during this 9-year period indicated that the estimated radiation doses to the

8 residents were to be low in general, and the residents' future radiation-induced risk was

9 considered low (UNSCEAR 2014). However, as we have pointed out (Kim et al. 2016a and c;

10 Kim et al. 2020; Kim and Kurihara 2020), further studies are still needed to improve the dose

11 assessment — in particular, the dose assessment for internal thyroid exposure from the short-

12 lived radionuclides (e.g., ^{131}I, ^{132}Te-^{132}I, and ^{133}I). The greatest obstacle has been the shortage

13 of direct human measurements at the early phase when the traces of ^{131}I, the main contributor

14 to the internal thyroid dose), were detectable. For this purpose, the early phase after the FDNPP

15 accident could be considered the period from the 11 March until the end of March or early April

16 2011 at the latest.

17 To address the problem of the lack of early phase direct human measurements, we proposed

18 a method that uses the results of direct human measurements taken with whole-body counters

19 (WBCs) by Japan's National Institute of Radiological Sciences (NIRS, reorganized in 2016 as

20 the National Institutes of Quantum and Radiological Science and Technology, QST) and the

21 Japan Atomic Energy Agency (JAEA) (Kim et al. 2016a and b; Kurihara et al. 2018). Although

22 the target radionuclides of these measurements were limited to ^{134}Cs and ^{137}Cs only, we derived

23 the intake ratio of ^{131}I to Cs at the early phase from the results of two independent direct

24 measurements (to assess the thyroid dose for children and the whole-body dose for adults), and

25 used this ratio to estimate the internal thyroid dose. However, one critical question later arose

26 regarding this method, namely whether the Cs detected in the WBC measurements that were

3

1 performed several months after the accident or later reflect the trace of the early intake or not.

2 In the Cs biokinetic model proposed by the International Commission on Radiological

3 Protection (ICRP 1989), the biological half-lives for Cs in the systemic body for adults, 10

4 year(-yr)-olds, and 5-yr-olds were assumed to be 110, 50, and 30 days, respectively. We

5 attempted to solve this question by conducting analyses of the WBC and personal behavioral

6 data of residents who were living near the FDNPP at the time of the nuclear accident. The results

7 revealed a distinct difference in the residual Cs body contents among individuals depending on

8 the timepoint of their evacuation, which strongly indicates a causal relationship with the

9 hydrogen explosion event at the FDNPP's Reactor Unit 1 building on the afternoon of the day

10 following the FDNPP accident (at 15:36 Japanese Standard Time [JST] on 12 March 2011). In

11 other words, it was revealed that the Cs intake was much higher in the late evacuees compared

12 to the prompt evacuees from Namie-town, which is approximately 7-8km from the FDNPP

13 (Igarashi et al. 2020). We divided the residents into prompt- and late-evacuee groups of

14 residents depending on their whereabouts at 15:00 on 12 March 2011 (as described later). Our

15 analyses revealed that the Cs detection rates (and the 90th percentile values of the estimated

16 ^{137}Cs intakes of individuals) of the prompt and late evacuees were approximately 20%

17 $(5.4 \times 10^3$ Bq) and 60% $(1.6 \times 10^4$ Bq), respectively. Approximately 20% of the individuals

18 analyzed were categorized as late evacuees. Here, the ^{137}Cs intake of each individual was

19 calculated based on the residual ^{137}Cs whole-body contents detected in the WBC measurements

20 in combination with the intake scenario of acute inhalation on the possibly earliest intake day

21 (i.e., 12 March 2011), which is the most conservative intake scenario.

22 This finding is of great importance in terms of determining the true and precise exposure

23 situations of residents living in the areas adjacent to the FDNPP where evacuation was ordered

24 (NAIIC, 2012). We thus attempted to clarify these residents' exposures by making use of the

25 latest atmospheric transport and dispersion model (ATDM) simulation published in 2020 and

26 we discuss the feasibility of this simulation as a tool for estimating the early internal dose to the

1 residents involved in the accident.

2

3 **MATERIALS AND METHODS**

4 **Subjects analyzed in the present study**

5   The subjects examined in the present study were the same as those analyzed in our Igarashi

6 et al. (2020) study, i.e., residents from Namie-town, one of the municipalities most severely

7 affected by the FDNPP (shown in Fig. 1). However, the present subjects were limited to two

8 age groups: the Adults group (aged ≥18 years) and the 15-yr group (ages 13–17 yrs) who moved

9 toward Tsushima district of Namie-town or Minamisoma-city shortly after the accident and

10 spent time there (>24 hr) during the period between 0:00 on 12 March and 0:00 on 14 March.

11 Here, the ages of the subjects are those as of the time of the accident (on 11 March 2011). In

12 our present and previous studies, Tsushima district of Namie-town is defined as an area outside

13 the 20-km radius of the FDNPP. The subjects underwent WBC measurements at the JAEA

14 during the months from July to December in 2011 (mostly July and August). The minimum

15 detectable activity (MDA) of these WBC measurements for ^{134}Cs and ^{137}Cs were both

16 approximately 300 Bq per body (Kurihara et al. 2018). The two age groups were further

17 subdivided into prompt and late evacuation groups: the former was the residents who had

18 moved outside the FDNPP's 20-km radius as of 15:00 on 12 March, and the latter residents had

19 not done so. The numbers of the four groups were as follows: prompt evacuees moving toward

20 Tsushima: G1(T) (n=231), late evacuees moving toward Tsushima: G2(T) (n=37), prompt

21 evacuees moving toward Minamisoma: G1(M) (n=64), and late evacuees moving toward

22 Minamisoma: G2(M) (n=24). The number of the subjects analyzed in this study thus totaled

23 356. The data of the committed effective doses (CEDs) to these four groups from ^{134}Cs and

24 ^{137}Cs were as seen in Table 1. Details of the subjects' behavioral data are described in our

25 Igarashi et al. (2020) study. Briefly, the behavioral data of the subjects contains the history of

26 their whereabouts (i.e., the place name and its latitude and longitude), the time spent

5

indoors/outdoors or moving, and the type of building where the person stayed (e.g., a wooden

house or concrete building). The behavioral data were provided hourly until 25 March and daily

from 26 March to 11 July (only for representative places to stay and commute to/from); however,

the data for April and later months were missing for most of the subjects. Additional

information to the above is that the behavioral data provided only landmark places in the

prefecture of destination (e.g., a prefectural government office) when the person stayed or

moved outside Fukushima Prefecture. The locations of individuals during moving were

determined assuming a uniform linear motion between the places of departure and destination

in the same manner as our previous study (Igarashi et al. 2020). The use of the behavioral and

whole-body data in the present study was approved by the Research Ethics Committees of the

authors' institutes (QST-NIRS: No. 13-011, Fukushima Medical University: No. 1892).

ATDM simulation and calculation of residual ^{137}Cs whole-body contents

We used the latest ATDM simulation provided by Worldwide version of System for

Prediction of Environmental Emergency Dose Information (WSPEEDI) ver. 2 (Terada et al.

2020). WSPEEDI-II has been used to understand the behaviors of the radionuclides released

into the environment in the FDNPP accident (Terada et al. 2012; Kobayashi et al. 2013; Katata

et al. 2015; Chino et al. 2016). The local-scale version system (SPEEDI, which is used in

emergency situations at nuclear power plants in Japan) was developed and updated to perform

immediate ATDM simulations using real-time metrological data and a given source term (e.g.,

the information on the release rate of radionuclides) that is to be obtained from a stack monitor

(Chino 1986; Chino and Adachi 2003; Suda 2006). However, the real-time information on the

source term could not be obtained in the case of the FDNPP accident. The source term was thus

estimated by means of inverse calculations to reproduce observed monitoring data such as the

ambient dose rate and the ground deposition density. The latest simulation by Terada et al.

(2020) has been improved by using an optimized method based on Bayesian interference that

1 incorporated the newly published hourly ^{137}Cs air concentration dataset obtained from

2 suspended particulate matter (SPM) samples collected at air pollution monitoring stations.

3 Details of the analysis of SPM samples have been described elsewhere (Oura et al. 2015, 2020;

4 Tsuruta et al. 2014, 2018).

5   In the present study, we dealt with the intake via inhalation of ^{137}Cs during the early phase

6 of the accident only. ^{134}Cs was excluded from the present analyses in this study because the

7 WBC results for ^{134}Cs were similar to those of ^{137}Cs (Igarashi et al. 2020). The ^{137}Cs intake

8 amount was then calculated by using the following equation:

9

10
$$I = \sum_j A_j \cdot V \cdot DRF_j \cdot \Delta T \tag{1}$$

11

12 where I is the intake amount of ^{137}Cs (Bq), A_j is the ^{137}Cs air concentration at the nearest grid

13 cell in a computational domain of WSPEEDI-II from the place where the subject stayed at the

14 time j (Bq m^{-3}), V is the hourly ventilation volume (m^3 hr^{-1}), DRF is the dose reduction factor

15 due to staying indoors (dimensionless), and ΔT is the time span of the database generated from

16 simulations by WSPEEDI-II (1 hr). This database contains a dataset of the horizontal two-

17 dimensional (2D) distribution of the ^{137}Cs air concentration (averaged hourly) at the ground

18 level for the time period between 01:00 on 12 March and 00:00 on 1 April, 2011 (480 [$= 24 \times 20$

19 days] outputs in total). The dataset used for dose calculations in this study was obtained from a

20 regional-scaled ATDM simulation by WSPEEDI-II (570×570 km^2 with 3-km resolution); we

21 also used a local-scaled ATDM simulation (190×190 km^2 with 1-km resolution) for a detailed

22 visualization of the ^{137}Cs air concentration (described below). The time integration in Equation

23 (1) was performed up to the end of March or 25 March 2011 depending on the analyses. The

24 value of the hourly ventilation volume was set at 0.925 m^3 h^{-1} (22.2 m^3 per day) for Adults and

25 0.838 m^3 h^{-1} (20.1 m^3 per day) for the 15-yr groups in reference to the ICRP publication 71

26 (1995). The DRF was set at 0.5 when the subject stayed indoors (described later), and at 1.0

1 when the subject stayed outdoors or was moving.

2 The residual ^{137}Cs body contents of a given subject, which were to be compared with the

3 results of the subject's whole-body measurements, were calculated using the following

4 equation:

5

$$M = \sum_k I_k \cdot R(T_M - T_k) \tag{2}$$

7

8 where I_k is the ^{137}Cs intake amount (Bq) on the day T_k, and $R(T_M - T_k)$ is the ^{137}Cs retention rate

9 (Bq per Bq intake, dimensionless) for the whole-body as a function of the elapsed days from T_k

10 to the measurement day, T_M. The data of $R(t)$ for the Adults and 15-yr groups were taken from

11 the MONDAL system developed by NIRS (Ishigure et al. 2004). Here $R(t)$ was calculated using

12 the default parameters set to assess the public exposure by inhalation: 1 μm in an activity

13 median aerodynamic diameter (AMAD) and Type F (fast absorption) for inhaled particulate

14 aerosols (ICRP 1995). The time integration in Equation (2) was performed up to the end of

15 March 2011, as in Equation (1). The data manipulation and visualization (e.g., the locations of

16 individuals and the horizontal 2D distribution of the ^{137}Cs air concentration on maps) were

17 implemented using programs written in Python by the authors.

18

19 Residents' evacuation

20 For a later discussion, the information on the residents' evacuation is provided next.

21 According to the records published by Namie-town (2018) and another relevant report

22 (Zengenkyo, 2012), the town decided to evacuate residents on a voluntary basis, based on

23 information from television reports. TEPCO was supposed to report the plant's situation to

24 Namie-town without delay based on a mutual agreement between the contractor and the town

25 in cases of emergency, but they could not. The Japanese central government issued evacuation

26 orders to municipalities adjacent to the FDNPP and adjacent to another facility, the Fukushima

1   Daini Nuclear Power Plant (located ~12 km south of the FDNPP); however, these orders did

2   not reach Namie-town directly (or via Fukushima Prefecture) due to communication failures.

3   Shortly after the earthquake at 14:46 on 11 March, Namie-town announced an immediate

4   evacuation order to residents living in its coastal area based on the forecast of a tsunami's arrival,

5   and most of those residents then evacuated to the town office (located 7–8 km away from the

6   FDNPP), the community center and many other shelters. The coastal area of the town was

7   seriously damaged due to the earthquake and massive tsunami. Table 2 provides the time chart

8   of countermeasures taken by Namie-town as well as the evacuation orders by the government.

9   The residents' evacuation was performed in two main steps. In the first evacuation on 11 and

10   12 March, residents moved to areas outside the 10-km radius and then outside the 20-km radius

11   of the FDNPP by private vehicles and buses. The town office was also transferred to Tsushima

12   district on that day. The evacuation took more than several hours (normally 30–40 min) due to

13   a heavy traffic jam on Route 114. Note that the evacuation to areas outside the 20-km radius

14   was made earlier than the evacuation order by the Japanese central government (at 18:25). In

15   the second evacuation on 15 March, the residents moved further to Nihonmatsu-city (~50 km

16   west of the FDNPP) or other municipalities (e.g., Fukushima-city, Koriyama-city, and others).

17   Akahane et al. (2013) considered 18 representative evacuation scenarios to perform the

18   preliminary external dose estimation for residents of Fukushima Prefecture; two of the 18

19   scenarios (Scenario 7 and Scenario 13) were for Namie-town residents (Fig. 2). In our previous

20   study we observed that some of the Namie-town residents moved toward Minamisoma-city,

21   which was not included in the 18 scenarios. A subsequent mass evacuation was held on 5 April

22   2011 or later. About 200 shelters were opened in various municipalities of Fukushima

23   Prefecture to receive the residents.

24   The numbers of Namie-town's residents who evacuated inside and outside Fukushima

25   Prefecture were 14,184 and 7,216, respectively (unknown for 34 persons). No instructions were

26   received from the local government or the prefecture about the distribution and administration

1 of stable iodine (KI). Namie-town had a stockpile of 25,000 KI tablets; however, they did not

2 use them.

3

4 **RESULTS**

5 **Movement of the subjects and behavior of aerial ^{137}Cs**

6 Figs. 3 and 4 illustrate the locations of individuals on the maps at several time points on 12

7 and 15 March. The ^{137}Cs air concentration at the ground level (created by the local-scaled

8 ATDM simulation) is superimposed on the same maps at the same time points. The symbols in

9 the figures denote each group described above; the blue symbols are the persons moving toward

10 Tsushima district, i.e., G1(T) and G2(T), and the red symbols are the persons moving toward

11 Minamisoma-city, i.e., G1(M) and G2(M). The same figures but at other time points and on

12 other days are provided in Appendix A. As shown in the figures, the locations of the subjects

13 become widely scattered with the increase in the distance from the FDNPP along with the

14 elapsed time. The locations of the subjects on 12 March (Fig. 3) indicates the crowded nature

15 of the evacuation routes mentioned above.

16 In the ATDM simulation, the release of ^{137}Cs began in the morning on 12 March and then

17 increased in the afternoon as a result of the hydrogen explosion at Reactor Unit 1. The aerial

18 ^{137}Cs that originated from this event flowed mainly to the north afterward and covered the

19 locations of some subjects, in particular those staying close to the FDNPP or moving toward

20 Minamisoma-city. On March 15 (when the largest release event was expected to occur), the

21 aerial ^{137}Cs flowed to the south in the morning, and its direction then turned clockwise in the

22 afternoon, resulting in the generation of a high-radiation background area in the northwest due

23 to wet deposition at night. As can be seen in the Figs. 3 and 4, many of the subjects appear to

24 have been exposed to the aerial ^{137}Cs at various places apart from the FDNPP on that day. Fig.

25 5 presents the time series of the ratios of subjects in each group who stayed outside the 20-km

26 radius of the FDNPP. As shown, the ratios were almost 1 (100%) for each group on 13 March

1 and later; in other words, no apparent difference was found in the ratios among the four groups

2 except for those on 12 March.

3

4 **^{137}Cs inhalation intake of the subjects**

5   Fig. 6 presents the total ^{137}Cs intake amounts (via inhalation up to 25 March) calculated

6 based on the ATDM simulation for each group in box-whisker plots; the two age groups are

7 also individually displayed. As shown in the figure, the ^{137}Cs intake amounts are higher in the

8 late-evacuation groups than in the prompt-evacuation groups: G1(T) < G2(T), and G1(M) <

9 G2(M). The ^{137}Cs intake amounts of the persons moving toward Minamisoma-city tend to be

10 higher than those moving toward Tsushima district: G1(T) < G1(M), and G2(T) < G2(M). The

11 ratio of the persons whose ^{137}Cs intake amounts were >1,000 Bq was 17% of the subjects

12 analyzed in this study (356 persons in total), whereas the same ratio in the WBC measurements

13 was 32%. Fig. 7 presents the relative daily ^{137}Cs intake amounts for each group in bar charts as

14 100% of the total (up to 25 March). Each bar in the figure is the average of the subjects whose

15 total ^{137}Cs intake amounts exceeded 500 Bq. One remarkable finding is the distinct difference

16 in the ^{137}Cs intake on 12 March between the G1(T) and G2(T) groups; however, such a

17 difference does not appear between the G1(M) and G2(M) groups. The contribution of the

18 intake on 15 March is also unique to each group; for example, it is the highest in the G1(T)

19 group, whereas is the lowest in the G2(M) group.

20

21 **Comparison of the residual ^{137}Cs body contents between the ATDM simulation and the**

22 **WBC measurements**

23   Fig. 8 presents the residual ^{137}Cs body contents for each group in box-whisker plots; the left

24 panel displays the results from the ATDM simulation using Equation (2) and the right panel

25 displays the results from the WBC measurements. Note that more than one-half of the G1(T)

26 and G1(M) subjects' values were below the MDA level in the WBC measurements. As seen in

the figure, the residual ^{137}Cs body contents calculated based on the ATDM simulation were considerably lower than the result of the WBC measurements; note that the scale of the vertical axis is different between the left and right panels in the figure. In the ATDM simulation, the body contents of only eight individuals exceeded 300 Bq (corresponding to the MDA) of the WBC measurements. The ratios of the two methods (ATDM/WBC) were roughly 0.1–0.2 at the 75th and 90th percentiles.

DISCUSSION

As described in the Introduction, the reconstruction of the early internal dose to residents in the FDNPP accident has been challenging because of the shortage of direct human measurements for ^{131}I. The total of those measurements was only approximately 1,300, and the measurements were gathered from relevant publications (Tokonami et al. 2012; Matsuda et al. 2013; Kim et al. 2020). To solve this problem, we have attempted to apply ATDM simulations to the estimation of the internal thyroid doses due to the inhalation of ^{131}I as a supplementary method (Kim et al. 2016a and d). Other researchers have used ATDM simulations for a similar purpose. Kawai et al. (2018) and Miyatake et al. (2020) attempted to reconstruct a time-series profile of the ^{131}I concentration in tap water available in the areas of concern after the FDNPP accident with the help of ATDM simulations by WSPEEDI-II to estimate the ingestion dose. Ohba et al. (2020) and Takagi et al. (2020) estimated the internal thyroid doses due to the inhalation of ^{131}I by using the latest ATDM simulations available. Our present study used the same database generated by WSPEEDI-II as that used by Ohba et al. (2020); however, we had a different focus, namely to confirm the validity of the application of ATDM simulations to future dose reconstructions for individuals by comparing the simulation results with the results of WBC measurements.

The critical finding of the present study is that the estimation based on the ATDM simulation could not reproduce the residual ^{137}Cs body contents from the WBC measurements of the

1 subjects analyzed. The values of the ATDM simulation were only 0.1–0.2 times as large as

2 those of the WBC measurements. This large discrepancy should be examined from the

3 perspective of at least two possibilities (assuming that there is no error in the WBC

4 measurements); one is the intake by routes other than inhalation at the early phase, and the other

5 is the underestimation of the ^{137}Cs air concentration computed by the ATDM simulation.

6 Regarding the first possibility, we note that a small amount of the daily intake due to

7 ingestion would increase the residual ^{137}Cs body contents observed in the WBC measurements,

8 resulting in the overestimation of the Cs intake at the early phase due to the conservative intake

9 scenario used. In fact, several studies revealed that the dietary intake of $^{134/137}$Cs in Fukushima

10 Prefecture in the first year after the accident was expected to be a few Bq per day or occasionally

11 more (Koizumi et al. 2012; Harada et al. 2013). Even such a small daily intake amount could

12 have a significant influence on the results of the WBC measurements if accumulated. For

13 example, the residual ^{137}Cs body content increases up to ~100 Bq in the case of adults on the

14 150th day of chronic ingestion with a uniform intake of 1 Bq per day (Kurihara et al. 2018).

15 The incidental ingestion of contaminated soil can also be considered as a possible exposure

16 pathway (IRSN 2012). In terms of inhalation, the dust sampling at several locations within ~30

17 km of the FDNPP demonstrated value that were mostly below the detection limits in April or

18 later (NRA 2011). On the other hand, the Cs air concentration at a parking lot in Fukushima-

19 city ranged fom 10 to 30 mBq m^{-3} during the period from September to December 2011

20 (Akimoto 2015), which was caused by the migration from the heavily contaminated areas

21 around the FDNPP or its resuspension from the ground. The Cs air concentration at this site

22 would be higher at the earlier time points (although the data are missing). Thus, the occasional

23 intake after the early phase could occur via both ingestion and inhalation. Such a possibility is

24 expected to exist evenly in all groups, because residents of Namie-town evacuated to various

25 places inside and outside Fukushima Prefecture (Namie-town, 2018). As a result, the

26 differences among the groups in their early intake amount between the groups would become

1 relatively small with time and disappear in subsequent WBC measurements if the additional

2 intake was significant; however, this was not the case in our stud.

3 The relationship between the intake amount and the residual body content is determined

4 depending on the period of time between the intake event and the measurement. In the case of

5 the inhalation of ^{137}Cs as a Type F compounds with an AMAD of 1 μm, the whole-body

6 retention rates at the 150th days after intake for the Adult and 15-yr groups are 1.17×10^{-1} and

7 9.15×10^{-2}, respectively. The number of elapsed days from the first possible intake event (12

8 March 2011) until the WBC measurements for the subjects analyzed in this study was 155 days

9 (1σ =23 days). Fig. 9 presents the ^{137}Cs whole-body retention rate as a function of the number

10 of elapsed days along with the number of WBC measurements taken on each day, suggesting

11 that the ^{137}Cs residual body contents detectable in the WBC measurements were decreased to

12 only around 10% of the initial intake amounts via inhalation. Note that about one-half of the

13 intake amount is immediately removed by exhalation. In detail, the total deposition rate in the

14 respiratory tract is 48.58% for the Adult group and 46.38% for the 15-yr group (ICRP 1995) in

15 the case of inhaled particles with an AMAD of 1 μm. Thereby, the WBC measurements should

16 have detected only the persons whose ^{137}Cs intake amounts were >3,000 Bq at least (i.e., 10

17 times as large as the MDA value) if there was no additional intake as described above. However,

18 the ^{137}Cs intake amounts calculated from the ATDM simulation were <3,000 Bq for almost all

19 of the subjects (Fig. 6).

20 The actual physiochemical form of Cs-containing particles released from the FDNPP should

21 also be mentioned here because this can influence the above-described retention rate. Several

22 studies reported the measured aerosol sizes with AMAD values of 0.5–1.5 μm (Kaneyasu et al.

23 2012; Doi et al. 2013; Miyamoto et al. 2014). Taking into account the fact that the samples were

24 collected in distant places (>100 km) from the FDNPP in those studies, the aerosols potentially

25 inhaled by the present study's subjects are expected to be larger. The ^{137}Cs whole-body retention

26 rate for particulate aerosols with an AMAD of 5 μm is approximately 40% larger than that for

14

particulate aerosols with an AMAD of 1 μm because of the increase in the particle deposition

rate in the respiratory tract. A greater proportion of larger aerosols or submicron-sized aerosols

would lower the deposition rate. The gaseous form of cesium was found to be minor compared

to its particulate form (JAEA 2011). Regarding the absorption type, Type F would be a

reasonable assignment in light of the reported by Kaneyasu et al (2012) that soluble sulfate

aerosol was a potential transport media for Cs. By contrast, other studies revealed the existence

of insoluble Cs particles released from the nuclear plant (Adachi et al. 2013; Igarashi et al.

2019), suggesting that Type S (slow absorption) would be an appropriate assignment instead.

However, the ^{137}Cs whole-body retention rate is rather lower in Type S than in Type F until the

200th-day post-intake due to a larger fraction of direct fecal excretion without absorption in the

gastro-intestine tract, which is parameterized as the f_1 value in the dosimetric models (ICRP

1995): 1.0 for Type F and 0.01 for Type S. The assumption of Type S results in further

enhancing the underestimation of the residual ^{137}Cs body contents. The insoluble Cs particles

found in the vicinity of the FDNPP were characterized into two types based mainly on the

isotopic ratio of ^{134}Cs/^{137}Cs (Igarashi et al. 2019). One of the two types (Type B) has been

considered to originate from Reactor Unit 1, which had with a core inventory with a lower

^{134}Cs/^{137}Cs radioactivity ratio compared to those of Reactor Units 2 and 3, where the nuclear

fuel melt-down occurred. Type B particles found in soil had high radioactivity (~30–19,000 Bq

per particle) and large sizes (~40–400 μm). These particles would have rarely contributed to

inhalation because of their sizes. On the other hand, the trace of the plume passage from Unit 1

remained in the area at a length of about 15 km and a width of 3 km in the north-northwest

(NNW) direction from the FDNPP (Kobayashi et al 2017). Chino et al (2016) also reported the

direction of the same plume passage and reproduced it in their ATDM simulations. which were

succeeded in the study by Terada et al (2020). The ATDM prediction in our present study would

thus capture the sequence of exposure to the radioactive plume by the subjects in the afternoon

on 12 March, although the detailed characteristics of released particles were not considered in

1 the ATDM simulation used herein.

2 Regarding the second possibility, we directly compared the ATDM simulation with SPM

3 data in terms of the ^{137}Cs air concentration at several locations. Fig. 10 illustrates the results of

4 our comparison of the daily-integrated values of the ^{137}Cs air concentrations at Haramachi (the

5 middle part of Minamisoma-city) and Fukushima-city. Table 3 provides the time-integrated

6 ^{137}Cs air concentration values from 12 to 22 March at five locations on the evacuation routes of

7 some subjects. From these results, although significant underestimations were found for

8 Nihonmatsu-city and Fukushima-city with relatively low ^{137}Cs air concentration in the SPM

9 data, we consider that the ATDM simulation would be reasonably applied to the estimation of

10 the inhalation doses to some of the subjects in the G1(M) and G2(M) groups (i.e., the

11 individuals who moved toward Minamisoma-city shortly after the accident and then stayed

12 there for a while), whereas the ATDM simulation would be likely to underestimate the

13 inhalation doses to those who continued to stay in Fukushima-city or Nihonmatsu-city after the

14 accident, which corresponds to some of the G1(T) and G2(T) subjects.

15 The intake amount via inhalation could be estimated as long as the air concentration is

16 accurately reproduced from ATDM simulations. Although, to our knowledge, there has been

17 only one case study that examined the ratio of the ^{137}Cs intake amount estimated from WBC

18 measurements to that calculated from air sampling in the FDNPP accident, the ratios for three

19 adult males staying in Ibaraki Prefecture (adjacent to Fukushima Prefecture in the south, Fig.

20 1) during the arrival of major radioactive plumes on 15 March and later were found to be

21 roughly 0.7 on average (Kurihara et al. 2016), which was considered reasonable taking into

22 account the dose reduction factor due to staying indoors. Note that the WBC measurements in

23 this study were performed in a timely manner so that the number of occasions of incidental

24 ingestion was minimized.

25 From a different point of view, the results of the ATDM simulations presented herein may

26 indicate that the ^{137}Cs inhalation intake at the early phase would have been very minor enough

1 to be undetectable at the time of the WBC measurements. However, then what caused the

2 finding in our previous study, the distinct difference in the Cs internal dose between prompt and

3 late evacuees? One may doubt the possibility of intake from the body surface contamination by

4 unintentional habits (e.g., touching the face) at the early phase. A large number of residents

5 were examined for body surface contamination during their evacuation, and it was revealed that

6 there were some heavily contaminated individuals (Kondo et al. 2013). The intake would be

7 trivial for Cs because its radioactivity fraction in the contamination was found to be minor

8 compared to the short-lived radioiodines (Ohba et al. 2017). To address the above question, we

9 need to further evaluate the possibility of an additional intake by Fukushima residents. The

10 extremely-high residual Cs body contents (a few kBq or more) in late WBC measurements for

11 some residents were likely to be due to an accidental ingestion of highly-contaminated food

12 (Tsubokura et al. 2014). This may be partly true in our study population.

13   On the other hand, interestingly, the distribution profiles of the residual ^{137}Cs body contents

14 for each the present groups of subjects appear to be similar between the ATDM simulation and

15 the WBC measurements, (many plots of the latter values are not shown, in particular for the

16 prompt evacuees due to the existence of MDA) (Fig. 8). The magnitude relationship among the

17 four groups generally agreed with each other: G1(T) < G1(M) < G2(T) < G2(M) (Fig. 8). In

18 addition, the ATDM simulation results were consistent with our finding that 12 March was the

19 most influential day for late evacuees in terms of their possible internal exposure. One new

20 insight from the latest ATDM simulation is that the inhalation dose of ^{131}I was significantly

21 reduced in the areas around Tsushima district compared to that predicted by the previous ATDM

22 simulation (Kim et al. 2016d). It was also indicated that the inhalation dose in Minamisoma-

23 city would have been brought by the radioactive plumes arriving there several times (in

24 particular on 12–13 and 18–20 March). These results may be reflected in the WBC

25 measurements. The daily accumulated ^{137}Cs air concentration at different locations on two

26 national roads (Routes 114 and 6) from the ATDM simulation are provided in Appendix B; Fig

B1 and Table B1 demonstrate the locations at which the data were obtained, and Tables B2 and

B3 provide the data for the locations on Route 114 and Route 6, respectively. Route 6 was

expected to be used for residents who evacuated toward Minamisoma-city (Fig. 3), although it

was reported that the road was unavailable due to serious damage (Zengenkyo, 2012). Note that

the ^{137}Cs inhalation intake amount can be calculated by multiplying the values in Tables B2 and

B3 by the hourly ventilation volume. These data indicate that the ^{137}Cs inhalation intake is

higher in the north area than in the northwest, unlike the previous ATDM simulations. However,

in either case, it is certain that the residents' evacuation would have considerably reduced the

inhalation dose that the resident would have received in the FDNPP's neighboring areas. In this

regard, it would be notable that most of the residents completed evacuation outside the 20-km

radius much earlier than the evacuation order by the Japanese central government at 18:25 on

12 March (Fig. 5).

The limitations of the method applied herein are as follows. First, the subjects' behavioral

data used in this study were created from answer sheets collected from residents for the purpose

of estimating the individual external doses for the first four months after the FDNPP accident

as part of the Fukushima Health Management Survey (Ishikawa et al. 2015). These answer

sheets were self-administered, and thus their quality was greatly dependent on each subject's

memory. Missing or mistaken memories would be likely to occur although the behaviors right

after the nuclear accident are expected to have been vividly retained in one's memory due to

many impressive events for the residents, e.g., the immediate evacuation, the heavy traffic jam

during evacuation, the successive explosive events at the FDNPP, and so on. Second, the

locations of individuals during their evacuations were not strictly accurate in this study because

of the assumption of a uniform linear motion between the places of departure and destination

(as noted earlier). This problem would be solved by taking int account the realistic movement

of individuals on the roadmap (Appendix B). Third, uncertainties accompany the parameters

for the dose calculations, i.e., the ventilation volume and the dose reduction factor due to staying

indoors. The ventilation volume depends on the exercise level (sleep, sitting, light exercise, heavy exercise), which ranges from 0.45 to 3.0 m^3 hr^{-1} for adults and from 0.42 to 2.92 m^3 hr^{-1} for 15-yr-olds (ICRP 1995). The actual ventilation volumes of the subjects could be somewhat higher than the reference values used in this study, considering the situations under the urgent evacuation. Regarding the dose reduction factor, Ishikawa et al. (2014) demonstrated that the indoor-to-outdoor air concentration ratios for ^{131}I (particulate) and ^{137}Cs in Chiba Prefecture after the FDNPP accident were 0.64 and 0.58, respectively. Another study (JAERI 1987) reported that the ratios for aerosols and iodine gas were 0.62–0.72 and 0.45–0.74, respectively, in Japanese buildings based on observations of the fallout that originated from the Chernobyl nuclear power plant accident. Based on these studies, the indoor shielding factor of 0.5 applied in the present study would be reasonable in general.

In conclusion, regarding Cs, it is currently difficult to apply the ATDM simulation to the estimation of the early internal doses to individuals. The method considerably underestimated the residual ^{137}Cs body contents of the subjects from their WBC measurements. Persuasive reasons for this could not been obtained in this study; however, through the above considerations, the discrepancy between the ATDM simulation and WBC measurements can be expected to have been due to multiple reasons: (1) the underestimation of the ATDM prediction and the overestimation of the early intake from the WBC measurements due to the conservative intake scenario not assuming potential additional intake, and (2) uncertainties in the parameters used in the dose calculations. The direct comparison of the WBC data containing many low values (below the MDA) with the ATDM data would also amplify the discrepancy. Further studies are necessary to clarify the discrepancy between these two methods and to determine the precise magnitude of the inhalation dose from the FDNPP accident.

data of the latest ATDM simulation by WSPEEDI-II.

REFERENCES

Adachi K, Kajino M, Zaisen Y, Igarashi Y. Emission of spherical cesium-bearing particles from an early stage of the Fukushima nuclear accident. Sci Rep 3: 2554; 2013.

Akahane K, Yonai S, Fukuda S, Miyahara N, Yasuda H, Iwaoka K, Matsumoto M, Fukumura A, Akashi M. NIRS external dose estimation system for Fukushima residents after the Fukushima Dai-ichi NPP accident. Sci Rep 3:1670; 2013.

Akimoto K. Annual and weekly cycle of radioactivity concentration observed in Fukushima city. Health Phys 108(1): 32–38; 2015.

Chino M, Adachi T. Present status and future prospect on system for prediction of environmental emergency dose information, SPEEDI. Nihon-genshiryoku-gakkaishi 45(5): 296–301; 2003 (in Japanese).

Chino M, Terada H, Nagai H, Katata G, Mikami S, Torii T, Saito K, Nishizawa Y. Utilization of $^{134}Cs/^{137}Cs$ in the environment to identify the reactor units that caused atmospheric releases during the Fukushima Daiichi accident. Sci Rep 6: 31376; 2016.

Chino M. SPEEDI: System for Prediction of Environmental Emergency Dose Information. Hokenbutsuri 21: 285–294; 1986 (in Japanese).

Doi T, Masumoto K, Toyoda A, Tanaka A, Shibata Y, Hirose K. Anthropogenic radionuclide in the atmospheric observed at Tsukuba: characteristics of the radionuclides derived from Fukushima. J Environ Radioact 122: 55–62; 2013.

Harada K H, Fujii Y, Adachi A, Tsukidate A, Asai F, Koizumi A. Dietary intake of radiocesium in adult residents in Fukushima Prefecture and neighboring regions after the Fukushima nuclear power plant accident: 24-h food-duplicate survey in December 2011. Environ Sci Technol 47: 2520–2526; 2013.

International Commission on Radiological Protection; Age-dependent doses to members of the public from intake of radionuclides–Part 1 ICRP Publication 56. Ann. ICRP 20(2); 1989.

International Commission on Radiological Protection. Age-dependent doses to the members of the public from intake of radionuclides–Part 4 inhalation dose coefficients. Oxford: ICRP; Publication 71. Ann. ICRP 25(3–4); 1995.

Igarashi Y, Kim E, Hashimoto S, Tani K, Yajima K, Iimoto T, Ishikawa T, Akashi M, Kurihara O. Difference in the cesium body contents of affected area residents depending on the evacuation timepoint following the 2011 Fukushima nuclear disaster. Health Phys 119 (6): 737–745; 2020.

Igarashi Y, Kogure T, Kurihara Y, Miura H, Okumura T, Satou Y, Takahashi Y, Yamaguchi N. A review of Cs-bearing microparticles in the environment emitted by the Fukushima Dai-ichi Nuclear Power Plant accident. J Environ Radioact 205–206: 101–118; 2019.

Institute for Radiological Protection and Nuclear Safety. Fukushima, one year later Initial analyses of the accident and its consequences. Report IRSN/DG/2012–003; 2012.

Ishigure N, Matsumoto M, Nakano T, Enomoto H. Development of software for internal dose calculation from bioassay measurements. Radiat Protect Dosim 109:235–242; 2004. [MONDAL3 (updated version), online]. Available at *https://www.nirs.qst.go.jp/db/anzendb/RPD/gpmd.php*. Accessed 10 January 2021.

Ishikawa T, Yasumura S, Ozasa K, Kobashi G, Yasuda H, Miyazaki M, Akahane K, Yonai S, Ohtsuru A, Sakai A, Sakata R, Kamiya K, Abe M. The Fukushima Health Management Survey: estimation of external doses to residents in Fukushima Prefecture. Sci Rep 5: 12712; 2015.

Ishikawa T. Radiation doses and associated risk from the Fukushima nuclear accident: a review of recent publications. Asia Pac J Public Health 29(2S): 18S–28S; 2017.

Ishikawa T., Sorimachi A., Arae H., Sahoo S. K., Janik M., Hosoda M., Tokonami, S. Simultaneous sampling of indoor and outdoor airborne radioactivity after the Fukushima

23

Daiichi nuclear power plant accident. Environ Sci Technol 48: 2340–2435; 2014.

Japan Atomic Energy Agency. Results of the environmental radiation monitoring following the accident at the Fukushima Daiichi Nuclear Power Plant –interim report (ambient radiation dose rates, radioactivity concentration in the air and the radioactivity concentration in the fallout–. JAEA-Review 2011-035; 2011 (in Japanese).

Japan Atomic Energy Research Institute. Health Physics in JAERI. Ibaraki, Japan: JAERI; JAERI-M No.29. 87–147 [online] 1987 (in Japanese). Available at *https://jopss.jaea.go.jp/pdfdata/JAERI-M-87-147.pdf*. Accessed 10 January 2021.

Katata G, Chino M, Kobayashi T, Terada H, Ota M, Nagai H, Kajino M, Draxler R, Hort MC, Malo A, Torii T, Sanada Y. Detailed source term estimation of the atmospheric release for the Fukushima Daiichi nuclear power station accident by coupling simulations of atmospheric dispersion model with improved deposition scheme and oceanic dispersion model. Atoms Chem Phys 15:1029–1070; 2015.

Kaneyasu N, Ohashi H, Suzuki F, Okuda T, Ikemori F. Sulfate aerosol as a potential transport medium of radiocesium from the Fukushima nuclear accident. Environ Sci Technol46: 5720–5726; 2012.

Kawai M, Yoshizawa N, Suzuki G. [131]I dose estimation from intake of tap water in the

24

early phase after Fukushima Daiichi nuclear power plant accident. Radiat Prot Dosim 179(1): 43–48; 2018.

Kim E, Kurihara O, Kunishima N, Momose T, Ishikawa T, Akashi M. Internal thyroid doses to Fukushima residents – estimation and issues remaining. J Radiat Res 57(S1): i118–i126; 2016a.

Kim E, Kurihara O, Kunishima N, Nakano T, Tani K, Hachiya M, Momose T, Ishikawa T, Tokonami S, Hosoda M, Akashi M. Early intake of radiocesium by residents living near the TEPCO Fukushima Dai-ichi nuclear power plant after the accident. Part 1: Internal doses based on whole-body measurements by NIRS. Health Phys 115(5): 451–464; 2016b.

Kim E, Kurihara O, Tani K, Ohmachi Y, Fukutsu K, Sakai K, Akashi M. Intake ratio of ^{131}I to ^{137}Cs from thyroid and whole-body doses to Fukushima residents. Radiat Prot Dosim 168(3): 408–418; 2016c.

Kim E, Kurihara O. Thyroid doses in children form radioiodine following the accident at the Fukushima Daiichi nuclear power plant. J Radiat Prot Res 45(1): 2–10; 2020.

Kim E, Tani K, Kunishima N, Kurihara O, Sakai K, Akashi M. Estimation of early internal doses to Fukushima residents after nuclear disaster based on atmospheric

dispersion simulation. Radiat Prot Dosim 171(3): 398–404; 2016d.

Kim E, Yajima K, Shozo Hashimoto, Tani K, Igarashi Y. Iimoto T, Ishigure N, Tatsuzaki N, Akashi M, Kurihara O. Reassessment of internal thyroid doses to 1,080 children examined in a screening survey after the 2011 Fukushima nuclear disaster. Health Phys 118(1): 36–52; 2020.

Kobayashi T, Nagai H, Chino M, Kawamura H. Source term estimation of atmospheric release due to the Fukushima Dai-ichi nuclear power plant accident by atmospheric and oceanic dispersion simulations. J Nucl Sci Technol 50(3): 255–264; 2013.

Kobayashi S, Shinomiya T, Ishikawa T, Imaseki H, Iwaoka K, Kitamura H, Kodaira S, Kobayashi K, Oikawa M, Miyaushiro N, Takashima Y, Uchihori Y. Low 134Cs/137Cs ratio anomaly in the north-northwest direction from the Fukushima Dai-ichi Nuclear Power Station. J Environ Radioact 178–179: 84–94; 2017.

Koizumi A, Harada K H, Niisoe T, Adachi A, Fujii Y, Hitomi H, Wada Y, Watanabe T, Ishikawa H. Preliminary assessment of ecological exposure of adult residents in Fukushima Prefecture to radioactive cesium through ingestion and inhalation. Environ Health Prev Med 17: 292–298; 2012.

Kondo H, Shimada J, Tase C, Tominaga T, Tatsuzaki H, Akashi M, Tanigawa K, Iwasaki

Y, Ono T, Ishihara M, Kohayagawa Y, Koido Y. Screening of residents following the Tokyo Electric Fukushima Daiichi Nuclear Power Plant accident. Health Phys 105(1): 11–20; 2013.

Kurihara O, Chunsheng L, Lopez M A, Kim E, Tani K, Nakano T, Takada C, Momose T, Akashi M. Experiences of population monitoring using whole-body counters in response to the Fukushima nuclear accident. Health Phys 115(2): 259–274; 2018.

Kurihara O, Nakagawa T, Takada C, Tani K, Kim E, Momose T. Internal doses of three persons staying 110 km south of the Fukushima Daiichi nuclear power station during the arrival of radioactive plumes based on direct measurements. Radiat Prot Dosim 170(1–4): 420–424; 2016.

Matsuda N, Kumagai A, Ohtsuru A, Morita N, Miura M, Yoshida M, Kudo T, Takamura N, Yamashita S. Assessment of internal exposure doses in Fukushima by a whole body counter within one month after the nuclear power plant accident. Radiat Res 179:663–668; 2013.

Miyamoto Y, Yasuda K, Magara M. Size distribution of radioactive particles collected at Tokai, Japan 6 days after the nuclear accident. J Environ Radioact 132: 1–7; 2014.

Miyatake H, Kawai M, Yashizawa N, Suzuki G. Estimation of internal dose from tap

water after the Fukushima Daiichi nuclear power station accident using newly obtained data. J Radiat Res 61(2): 231–236; 2020.

Nuclear Regulation Authority. Monitoring information of environmental radioactivity level. [online] 2011 (in Japanese). Available at *https://radioactivity.nsr.go.jp/ja/list/485/list-1.html*. Accessed on 10 January 2021.

The National Diet of Japan Fukushima Nuclear Accident Independent Investigation Commission (NAIIC). Reports [online]. 2012. Available at *https://www.cas.go.jp/jp/seisaku/icanps/eng/final-report.html*. Accessed 10 January 2020.

Namie-town. Earthquake record of Namie-town [online]. 2018 (in Japanese). Available at *https://www.town.namie.fukushima.jp/soshiki/1/18101.html*. Accessed 10 January 2021.

Ohba T, Hasegawa A, Kohayagawa Y, Kondo H, Suzuki G. Body surface contamination levels of residents under different evacuation scenarios after the Fukushima Daiichi Nuclear Power Plant accident. Health Phys 117(3): 175–182; 2017.

Ohba T, Ishikawa T, Nagai H, Tokonami S, Hasegawa A, Suzuki G. Reconstruction of residents' thyroid equivalent doses from internal radionuclides after the Fukushima Daiichi nuclear power station accident. Sci Rep 10: 3639; 2020.

28

Oura Y, Ebihara M, Tsuruta H, Nakajima T, Ohara T, Ishimoto M, Sawahata H, Katsumura Y, Nitta W. A database of hourly atmospheric concentrations of radiocesium (^{134}Cs and ^{137}Cs) in suspended particulate matter collected in March 2011 at 99 air pollution monitoring stations in Eastern Japan. J Nucl Radiochem Sci 15(2): 1–22; 2015.

Oura Y, Tsuruta H, Ebihara M, Ohara T, Nakajima T. Determination of atmospheric radiocesium by analyzing filter-tapes used in automated suspended particulate matter monitor. Bunseki Kagaku 69(1-2): 1–9; 2020 (in Japanese).

Suda N. The present status and future prospectus of the SPEEDI network system. Hoken-Butsuri 41(2): 88–98; 2006 (in Japanese).

Takagi M, Ohara T, Goto D, Morino Y, Uchida J, Sekiyama T T, Nakayama S F, Ebihara M, Oura Y, Nakajima T, Tsuruta H, Moriguchi Y. Reassessment of early ^{131}I inhalation doses by the Fukushima nuclear accident based on atmospheric ^{137}Cs and ^{131}I/^{137}Cs observation data and multi-ensemble of atmospheric transport and deposition models. J Environ Radioact 218: 106223; 2020.

Terada H, Katata G, Chino M, Nagai H. Atmospheric discharge and dispersion of radionuclides during the Fukushima Dai-ichi nuclear power plant accident. Part II: verification of the source term and analysis of regional-scale atmospheric dispersion. J Environ Radioact 112: 141–154; 2012.

Terada H, Nagai N, Tsuduki K, Furuno A, Kadowaki M, Kakefuda T. Refinement of source term and atmospheric dispersion simulations of radionuclides during the Fukushima Daiichi nuclear power station accident. J Environ Radioact 213: 106104; 2020.

Tokonami S, Hosoda M, Akiba S, Sorimachi A, Kashiwakura I, Balonov M. Thyroid doses for evacuees from the Fukushima nuclear accident. Sci Rep 2:507:1–4; 2012.

Tsubokura M, Kato S, Nomura S, Gilmour S, Nihei M, Sakuma Y, Oikawa T, Kanazawa Y, Kami M, Hayano R. Reduction of high levels of internal radio-contamination by dietary intervention in residents of areas affected by the Fukushima Daiichi nuclear power plant disaster: a case series. PLOS ONE 9(6): e100302; 2014.

Tsuruta H, Oura Y, Ebihara M, Moriguchi Y, Ohara T, Nakajima T. Time-series analysis of atmospheric radiocesium at two SPM monitoring sites near the Fukushima Daiichi nuclear power plant just after the Fukushima accident on March 11, 2011. Geochemical J 52: 103–121; 2018.

Tsuruta H, Oura Y, Ebihara M, Ohara T, Nakajima T. First retrieval of hourly atmospheric radionuclides just after the Fukushima accident by analyzing filter-tapes of operational air pollution monitoring stations. Sci Rep 4: 6717; 2014.

United Nations Scientific Committee on the Effects of Atomic Radiation. Levels and Effects of Radiation Exposure Due to the Nuclear Accident After the 2011 Great East-Japan Earthquake and Tsunami. UNSCEAR 2013 Report Annex A; 2014.

Zengenkyo. Working group report on nuclear disaster [online]. 2012 (in Japanese). Available at *https://zengenkyo.org/data/*. Accessed 10 January 2021.

Footnote

*National Institutes for Quantum and Radiological Sciences and Technology, 4-9-1 Anagawa,

Inage-ku, Chiba-city, Chiba 263-8555, Japan

List of figure captions

Fig. 1. The locations of Fukushima Prefecture, Ibaraki Prefecture, Namie-town, and its adjacent municipalities (reproduced from Igarashi et al. 2020).

Fig. 2. Representative evacuation scenarios for Namie-town's residents. Scenario 7: The first evacuation route is from the town office (departure at 12:00) to the Tsushima vitalization center (arrival at 15:00) on 12 March, and the second evacuation route is from the Tsushima vitalization center (departure at 10:00) to the Adachi gymnasium in Nihonmatsu-city (arrival at 14:00) on 16 March. Scenario 13: The first evacuation is the same as that in Scenario 7, and the second evacuation is from the Tsushima vitalization center (departure at 10:00) to the Adachi gymnasium in Nihonmatsu-city (arrival at 14:00) on 23 March. The *circles* in the figure denote the rough locations of the offices of each administrative district. The national roads (Route 114 and Route 6, partly drawn in the figure) were thought to be used by most of the residents of Namie-town for their evacuation.

Fig. 3. The locations of individuals on the maps with the superimposed ^{137}Cs air concentrations at the ground level on 12 March. The *concentric circles* on the maps are drawn with the FDNPP at the center. The ^{137}Cs air concentrations are provided as hourly-averaged data, and the starting time is denoted at the top of each panel (*left panel:* 8:00, *middle panel:* 15:00, and *right panel:* 18:00). The symbols in the figure denote the four groups of residents (see text).

Fig. 4. The locations of individuals on the maps with the ^{137}Cs air concentrations at the ground level on 15 March. The *concentric circles* on the maps are drawn with the FDNPP at the center. The ^{137}Cs air concentrations are provided as hourly-averaged data, and the starting time is denoted at the top of each panel (*left panel:* 9:00, *middle panel:* 15:00, and *right panel:* 21:00). The symbols in the figure denote each of the four resident groups (see text).

Fig. 5. The ratio of subjects staying outside the 20-km radius of the FDNPP for each group (see the text). *Left panel:* The period from 12 to 15 March. *Right panel:* The period from 12 to 25 March.

Fig. 6. The total ^{137}Cs intake amounts (Bq) for each group based on the ATDM simulation. The

33

boxes cover the 25th percentile to the 75th percentile of the distribution. The right panel expands the vertical axis of the left panel to make it easy to see the distribution in the small range. The lines in the boxes are the 50th percentile (median) of the distribution. The whiskers cover the first quantile − 1.5 × IQR (interquartile range) to the third quintile + 1.5 × IQR. The outliers are marked as *circles*.

Fig. 7. The relative daily ^{137}Cs intake amounts (Bq) for each group of the subjects with their total ^{137}Cs intake exceeding 500 Bq. *Left panel:* G1(T) and G2(T). *Right panel:* G1(M) and G2(M). Error bars: 1σ.

Fig. 8. The residual ^{137}Cs body contents (Bq) for each group. *Left panel:* ATDM simulation. *Right panel:* WBC measurement. The figure is in the same format as Fig. 6. The individuals with no detection in the WBC measurements are treated as zero (in the right panel). The 50th percentile of the distribution is not seen in the G1(T) group or G2(T) group in the WBC measurements due to the large number of subjects without detection. All subjects with detection are displayed as outliers for G1(T) group.

Fig. 9. The ^{137}Cs whole-body retention rate as a function of the number of elapsed days after intake along with the number of WBC measurements on each day.

Fig. 10. Comparison of the daily-integrated values of the ^{137}Cs air concentration between the ATDM simulation and the SPM data at Haramachi (Minamisoma-city) (*left panel*) and Fukushima-city (*right panel*). The SPM data for Fukushima-city are the average and 1σ of four locations in the city.

Appendix A

The locations of individuals and the ^{137}Cs air concentration on the map at every hour on 12, 13, 15, 16, 18, 19, 20 and 21 March (**Fig. A1** to **Fig. A32**). The *concentric circles* on the maps are drawn with the FDNPP at the center. The ^{137}Cs air concentration is provided as hourly-averaged data, and the starting time is denoted at the top of each panel. The symbols in the figure denote the four groups of residents: prompt evacuees moving toward Tsushima: G1(T) (n=231), late evacuees moving toward Tsushima: G2(T) (n=37), prompt evacuees moving toward Minamisoma: G1(M) (n=64), and late evacuees moving toward Minamisoma: G2(M) (n=24).

Appendix B

The daily integrated ^{137}Cs air concentration (Bq m^{-3} hr) at different locations on Route 114 (denoted by 'A') and Route 6 (denoted by 'B').

Table 1. The CEDs (mSv) for the Adults and 15-yr subjects among the G1(T), G2(T), G1(M), and G2(M) groups (reproduced from **Table 5** in Igarashi et al. 2020).

Adults and 15yr groups	G1(T)	G2(T)	G1(M)	G2(M)
No. of subjects	231	37	64	24
CED: max.	4.9×10^{-1}	6.1×10^{-1}	1.2×10^{-1}	7.2×10^{-1}
95th percentile	1.2×10^{-1}	2.9×10^{-1}	1.0×10^{-1}	3.0×10^{-1}
90th percentile	6.4×10^{-2}	1.5×10^{-1}	7.7×10^{-2}	2.8×10^{-1}
75th percentile	n.d.[a]	8.9×10^{-2}	4.4×10^{-2}	1.4×10^{-1}
50th percentile (median)	n.d.	6.2×10^{-2}	n.d.	4.1×10^{-2}

[a] n.d.: not detected in the WBC measurements. CED: committed effective dose.

Table 2. The time chart of countermeasures by Namie-town along with evacuation orders by the Japanese central government.

Date and time, 2011		Events[†]
11 March	14:46[‡]	The disaster countermeasure headquarters was established in Namie-town.
	21:23	The evacuation order to the area within the 3-km radius of F1 and the order to take shelter indoors for the area within 3–10 km of F1.
12 March	5:44	The evacuation order to the area within the 10-km radius of F1.
	6:35[‡]	The emergency broadcast system of Namie-town announced the evacuation order to the area within the 10-km radius of F1 and instructed residents to evacuate to the west part of the town (and to Tsushima's elementary school or Tsushima's junior high school via Route 114 for individuals who could evacuate by themselves).
	7:15[‡]	Same as the above, but Tsushima's rehabilitation center and Tsushima's branch of Namie-town's high school were added to the designated shelters.
	7:45	The evacuation order to the area within the 3-km radius of F2 and the order to take shelter indoors for the area within 3–10 km of F2.
	8:40[‡]	Evacuation to shelters outside the 10-km radius of F1 using buses.
	14:47[‡]	The emergency broadcast system of Namie-town announced that the town office was moving to the Tsushima branch (completed at 16:45).
	17:39	The evacuation order to the area within the 10-km radius of F2.
	18:25	The evacuation order to the area within the 20-km radius of F1.
	18:25[‡]	The order to evacuate individuals who evacuated in the east of Hirusone district (located at the border of the 20-km radius of F1).
15 March	7:30[‡]	The town mayor requested Nihonmatsu-city to accept evacuees (approval).
	10:00[‡]	The evacuation order to areas outside the 20-km radius of F1, and the disaster countermeasure headquarters was transferred to Nihonmatsu-city.
	11:00	The order to take shelter indoors for the area within 20–30 km of F1.
	13:00[‡]	Starting voluntary evacuation by private vehicles and buses.
5 April[‡]		The subsequent mass evacuation was started.

[†] F1: Fukushima Daiichi Nuclear Power Plant, F2: Fukushima Daini Nuclear Power Plant.

[‡] Countermeasures by Namie-town.

Table

Table 3. Comparison of the time-integrated ^{137}Cs air concentration values (Bq m^{-3} hr) from 12 to 22 March between the ATDM simulation and the SPM data.

	Haramachi (Minamisoma-city)	Soma-city	Shinchi-town	Fukushima-city	Nihonmatsu-city
ATDM	7,450	3,900	3,830	80	20
SPM[†]	5,660	3,120	930	520±40[‡]	950[¶]

The last digit of the values is rounded.

[†] The data below detection limits (D.L.) were treated as D.L.

[‡] The average and 1σ of the SPM data at four locations in Fukushima-city.

[¶] No measurements on 12–14 or 17–20 March.

Table B1. The latitude and longitude of the points listed in Tables B2 and B3

Location ID	Latitude	Longitude	Location ID	Latitude	Longitude
S	37.495503	141.001648			
A1	37.495768	140.983629	B1	37.508107	140.997701
A2	37.504654	140.942209	B2	37.524159	140.998829
A3	37.506077	140.910863	B3	37.543834	141.007335
A4	37.515075	140.891326	B4	37.563552	141.002349
A5	37.526104	140.879751	B5	37.579662	141.009811
A6	37.541736	140.86151	B6	37.603416	141.005654
A7	37.553386	140.834195	B7	37.612799	141.004335
A8	37.567287	140.800218	B8	37.636412	140.984145
A9	37.559674	140.761499	B9	37.650519	140.985436
A10	37.565547	140.743662	B10	37.678635	140.981321
A11	37.582256	140.719519	B11	37.702782	140.970943
A12	37.587623	140.690285	B12	37.729433	140.953269
A13	37.601039	140.67481	B13	37.743687	140.954165
A14	37.633008	140.639842	B14	37.760653	140.948646
A15	37.662754	140.595236	B15	37.791024	140.94395
A16	37.667619	140.576224	B16	37.808674	140.943432
A17	37.682376	140.5628	B17	37.838212	140.937562
A18	37.684875	140.548837	B18	37.897808	140.90169
A19	37.691433	140.52427			
A20	37.712967	140.502611			
A21	37.733697	140.47813			
A22	37.756645	140.473572			

Table B2. The daily accumulated ^{137}Cs air concentration (Bq m^{-3} hr) at different locations on Routes 114

Location	12	13	14	15	16	17	18	19	20	21	22	23	24	25	26	27	28	29	30	31
S	2,847	3,378	3,431	3,471	3,471	3,471	25,986	60,144	83,889	83,890	84,139	84,139	84,663	85,775	85,795	85,795	86,361	88,295	99,085	99,400
A1	2,324	2,814	2,814	5,036	5,048	5,048	24,830	33,571	46,242	46,244	46,382	46,382	46,486	46,773	46,778	46,778	46,997	49,644	55,819	55,921
A2	1,818	1,994	1,994	35,403	35,571	35,571	46,764	46,776	47,947	47,950	47,986	47,986	47,993	48,099	48,104	48,104	48,401	49,834	51,660	51,664
A3	136	138	138	35,546	35,680	35,680	42,318	42,318	42,999	43,005	43,036	43,036	43,037	43,094	43,094	43,094	43,130	43,191	43,234	43,234
A4	124	135	135	11,975	12,174	12,174	20,438	20,438	20,944	20,948	20,971	20,971	20,973	21,032	21,032	21,032	21,186	21,453	21,490	21,490
A5	2	2	2	15,095	15,656	15,656	23,841	23,841	24,292	24,301	24,320	24,320	24,321	24,364	24,364	24,364	24,378	24,394	24,412	24,412
A6	10	10	10	7,570	8,104	8,104	21,908	21,908	22,284	22,292	22,309	22,309	22,310	22,355	22,355	22,355	22,367	22,386	22,402	22,402
A7	0	0	0	4,817	5,463	5,463	13,409	13,409	13,782	13,790	13,805	13,805	13,805	13,842	13,842	13,842	13,842	13,843	13,846	13,846
A8	1	1	1	2,352	2,726	2,726	5,579	5,579	5,899	5,901	5,913	5,913	5,913	5,945	5,945	5,945	5,945	5,945	5,945	5,945
A9	0	0	0	1,673	1,832	1,832	2,660	2,660	2,774	2,775	2,785	2,785	2,785	2,802	2,802	2,802	2,802	2,802	2,802	2,802
A10	0	0	0	1,250	1,359	1,359	1,525	1,525	1,537	1,538	1,544	1,544	1,544	1,557	1,557	1,557	1,557	1,557	1,557	1,557
A11	0	0	0	884	1,232	1,232	1,418	1,418	1,462	1,464	1,473	1,473	1,473	1,484	1,484	1,484	1,484	1,484	1,484	1,484
A12	0	0	0	667	705	705	718	718	723	725	730	730	730	736	736	736	736	736	736	736
A13	0	0	0	443	446	446	446	446	453	457	463	463	463	464	464	464	464	464	464	464
A14	0	0	0	339	340	340	340	340	365	374	380	380	380	381	381	381	381	381	381	381
A15	0	0	0	187	191	191	191	191	225	238	244	244	244	245	245	245	245	245	245	245
A16	0	0	0	63	64	64	64	64	89	103	107	107	107	108	108	108	108	108	108	108
A17	0	0	0	61	64	64	64	64	94	103	108	108	108	109	109	109	109	109	109	109
A18	0	0	0	61	64	64	64	64	94	103	108	108	108	109	109	109	109	109	109	109
A19	0	0	0	12	14	14	14	14	45	55	59	59	59	60	60	60	60	60	60	60
A20	0	0	0	6	8	8	8	8	49	61	65	65	65	66	66	66	66	66	66	66
A21	0	0	0	6	8	8	8	8	49	61	65	65	65	66	66	66	66	66	66	66
A22	0	0	0	5	8	8	8	8	59	72	77	77	77	78	78	78	78	78	78	78

The values are integrated for the period until the end of March 2011. The ^{137}Cs air concentration data were obtained from those at the nearest grid to each location in the calculation domain by WSPEEDI-II.

Table B3. The daily accumulated ^{137}Cs air concentration (Bq m^{-3} hr) at different locations on Route 6

Location	12	13	14	15	16	17	18	19	20	21	22	23	24	25	26	27	28	29	30	31
B1	2,847	3,378	3,431	3,471	3,471	3,471	25,986	60,144	83,889	83,890	84,139	84,139	84,663	85,775	85,795	85,795	86,361	88,295	99,085	99,400
B2	3,582	4,177	4,192	4,195	4,195	4,195	8,687	29,966	40,760	40,761	40,895	40,895	41,157	41,797	41,797	41,797	42,187	42,732	50,670	50,841
B3	3,262	3,961	3,966	3,967	3,967	3,967	6,119	20,289	28,908	28,909	28,981	28,981	29,133	29,542	29,542	29,542	29,784	30,207	35,667	35,707
B4	3,262	3,961	3,966	3,967	3,967	3,967	6,119	20,289	28,908	28,909	28,981	28,981	29,133	29,542	29,542	29,542	29,784	30,207	35,667	35,707
B5	1,947	2,691	2,700	2,700	2,700	2,700	4,818	16,032	26,054	26,055	26,105	26,105	26,205	26,468	26,468	26,468	26,661	27,088	30,675	30,678
B6	1,286	2,041	2,066	2,066	2,066	2,066	4,036	14,570	21,366	21,367	21,406	21,406	21,472	21,630	21,630	21,630	21,791	22,118	25,168	25,169
B7	1,286	2,041	2,066	2,066	2,066	2,066	4,036	14,570	21,366	21,367	21,406	21,406	21,472	21,630	21,630	21,630	21,791	22,118	25,168	25,169
B8	558	1,220	1,232	1,232	1,232	1,232	3,568	8,046	11,150	11,151	11,220	11,220	11,253	11,431	11,431	11,431	11,487	11,715	12,839	12,839
B9	684	1,319	1,353	1,353	1,353	1,353	3,403	7,426	10,194	10,194	10,246	10,246	10,272	10,423	10,423	10,423	10,459	10,702	11,785	11,785
B10	886	1,491	1,550	1,550	1,550	1,550	3,207	8,149	10,269	10,269	10,309	10,309	10,331	10,437	10,437	10,437	10,458	10,689	11,958	11,958
B11	886	1,491	1,550	1,550	1,550	1,550	3,207	8,149	10,269	10,269	10,309	10,309	10,331	10,437	10,437	10,437	10,458	10,689	11,958	11,958
B12	757	1,339	1,361	1,363	1,364	1,364	2,569	5,037	6,584	6,584	6,633	6,633	6,646	6,757	6,757	6,757	6,757	6,959	7,790	7,790
B13	668	1,165	1,213	1,215	1,215	1,215	2,138	4,938	6,244	6,244	6,284	6,284	6,296	6,389	6,389	6,389	6,389	6,532	7,470	7,470
B14	650	1,095	1,170	1,171	1,171	1,171	1,882	4,330	5,338	5,339	5,372	5,373	5,384	5,456	5,456	5,456	5,456	5,571	6,555	6,559
B15	618	1,045	1,131	1,132	1,132	1,132	1,749	4,329	5,194	5,195	5,225	5,226	5,239	5,286	5,286	5,286	5,287	5,398	6,357	6,373
B16	618	1,045	1,131	1,132	1,132	1,132	1,749	4,329	5,194	5,195	5,225	5,226	5,239	5,286	5,286	5,286	5,287	5,398	6,357	6,373
B17	576	1,011	1,107	1,107	1,107	1,107	1,618	4,781	5,590	5,591	5,616	5,618	5,629	5,659	5,659	5,659	5,661	5,760	6,639	6,660
B18	386	623	630	631	631	631	715	3,265	3,682	3,682	3,701	3,703	3,713	3,728	3,728	3,728	3,729	3,755	4,432	4,476

The values are integrated for the period until the end of March 2011. The ^{137}Cs air concentration data were obtained from those at the nearest grid to each location in the calculation domain by WSPEEDI-II.
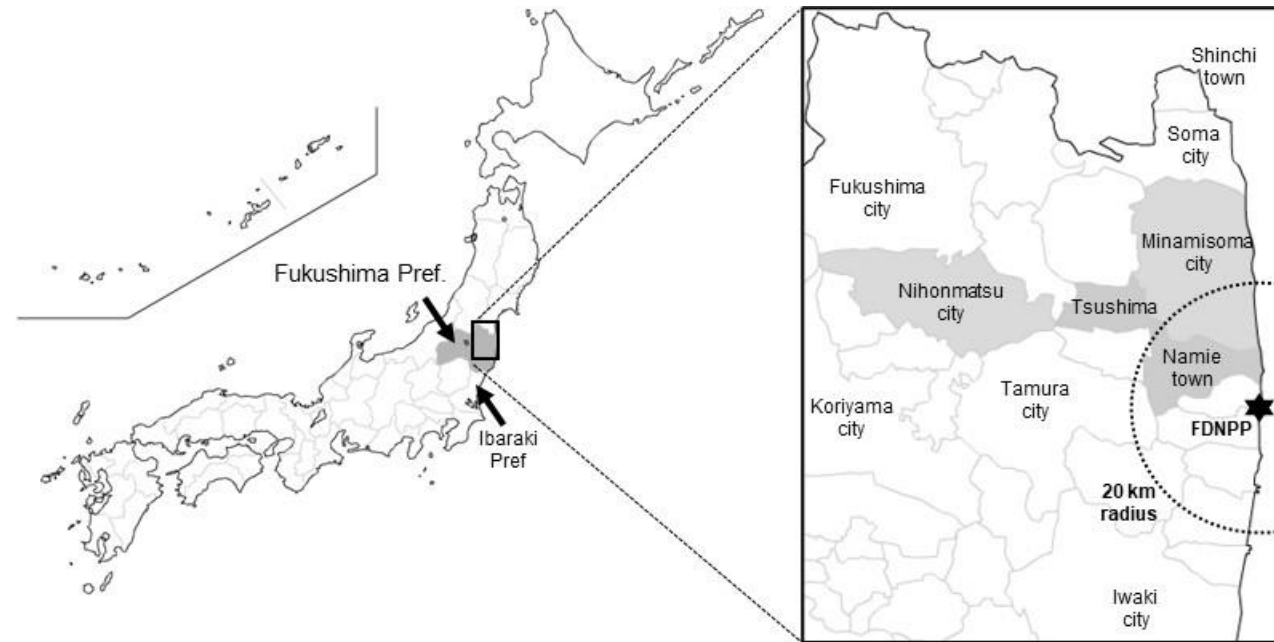
Figure1
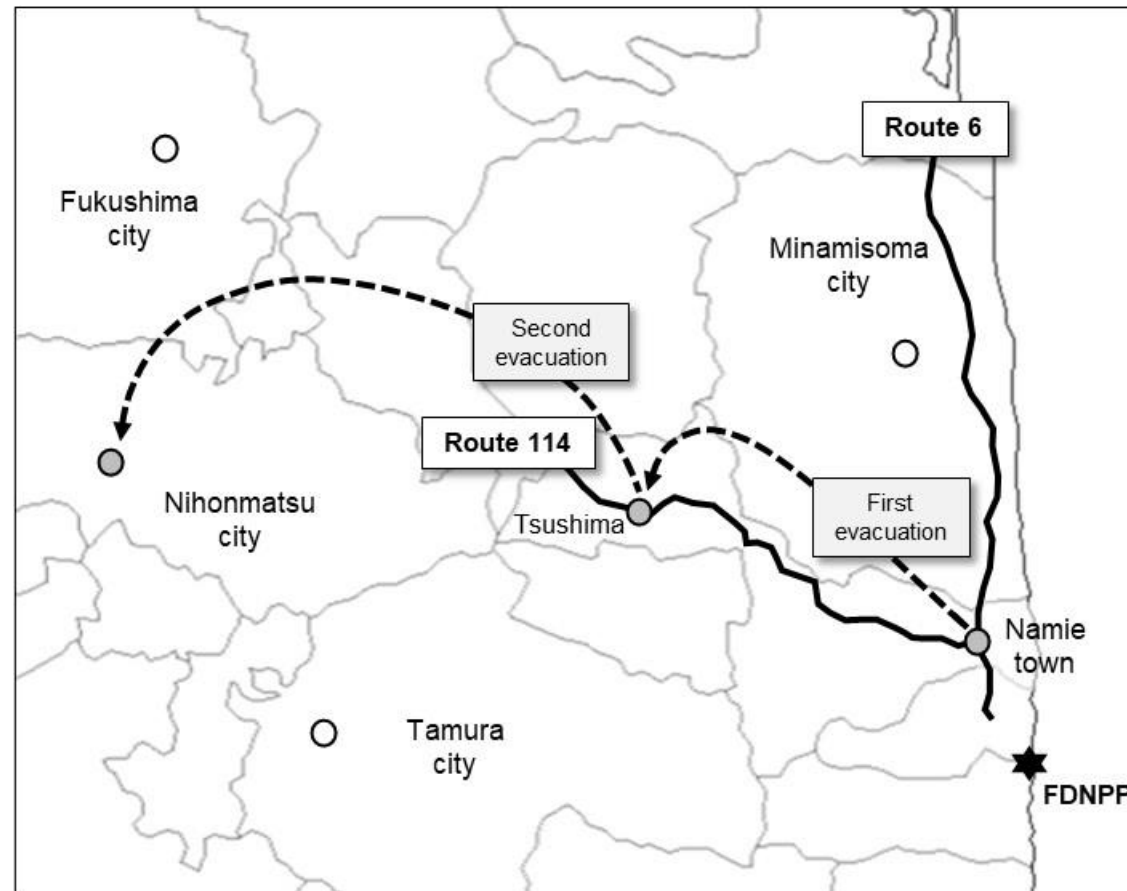
Fig. 1

Figure2

Fig. 2
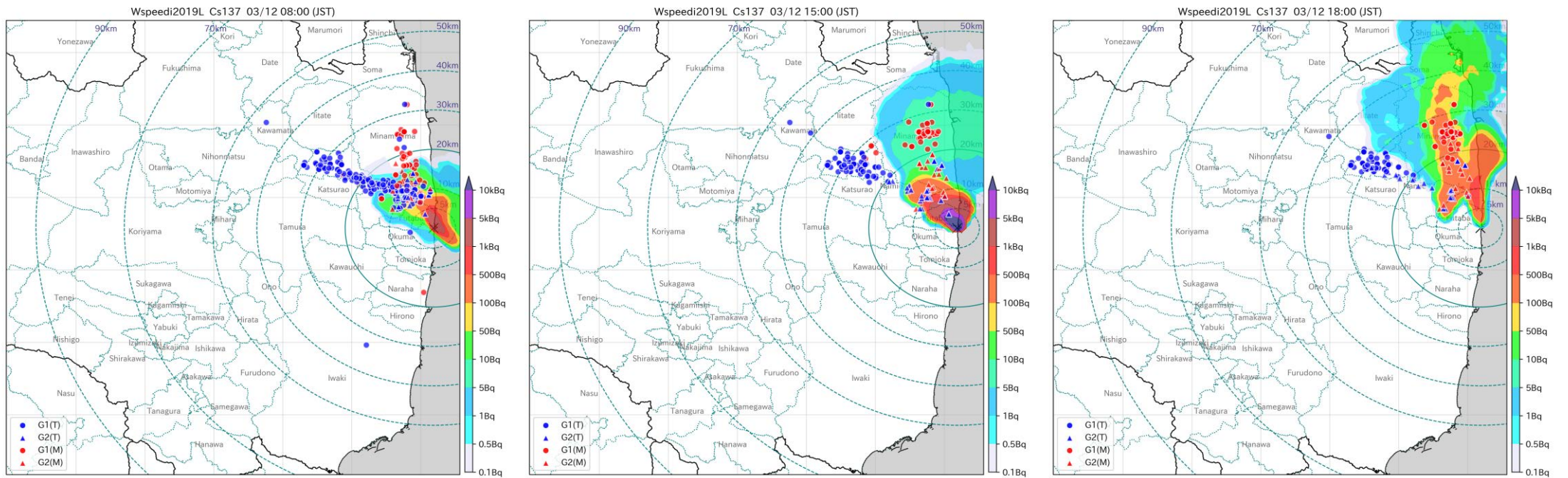
Figure3

Fig. 3

Figure4
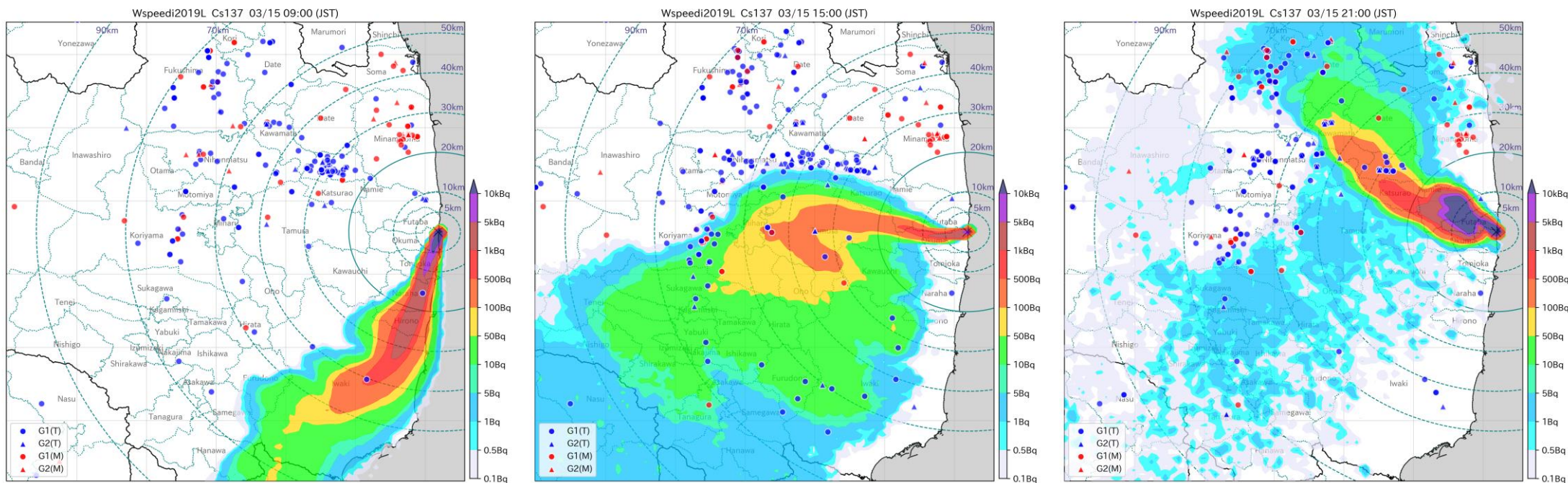
Fig. 4
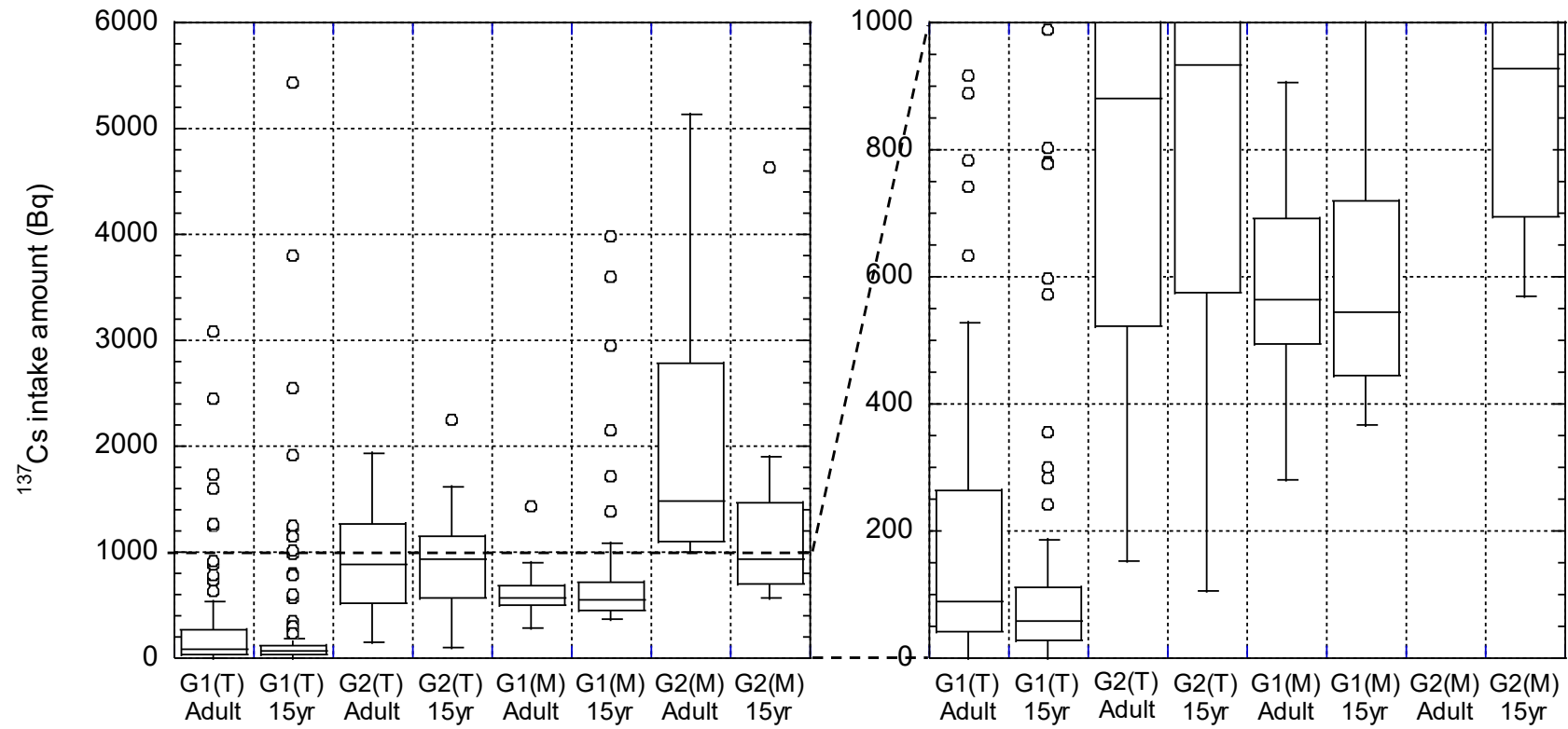
Figure5
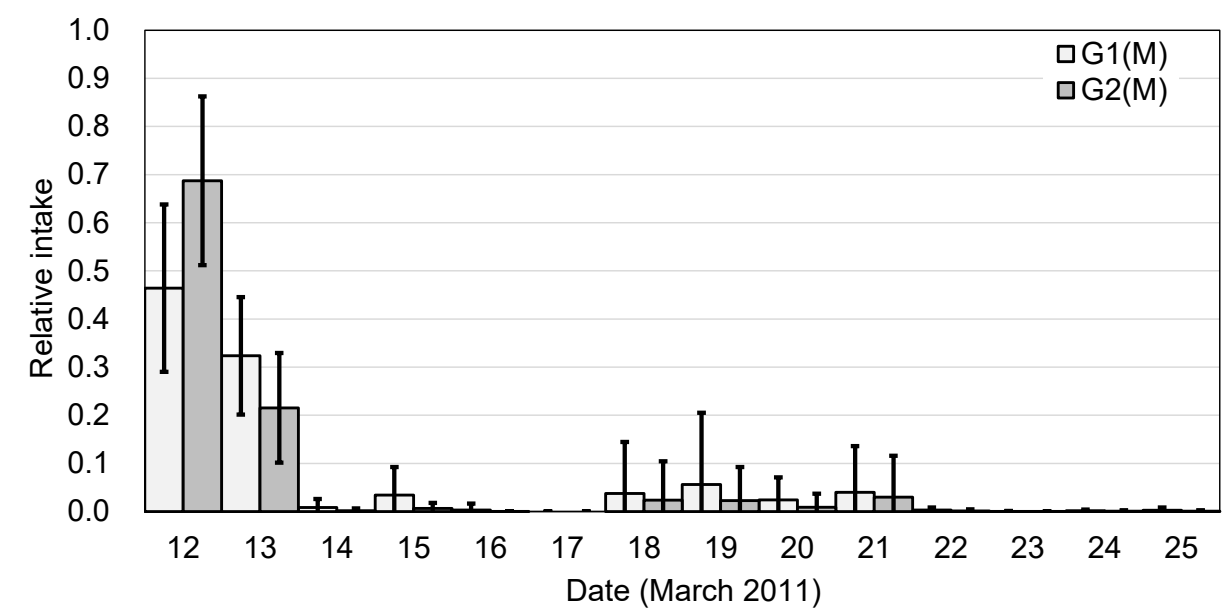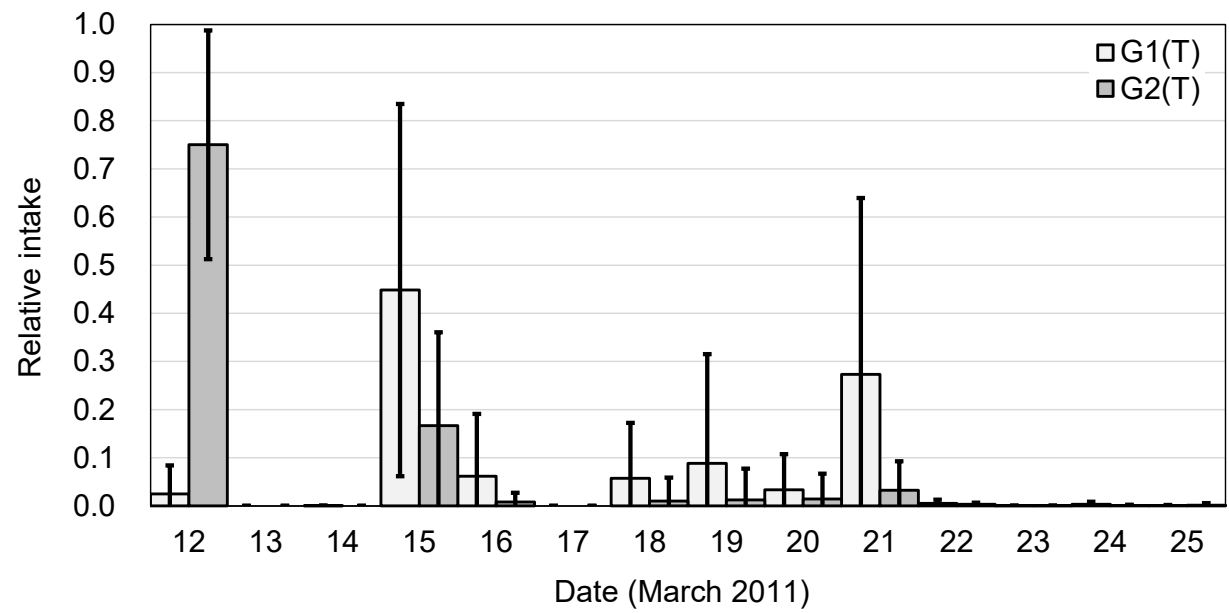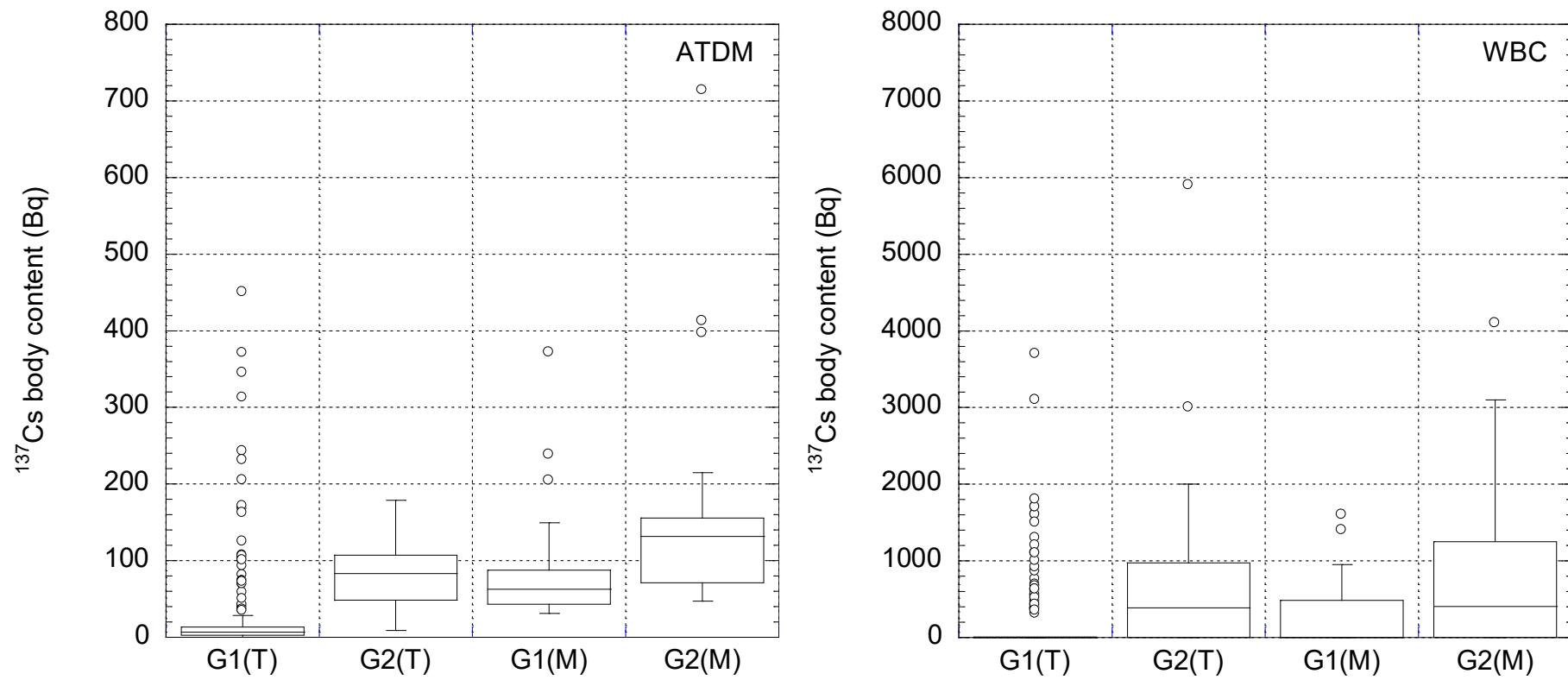
Fig. 5

Figure6

Fig. 6

Figure7

Fig. 7

Figure8
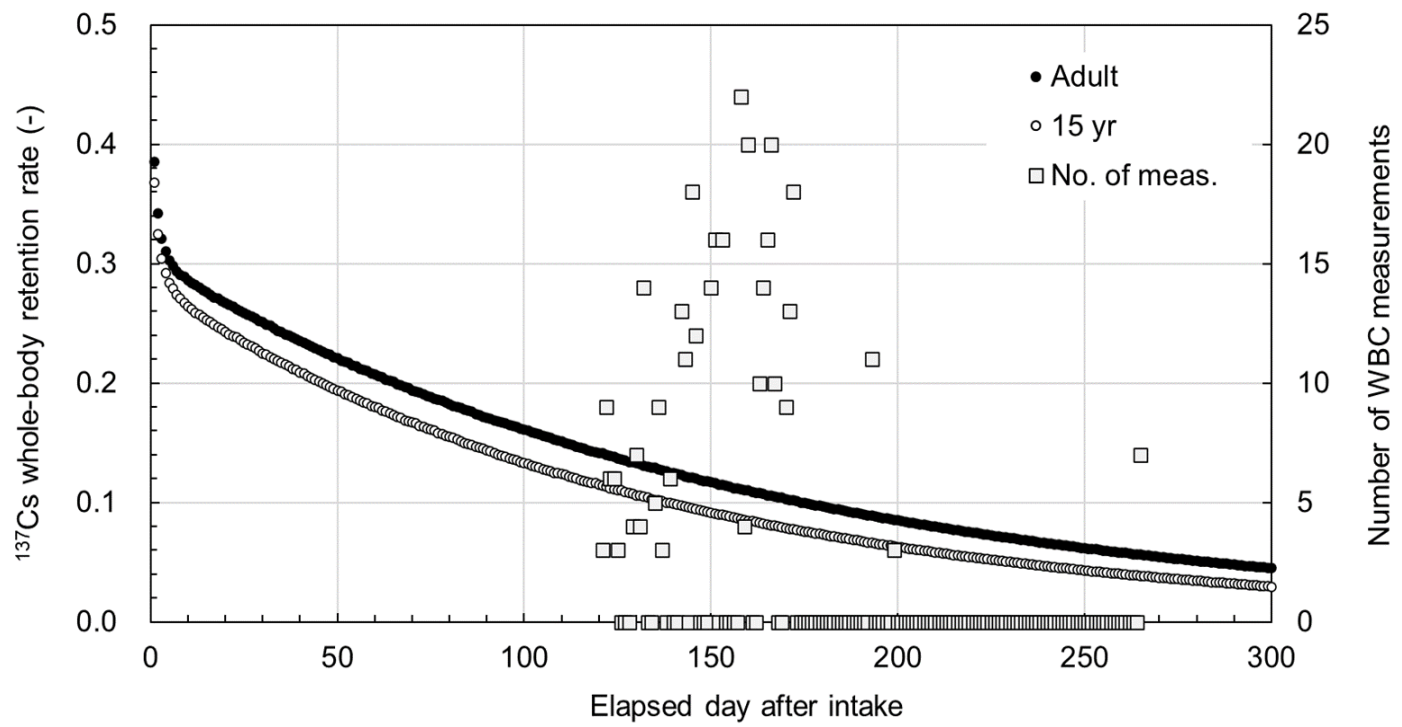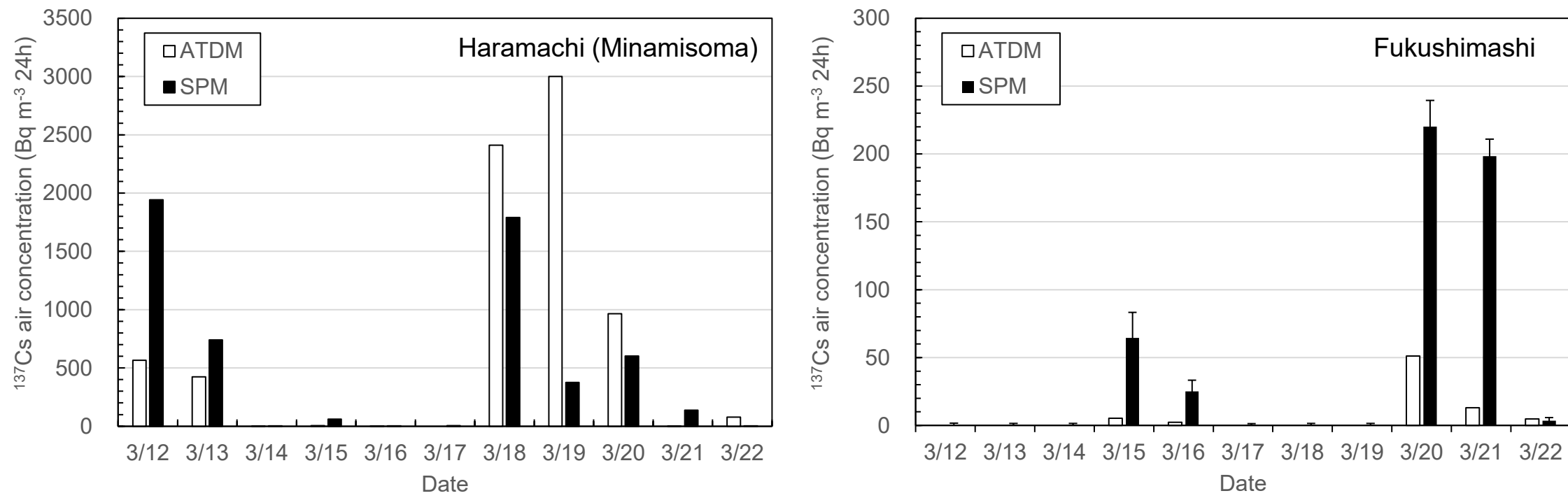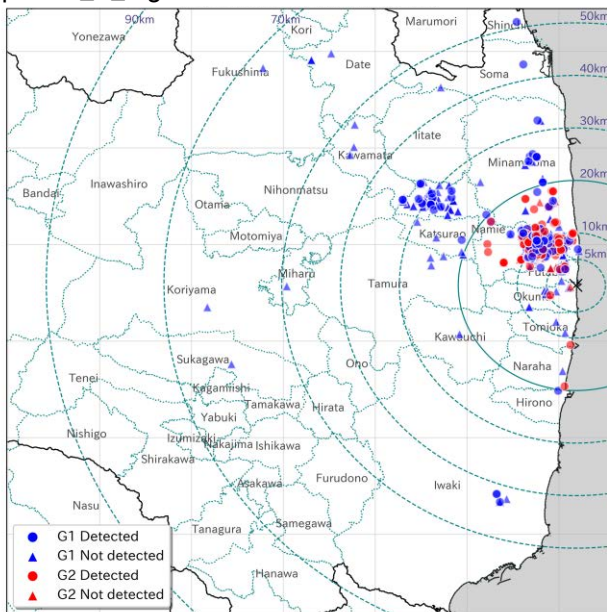
Fig. 8

Figure9

Fig. 9

Figure10

Fig. 10
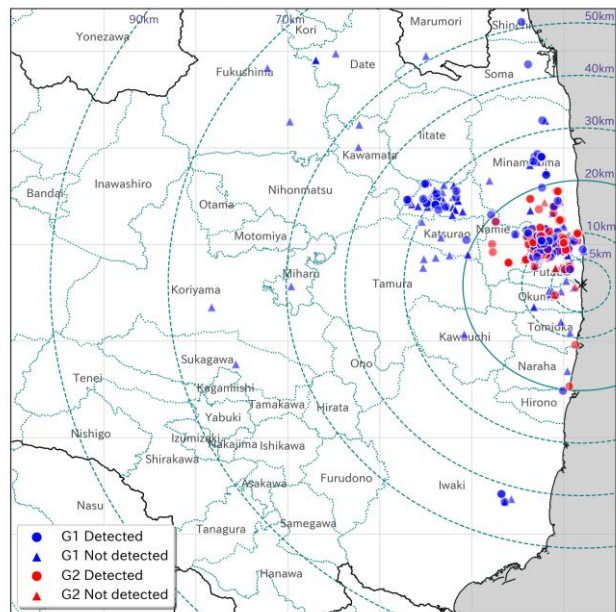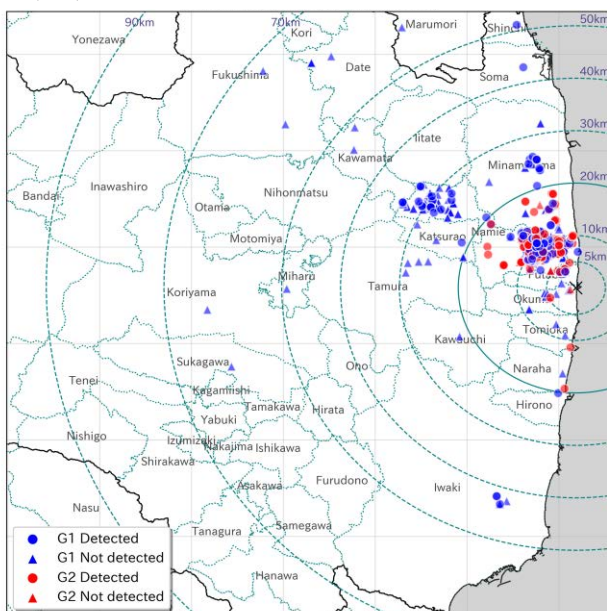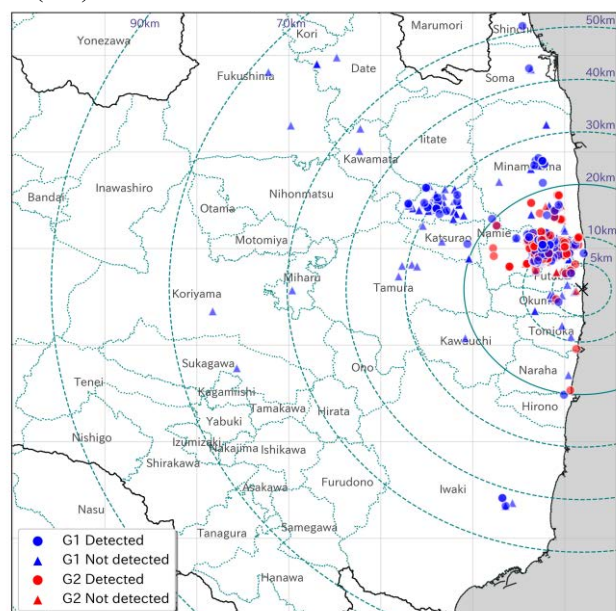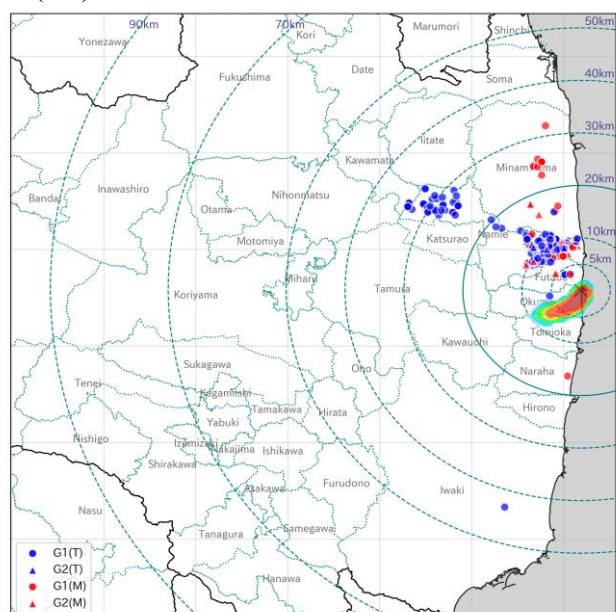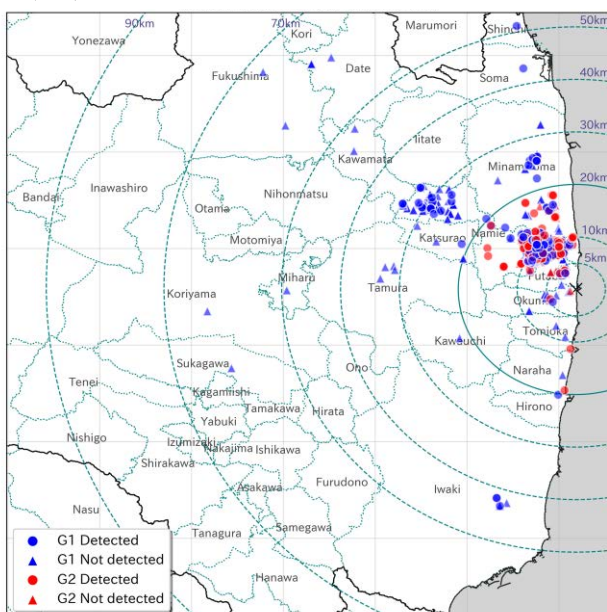
Fig. A1. The locations of individuals on the maps with the ^{137}Cs air concentration at the ground level at 12:00 a.m. on 12 March (1/6), 1:00 a.m. on 12 March (2/6), 2:00 a.m. on 12 March (3/6), 3:00 a.m. on 12 March (4/6), 4:00 a.m. on 12 March (5/6), and 5:00 a.m. on 12 March (6/6).
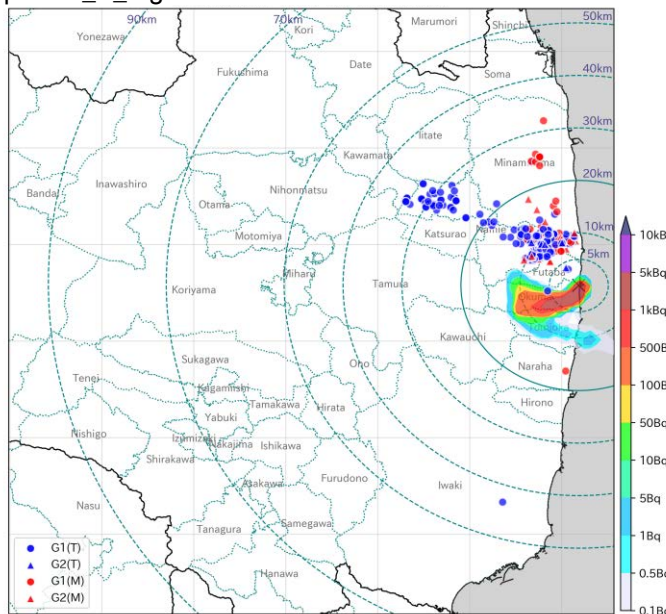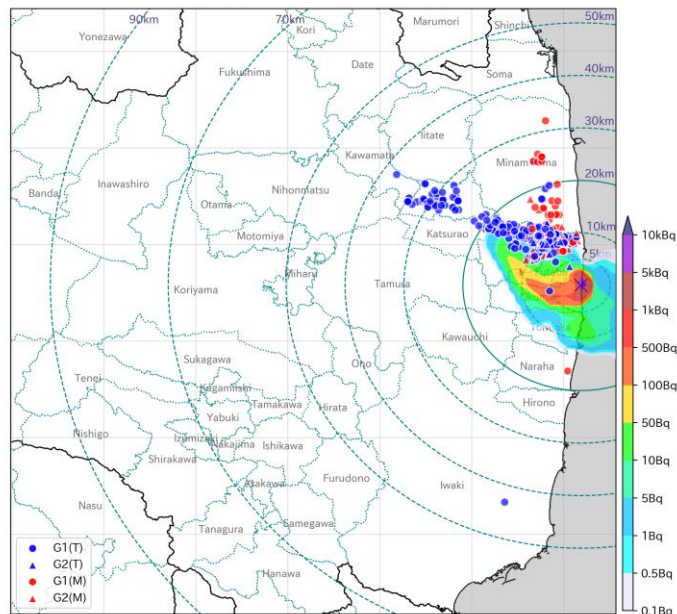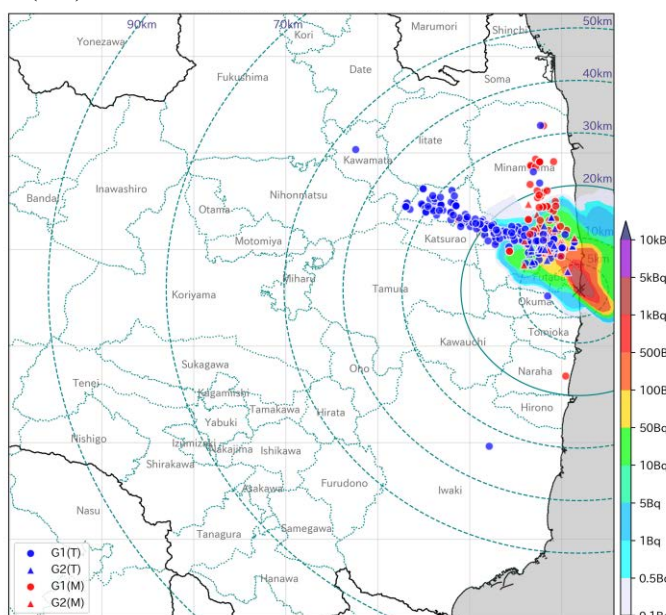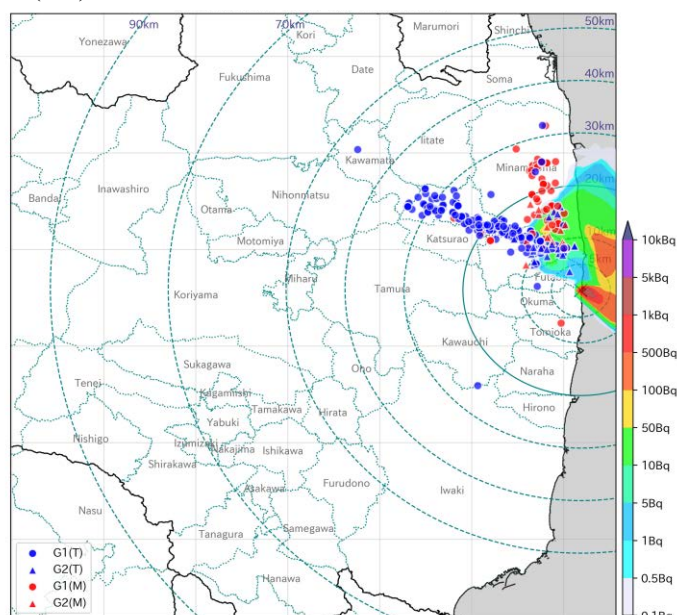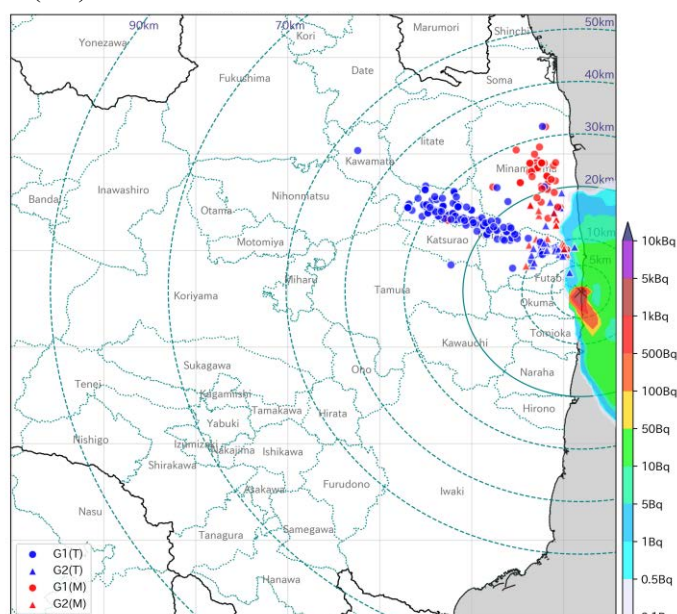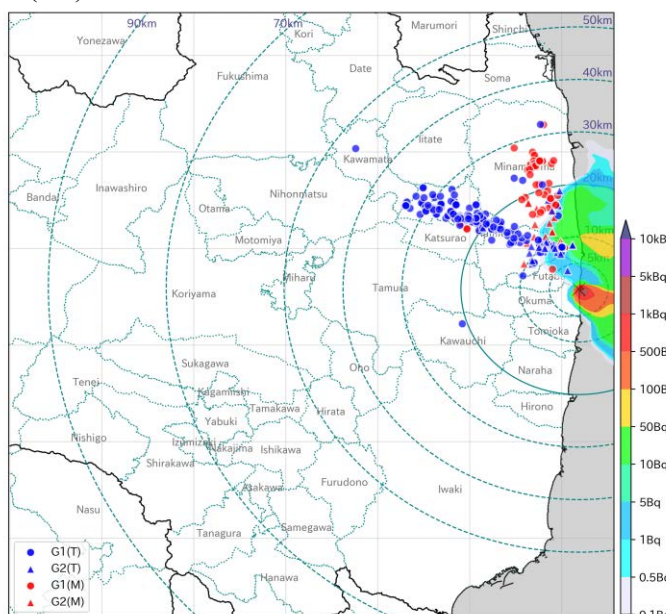
Fig. A2. The locations of individuals on the maps with the ^{137}Cs air concentration at the ground level at 6:00 a.m. on 12 March (1/6), 7:00 a.m. on 12 March (2/6), 8:00 a.m. on 12 March (3/6), 9:00 a.m. on 12 March (4/6), 10:00 a.m. on 12 March (5/6), and 11:00 a.m. on 12 March (6/6).
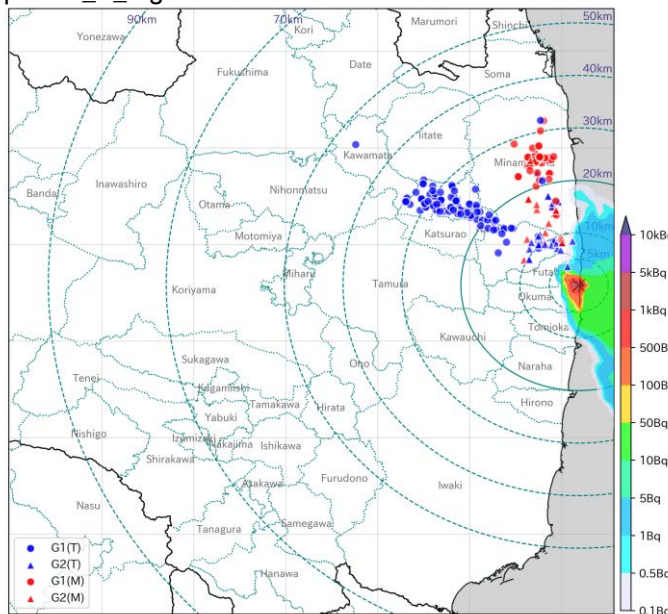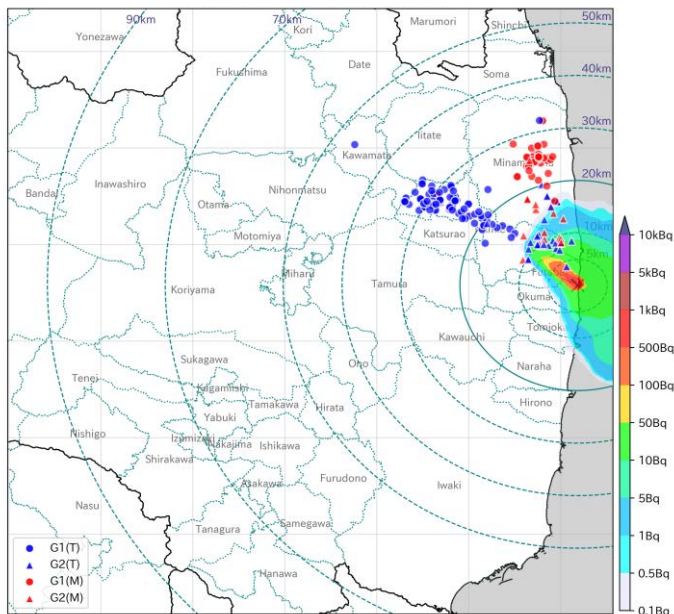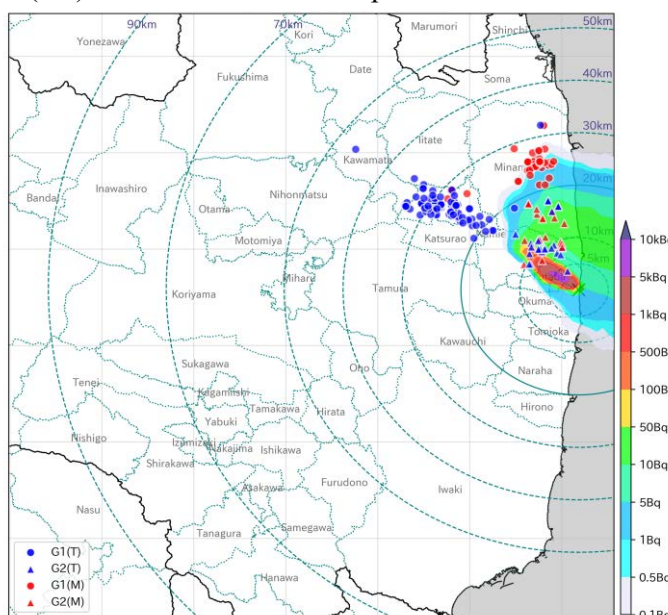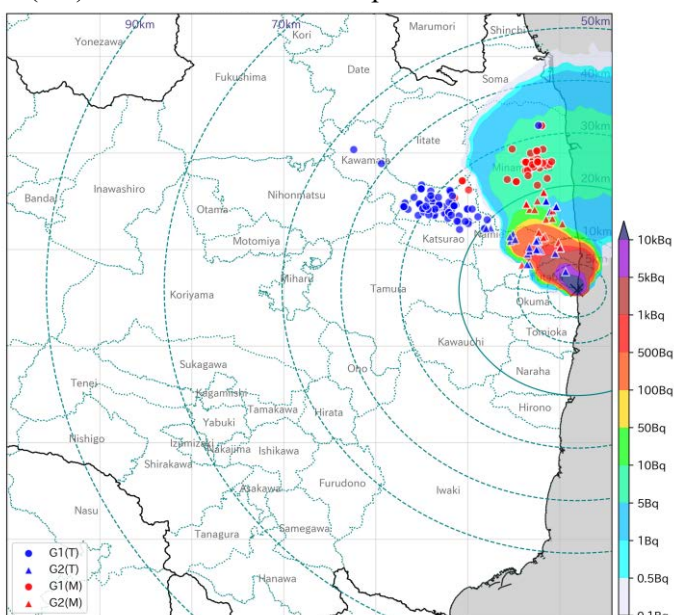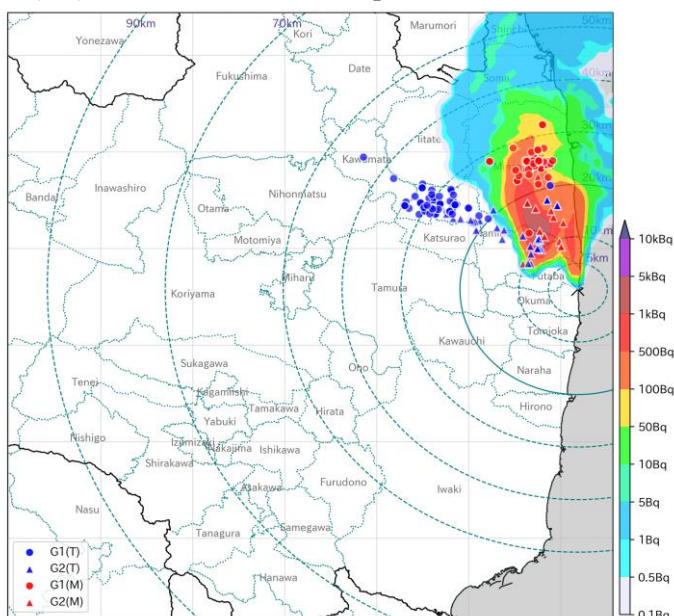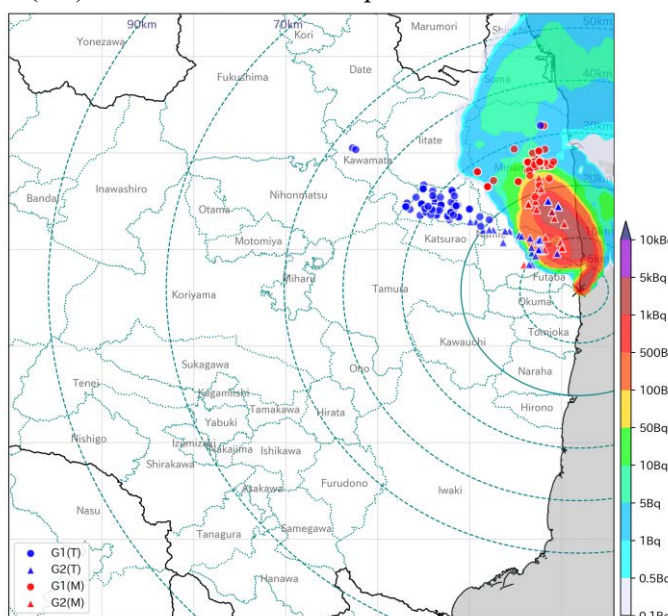
Fig. A3. The locations of individuals on the maps with the ^{137}Cs air concentration at the ground level at 12:00 p.m. on 12 March (1/6), 1:00 p.m. on 12 March (2/6), 2:00 p.m. on 12 March (3/6), 3:00 p.m. on 12 March (4/6), 4:00 p.m. on 12 March (5/6), and 5:00 p.m. on 12 March (6/6).
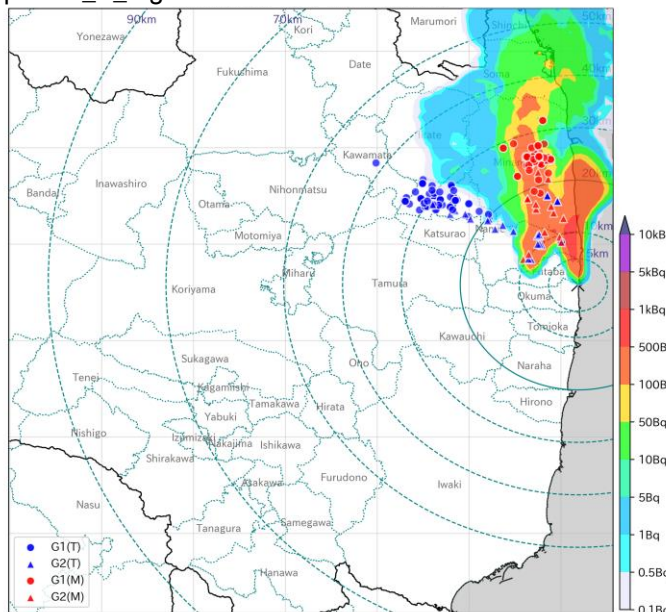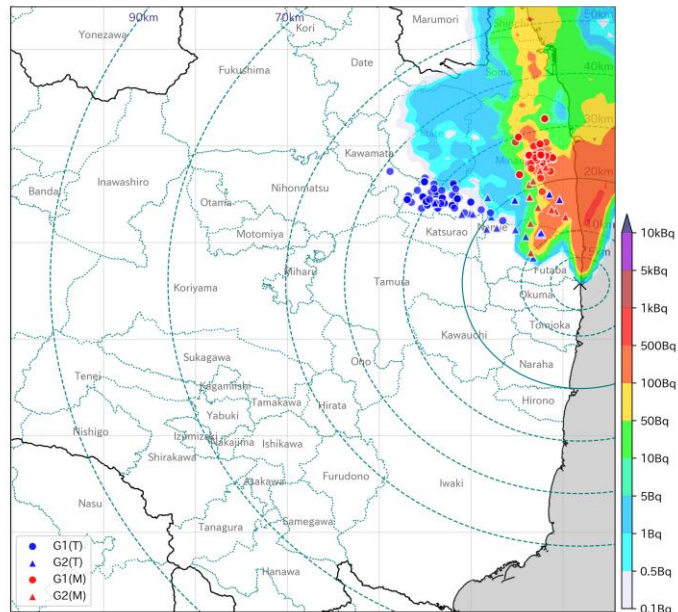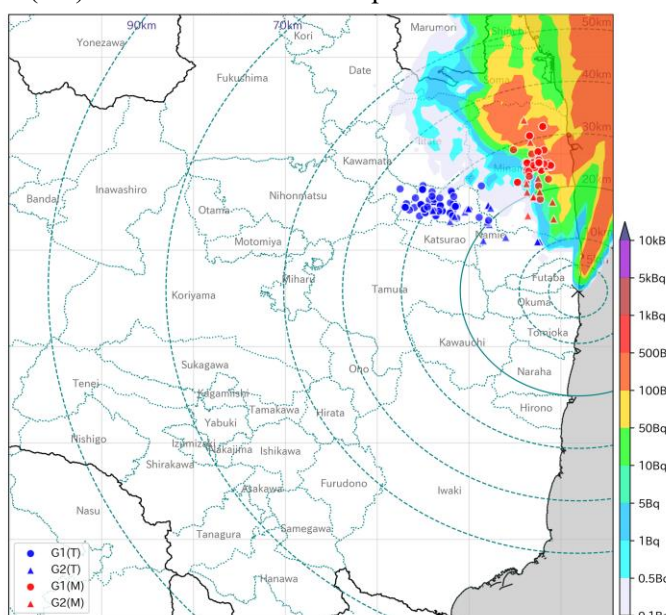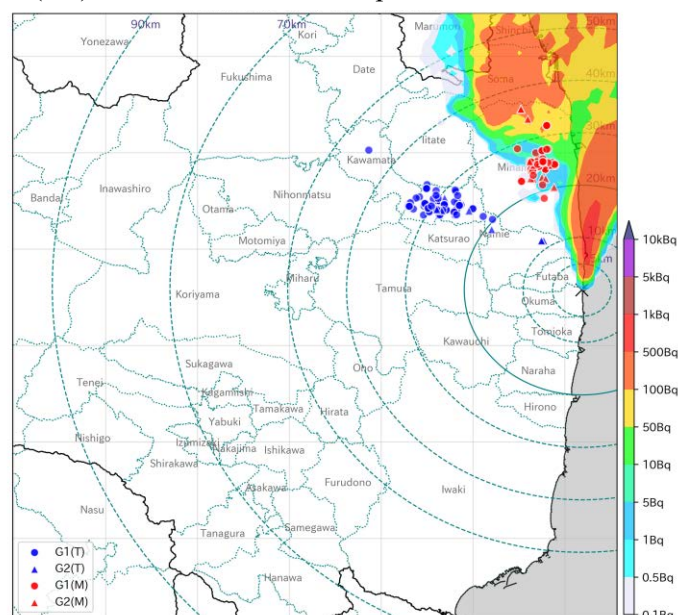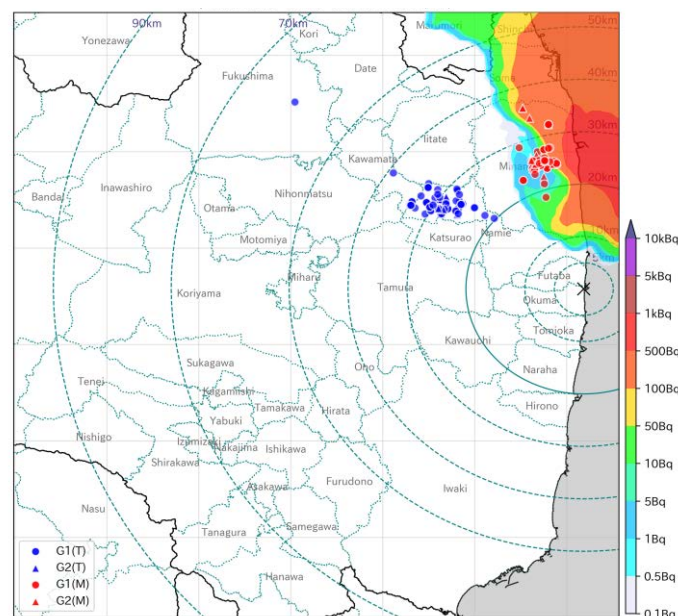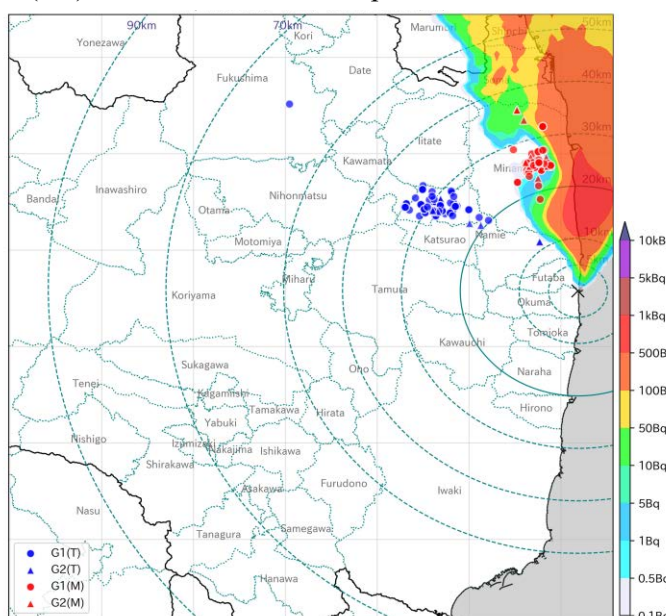
Fig. A4. The locations of individuals on the maps with the ^{137}Cs air concentration at the ground level at 6:00 p.m. on 12 March (1/6), 7:00 p.m. on 12 March (2/6), 8:00 p.m. on 12 March (3/6), 9:00 p.m. on 12 March (4/6), 10:00 p.m. on 12 March (5/6), and 11:00 p.m. on 12 March (6/6).
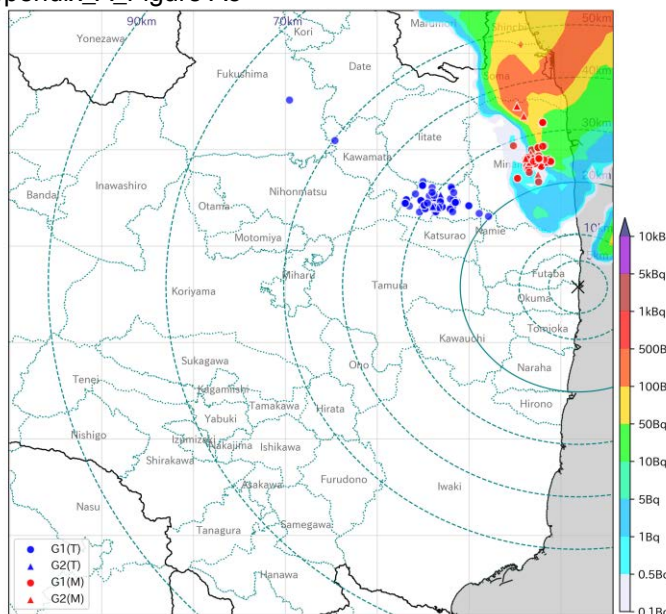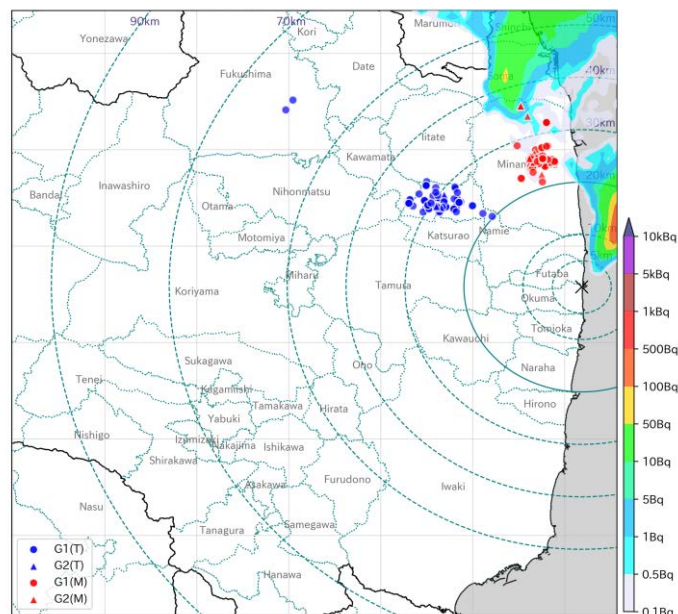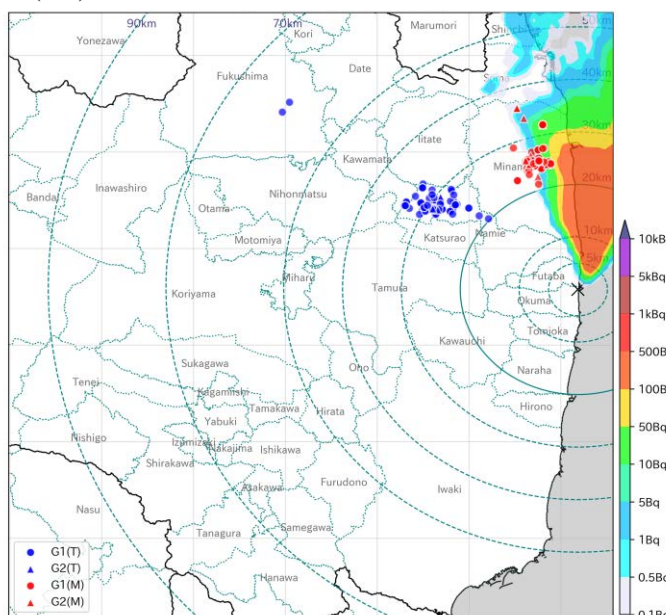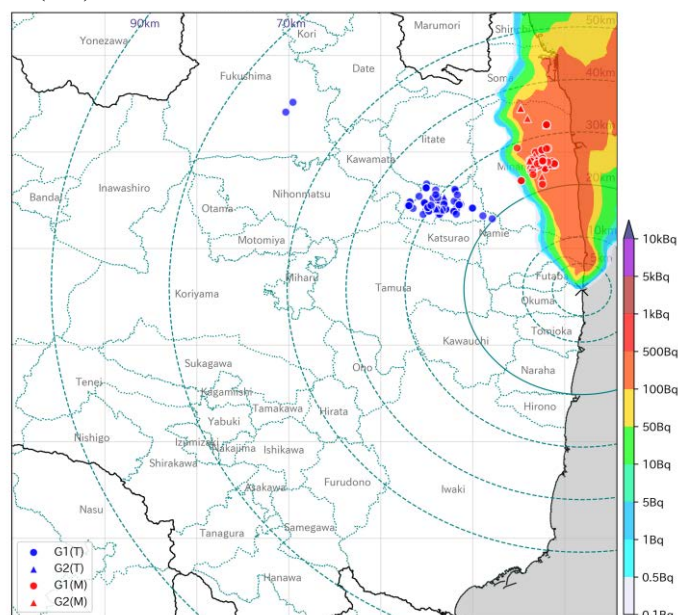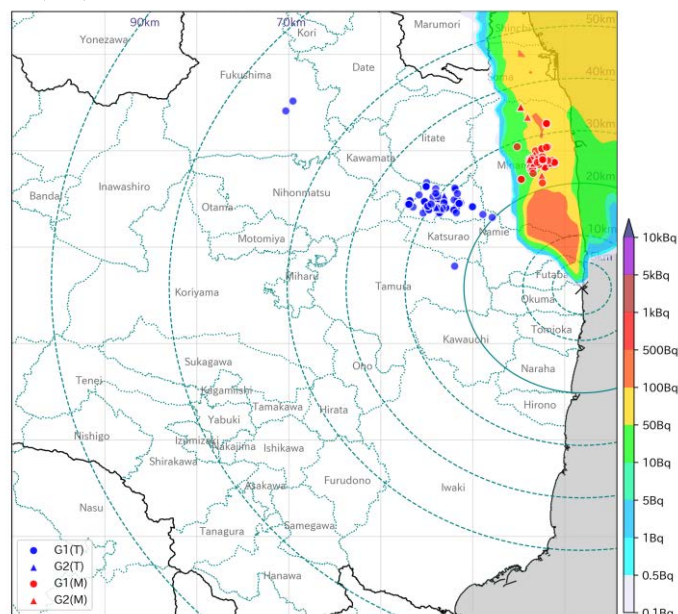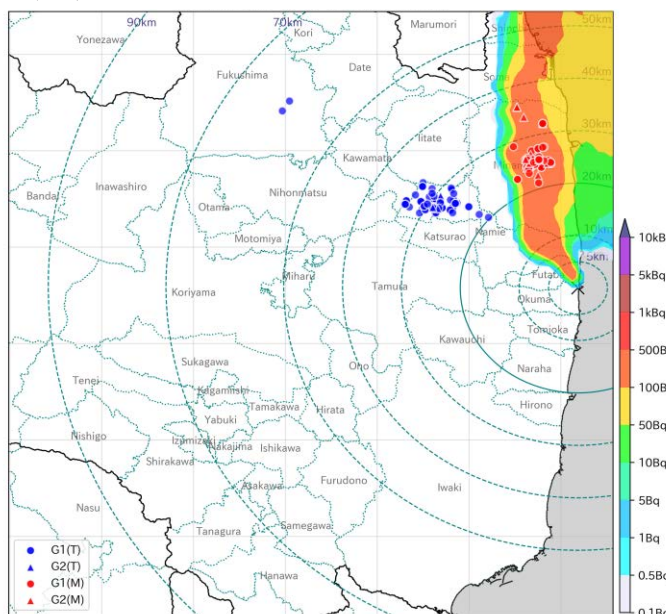
Fig. A5. The locations of individuals on the maps with the ¹³⁷Cs air concentration at the ground level at 12:00 a.m. on 13 March (1/6), 1:00 a.m. on 13 March (2/6), 2:00 a.m. on 13 March (3/6), 3:00 a.m. on 13 March (4/6), 4:00 a.m. on 13 March (5/6), and 5:00 a.m. on 13 March (6/6).
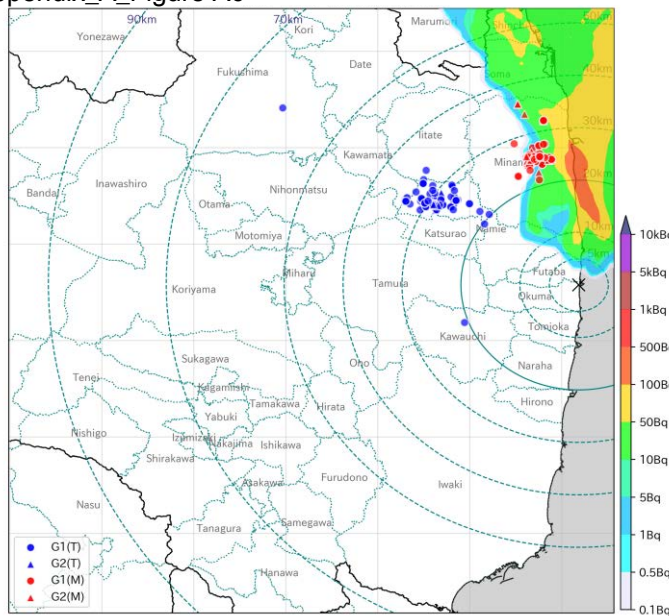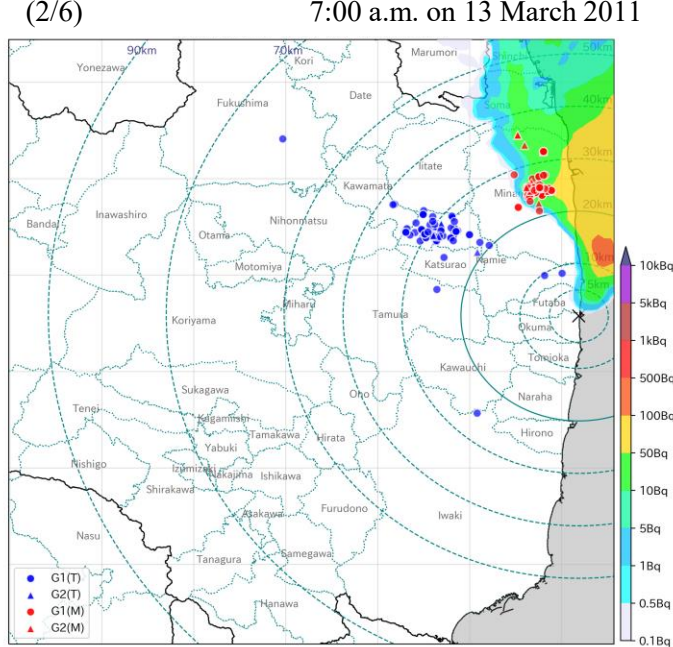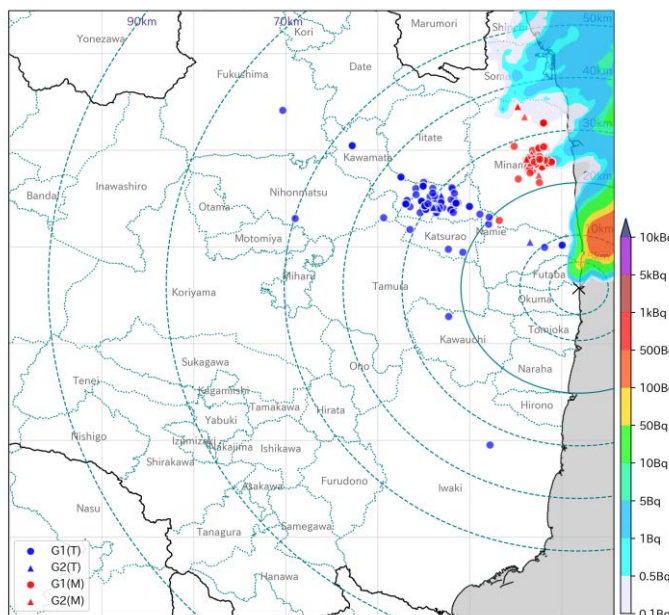
Fig. A6. The locations of individuals on the maps with the ^{137}Cs air concentration at the ground level at 6:00 a.m. on 13 March (1/6), 7:00 a.m. on 13 March (2/6), 8:00 a.m. on 13 March (3/6), 9:00 a.m. on 13 March (4/6), 10:00 a.m. on 13 March (5/6), and 11:00 a.m. on 13 March (6/6).
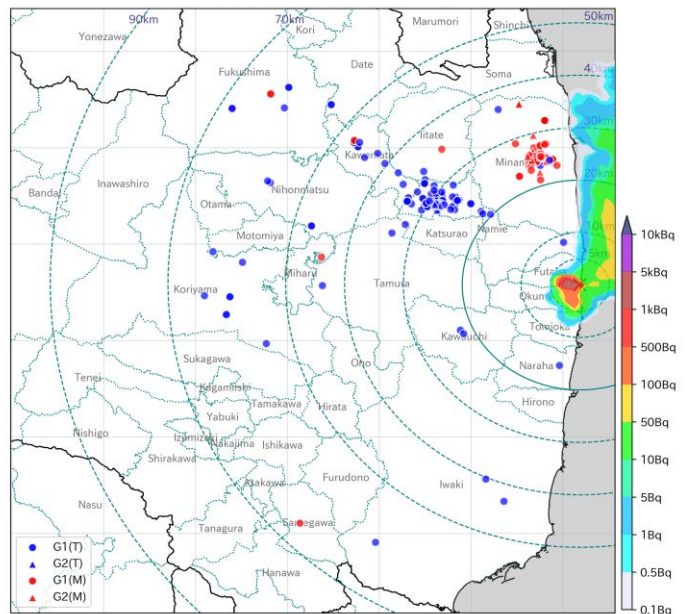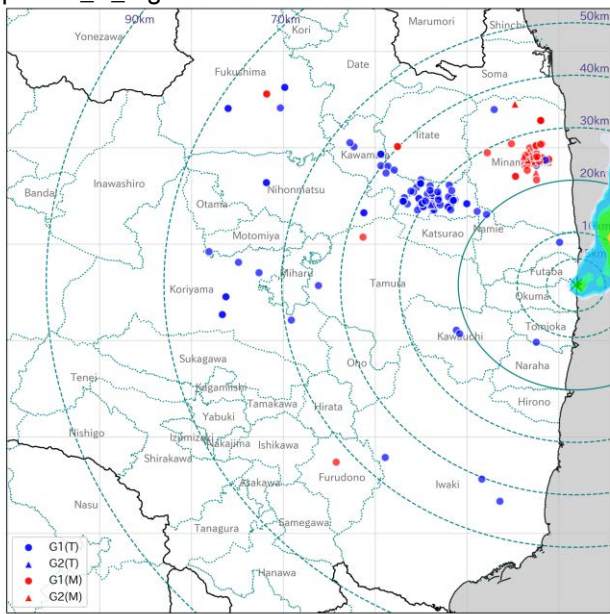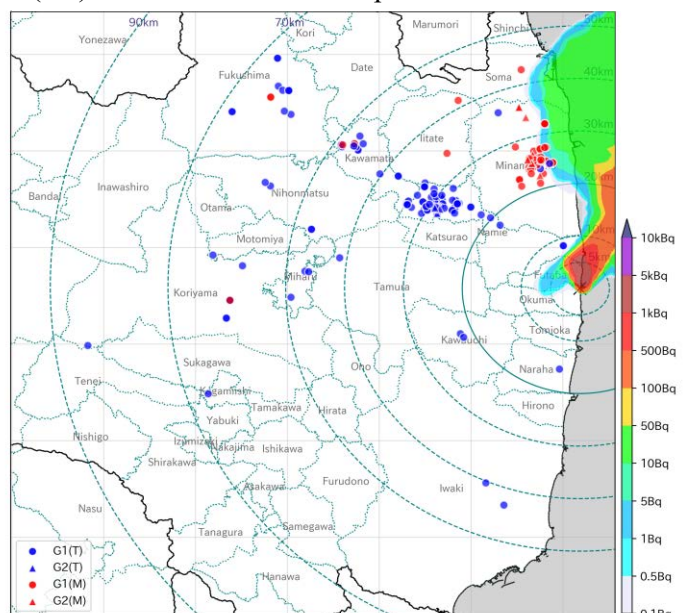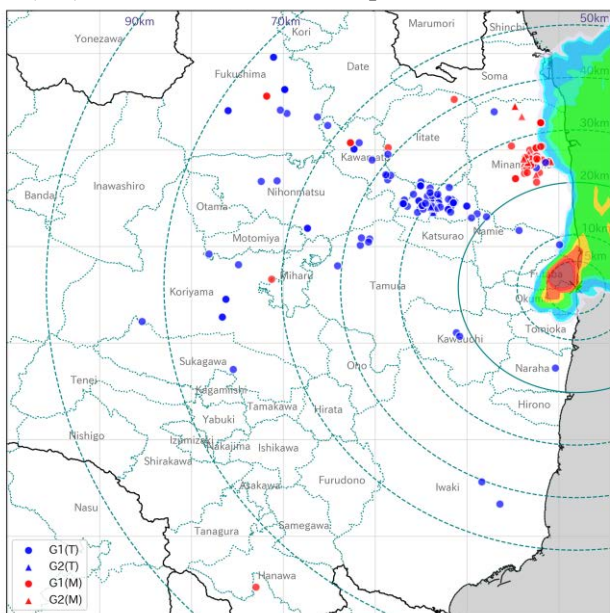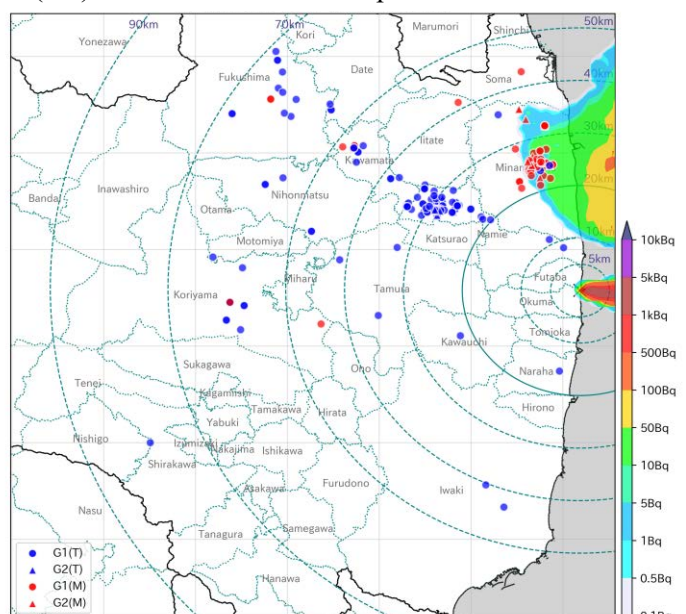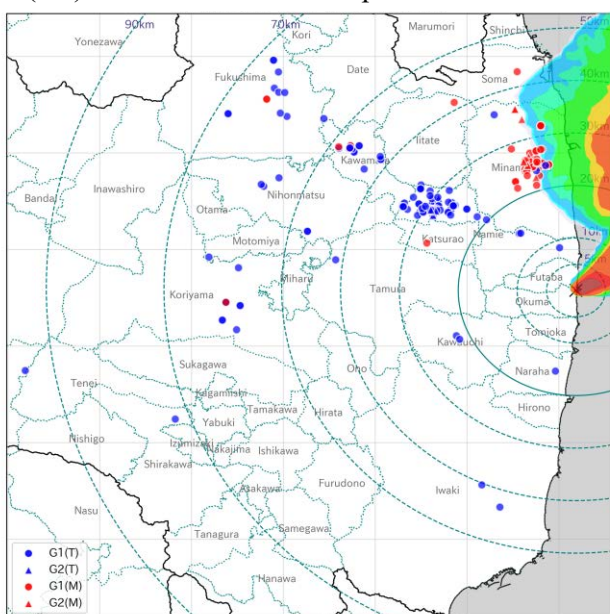
Fig. A7. The locations of individuals on the maps with the ^{137}Cs air concentration at the ground level at 12:00 p.m. on 13 March (1/6), 1:00 p.m. on 13 March (2/6), 2:00 p.m. on 13 March (3/6), 3:00 p.m. on 13 March (4/6), 4:00 p.m. on 13 March (5/6), and 5:00 p.m. on 13 March (6/6).
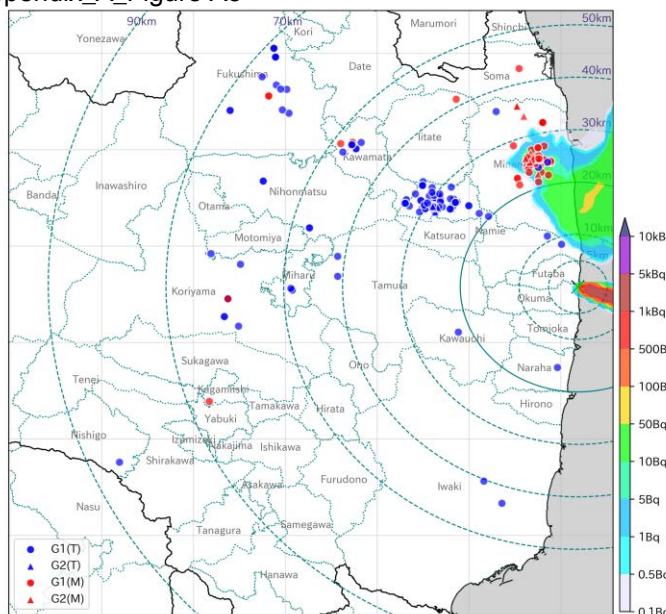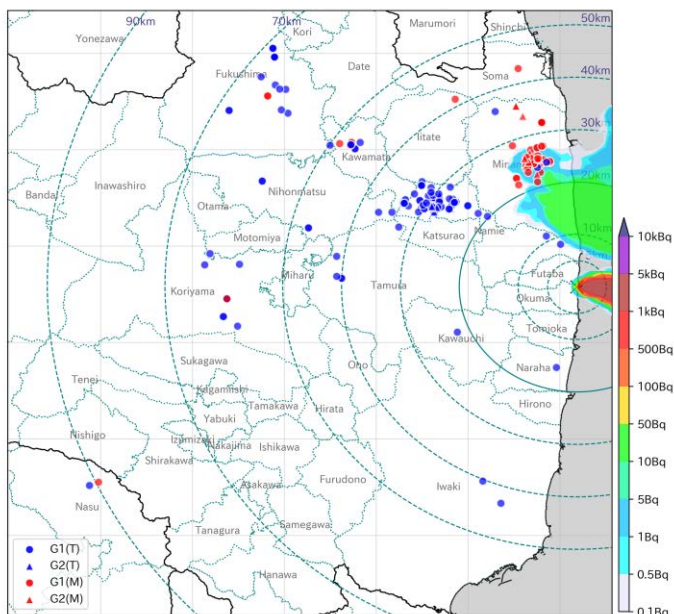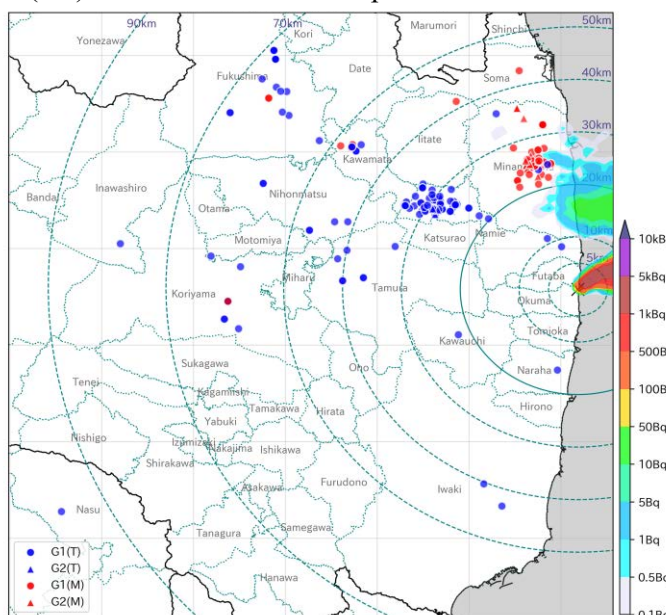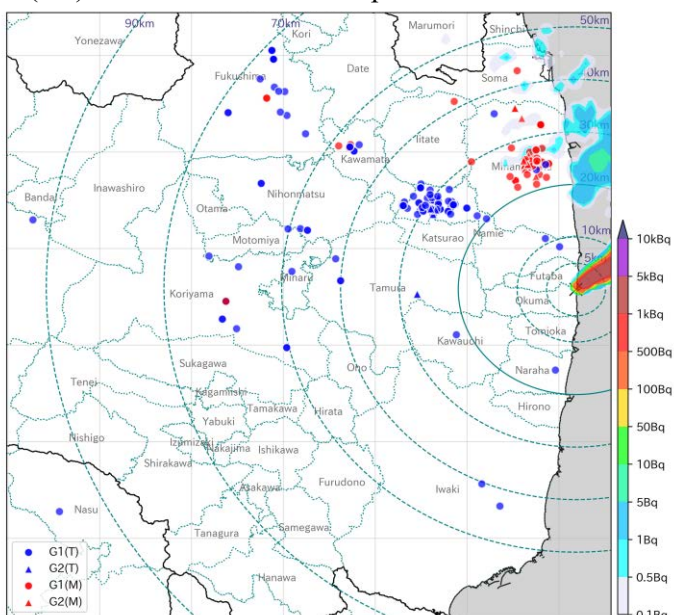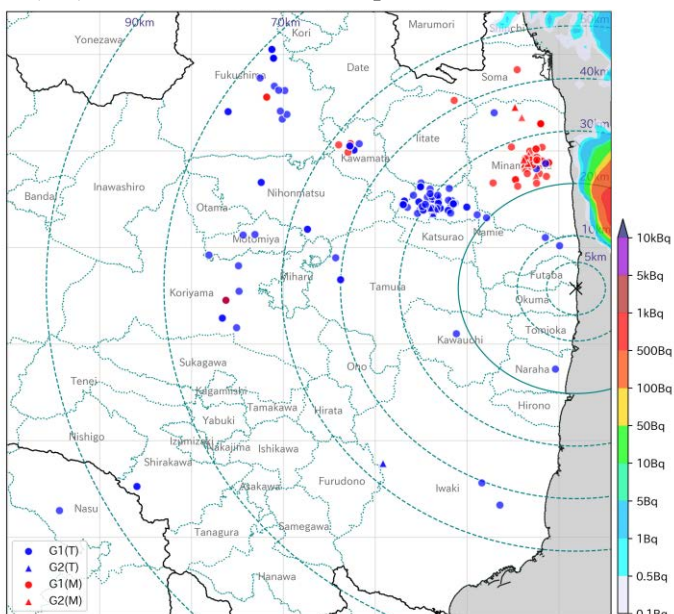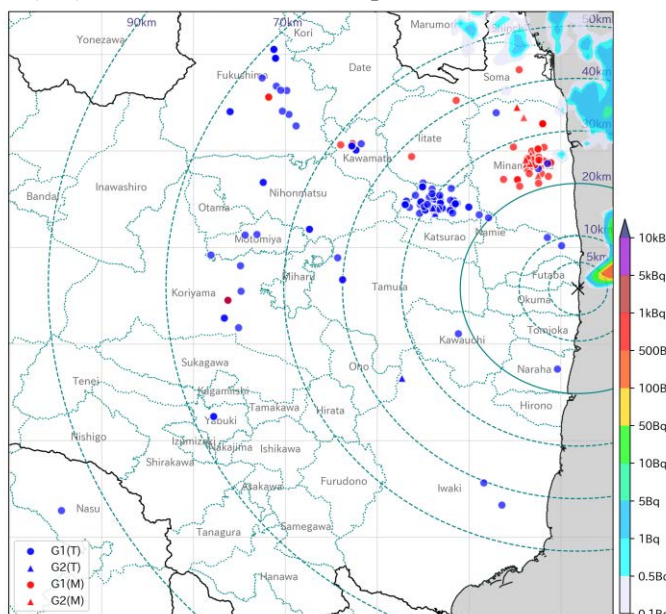
Fig. A8. The locations of individuals on the maps with the ^{137}Cs air concentration at the ground level at 6:00 p.m. on 13 March (1/6), 7:00 p.m. on 13 March (2/6), 8:00 p.m. on 13 March (3/6), 9:00 p.m. on 13 March (4/6), 10:00 p.m. on 13 March (5/6), and 11:00 p.m. on 13 March (6/6).
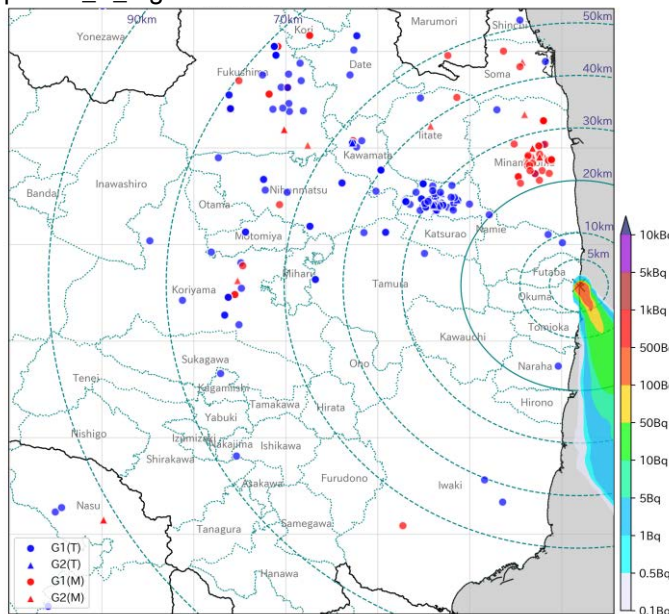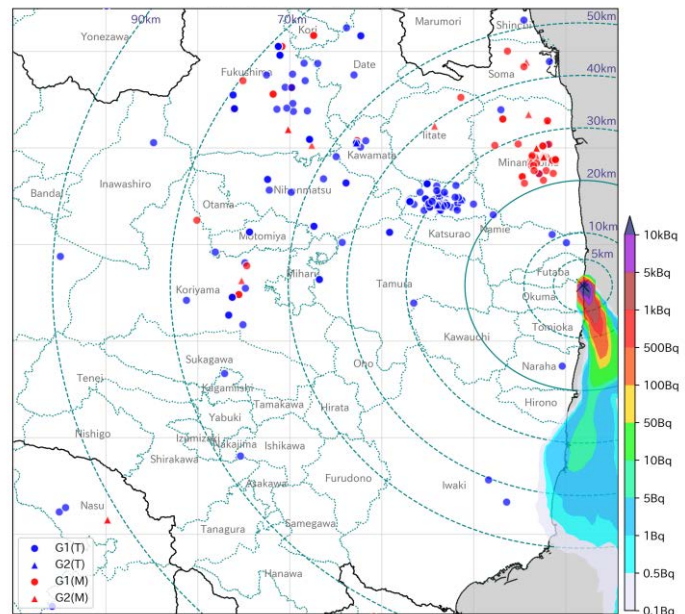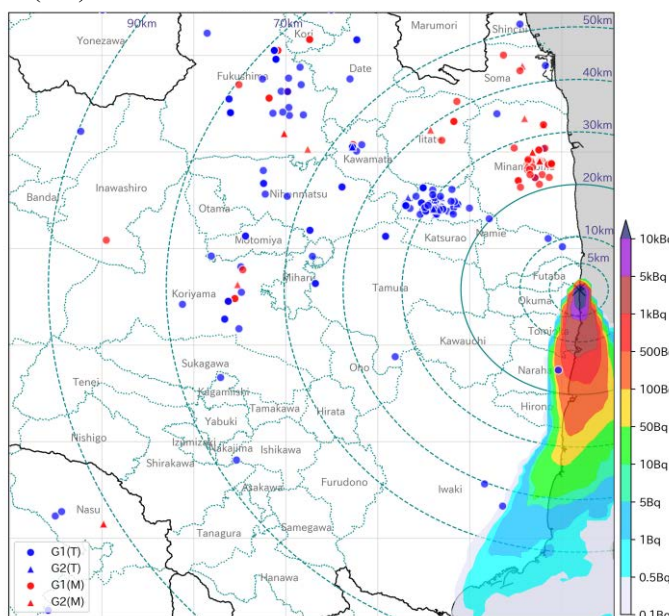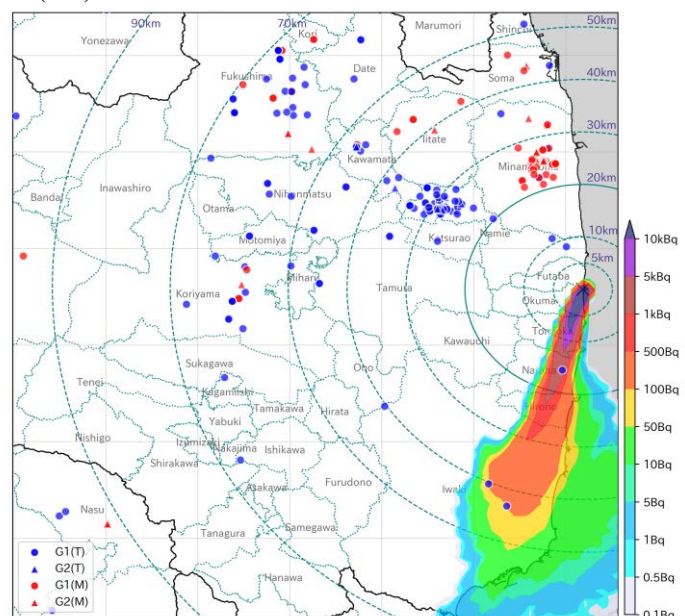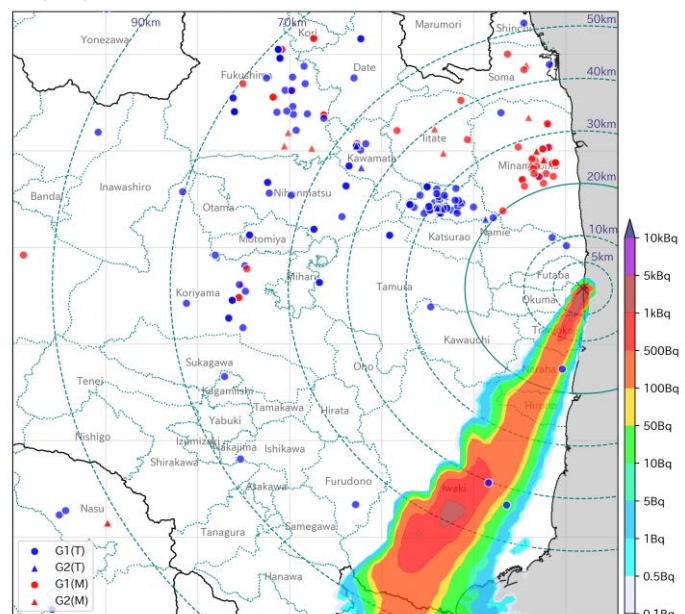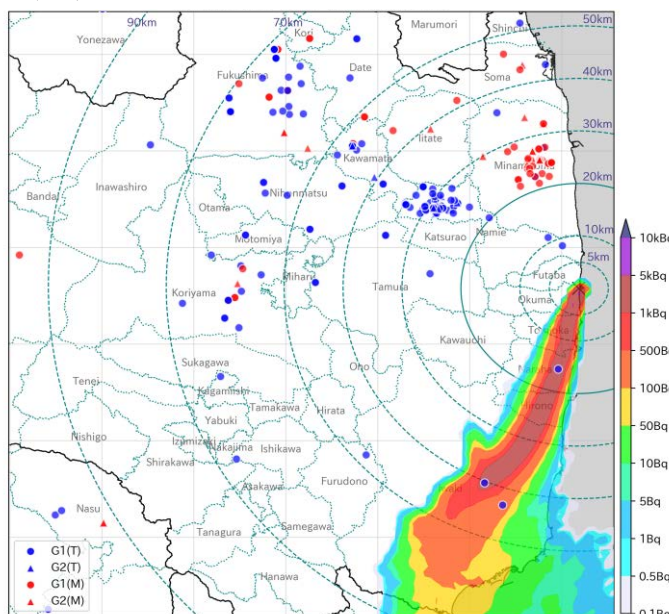
Fig. A9. The locations of individuals on the maps with the ^{137}Cs air concentration at the ground level at 12:00 a.m. on 15 March (1/6), 1:00 a.m. on 15 March (2/6), 2:00 a.m. on 15 March (3/6), 3:00 a.m. on 15 March (4/6), 4:00 a.m. on 15 March (5/6), and 5:00 a.m. on 15 March (6/6).
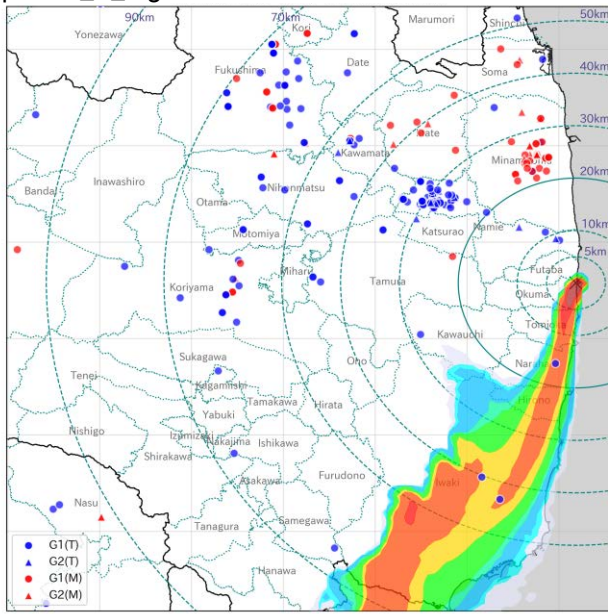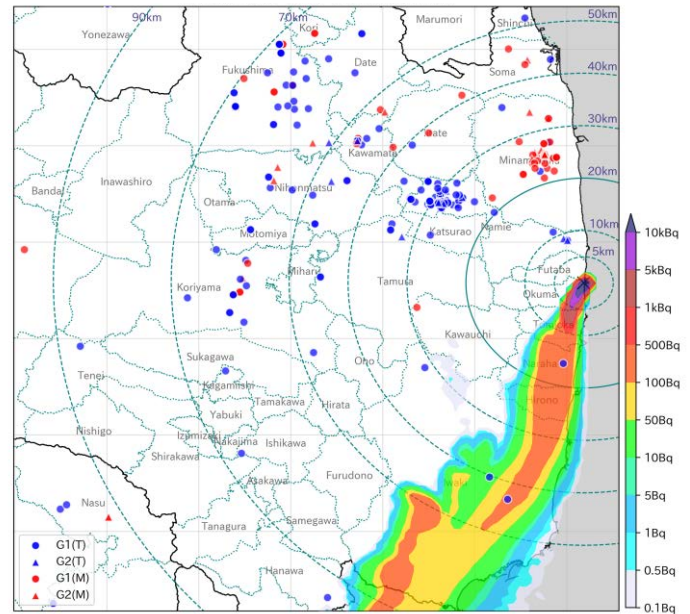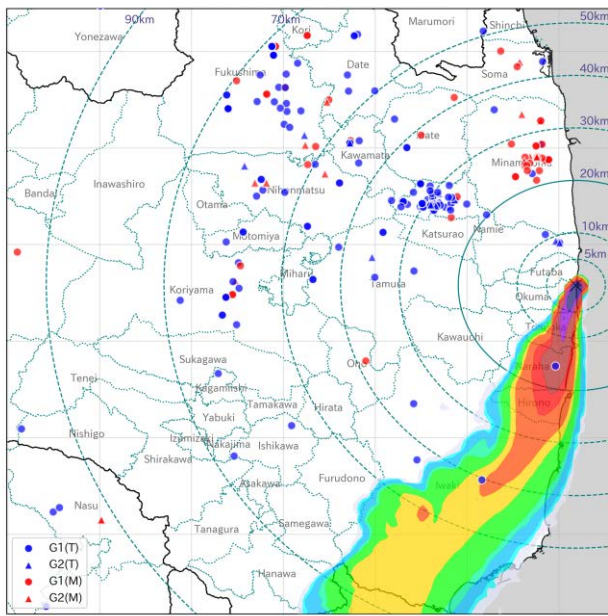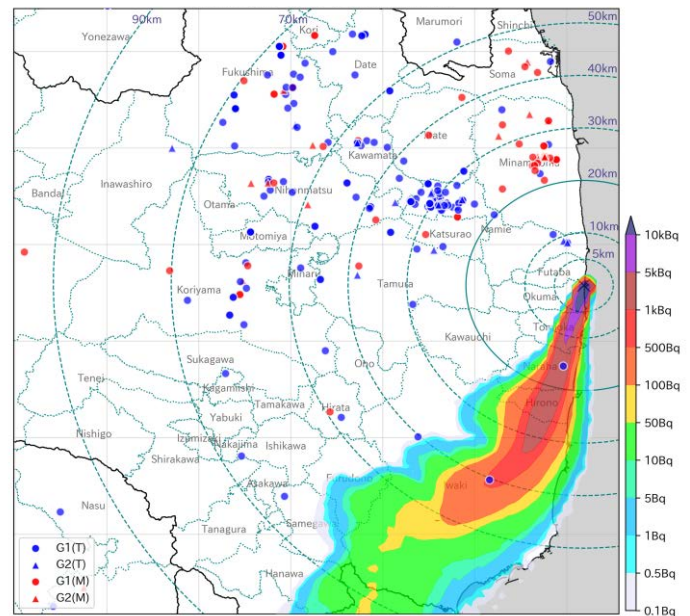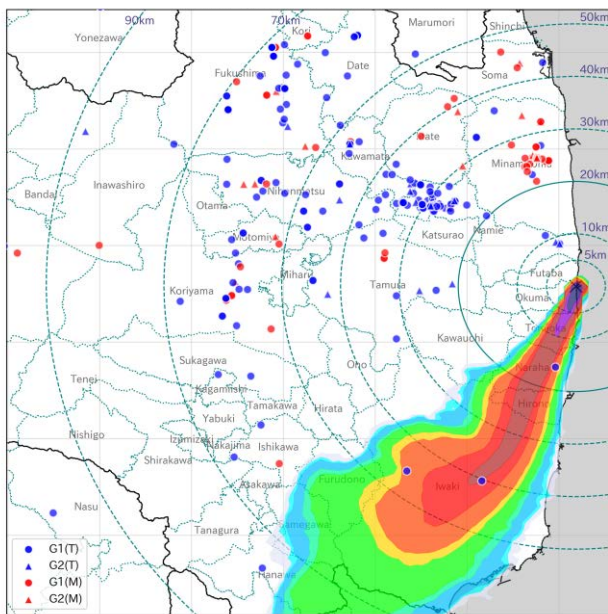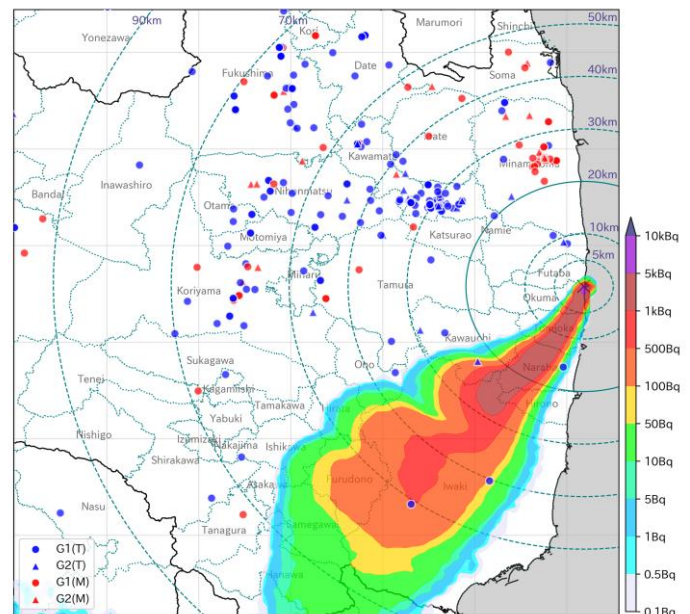
Fig. A10. The locations of individuals on the maps with the ^{137}Cs air concentration at the ground level at 6:00 a.m. on 15 March (1/6), 7:00 a.m. on 15 March (2/6), 8:00 a.m. on 15 March (3/6), 9:00 a.m. on 15 March (4/6), 10:00 a.m. on 15 March (5/6), and 11:00 a.m. on 15 March (6/6).
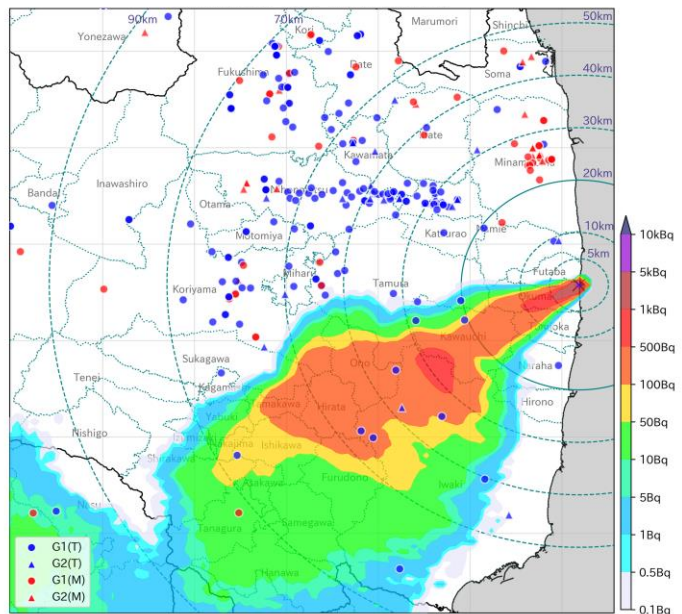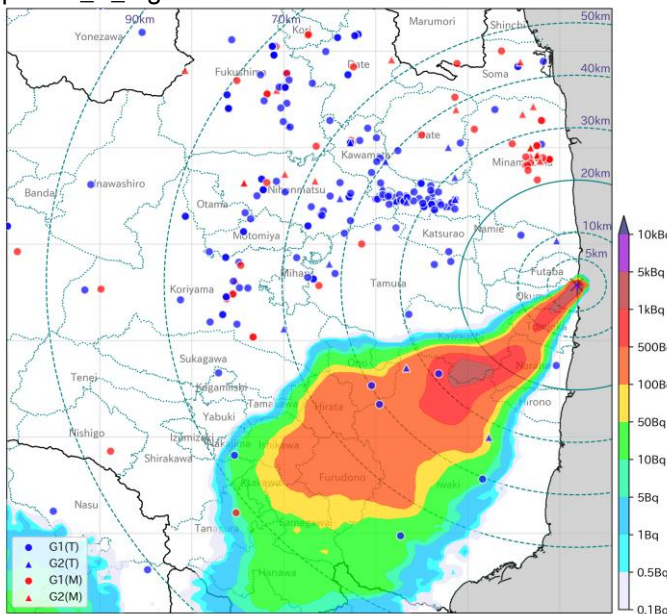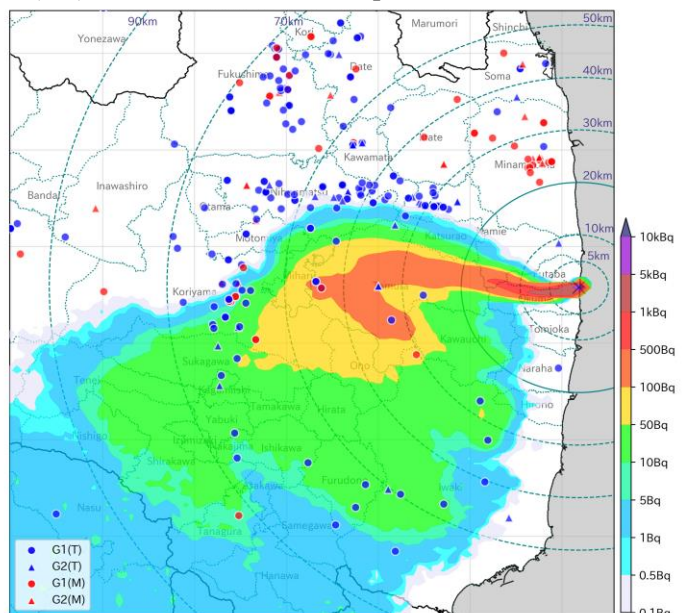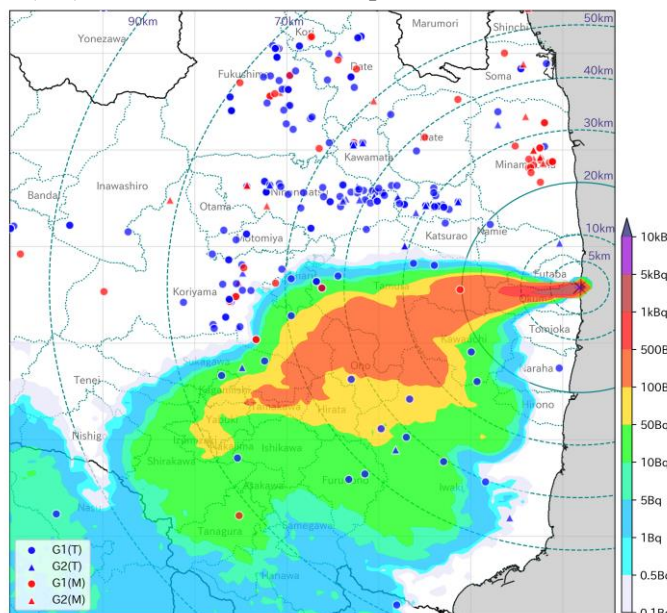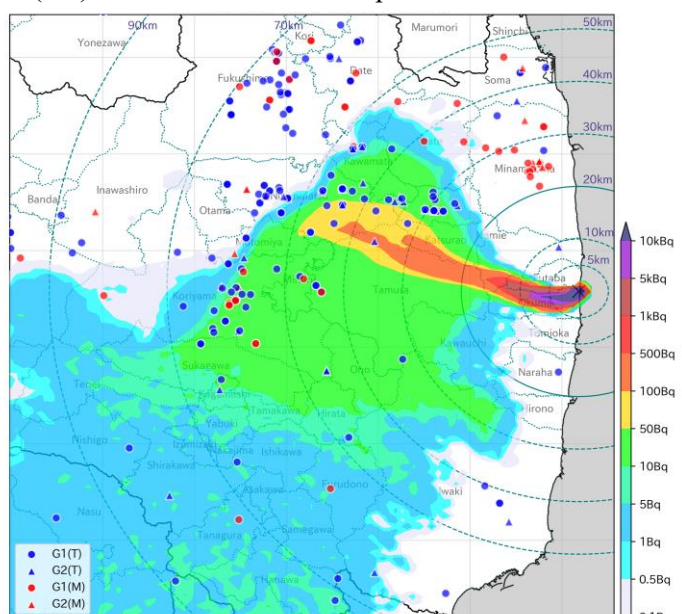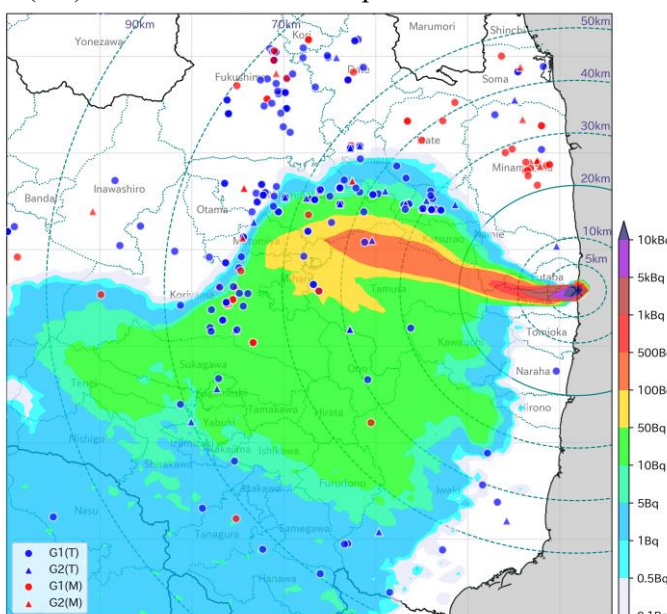
Fig. A11. The locations of individuals on the maps with the ^{137}Cs air concentration at the ground level at 12:00 p.m. on 15 March (1/6), 1:00 p.m. on 15 March (2/6), 2:00 p.m. on 15 March (3/6), 3:00 p.m. on 15 March (4/6), 4:00 p.m. on 15 March (5/6), and 5:00 p.m. on 15 March (6/6).
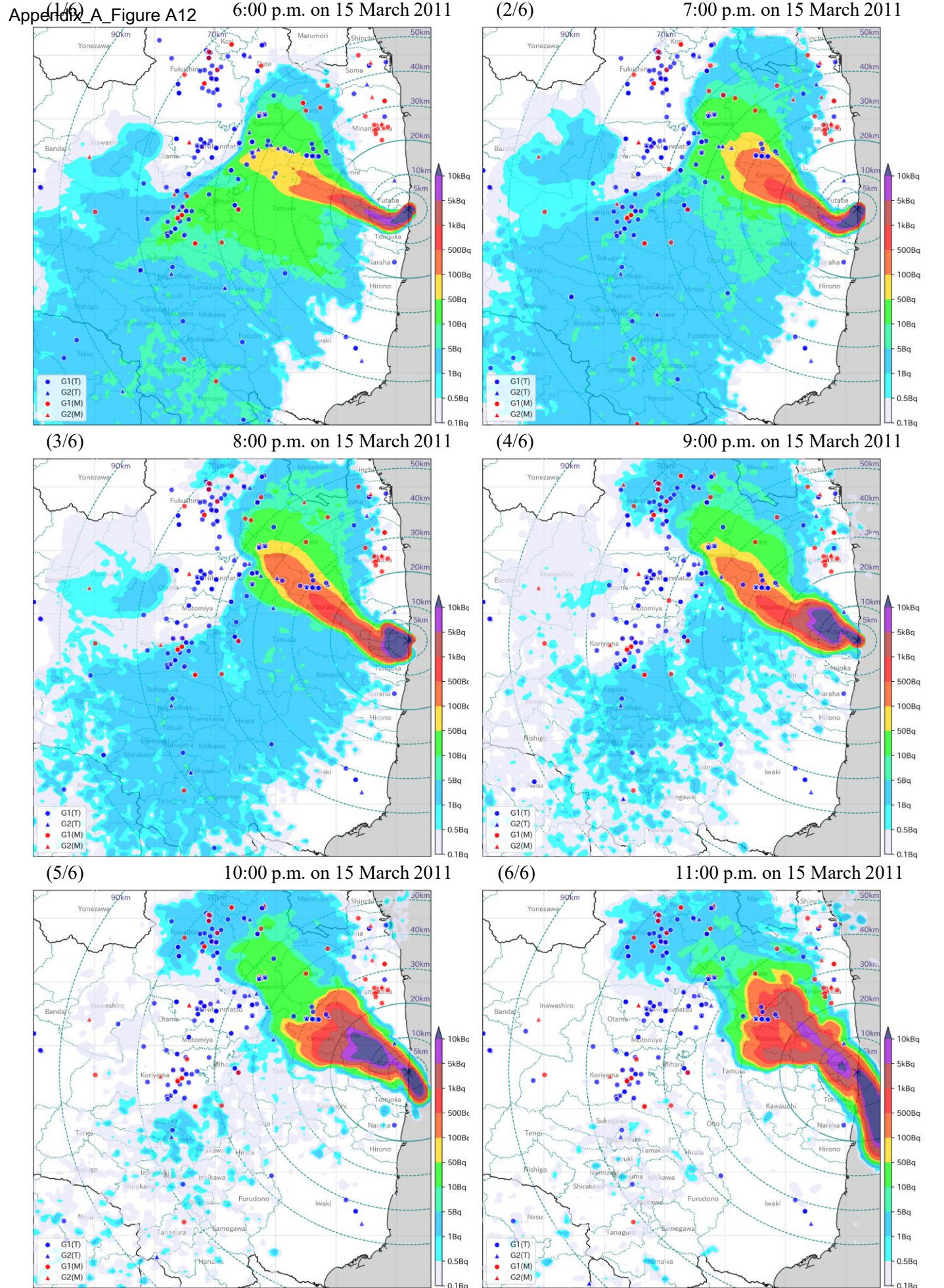
Fig. A12. The locations of individuals on the maps with the ^{137}Cs air concentration at the ground level at 6:00 p.m. on 15 March (1/6), 7:00 p.m. on 15 March (2/6), 8:00 p.m. on 15 March (3/6), 9:00 p.m. on 15 March (4/6), 10:00 p.m. on 15 March (5/6), and 11:00 p.m. on 15 March (6/6).
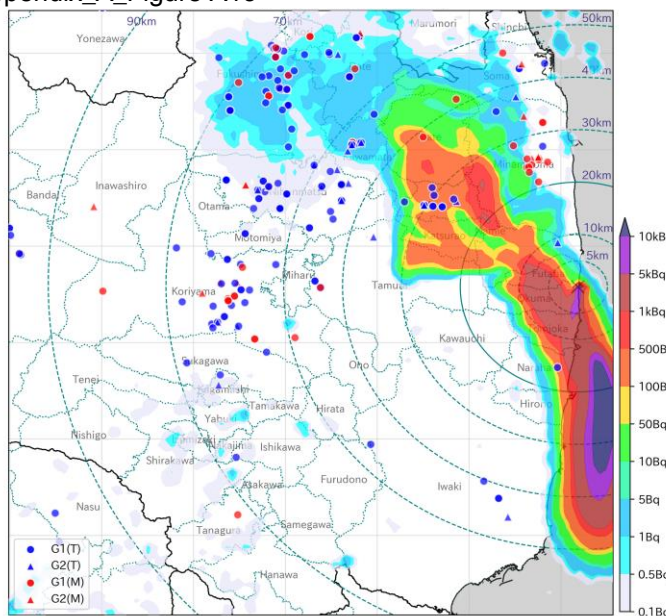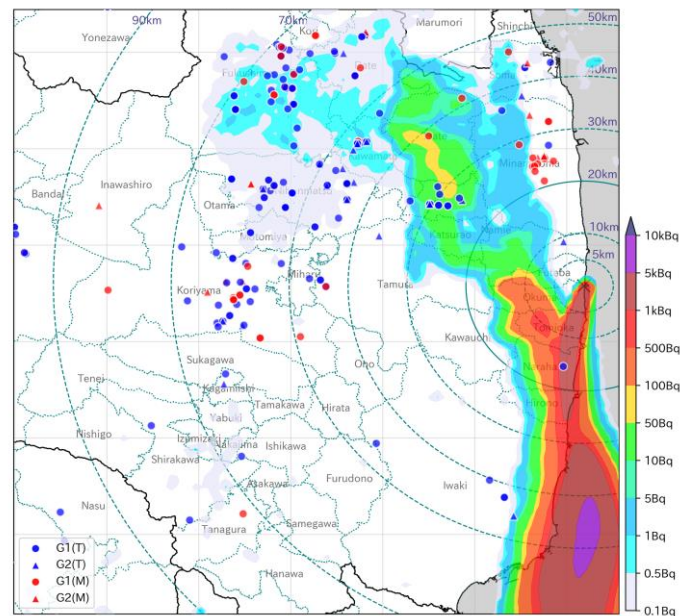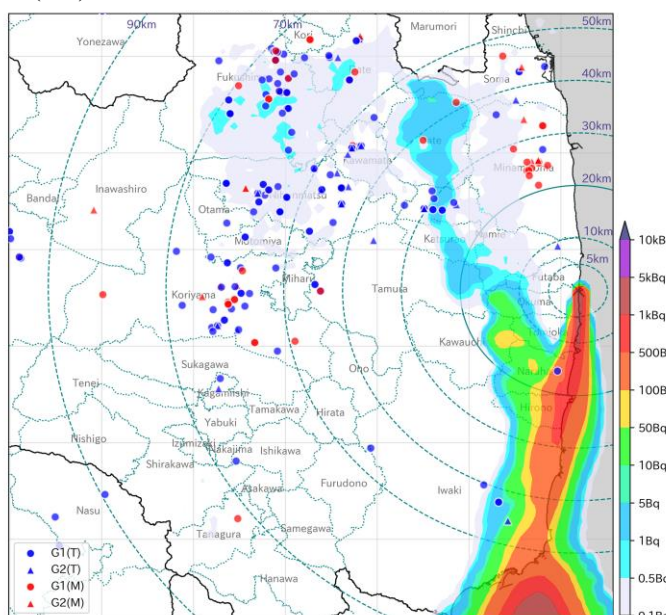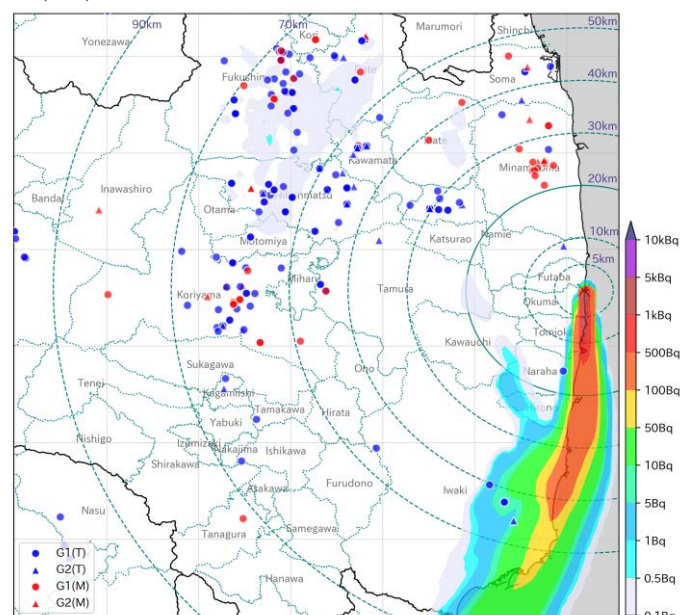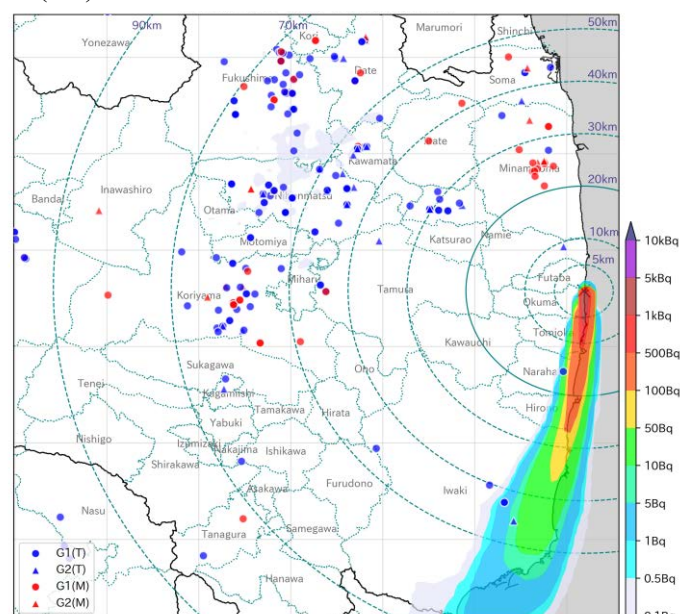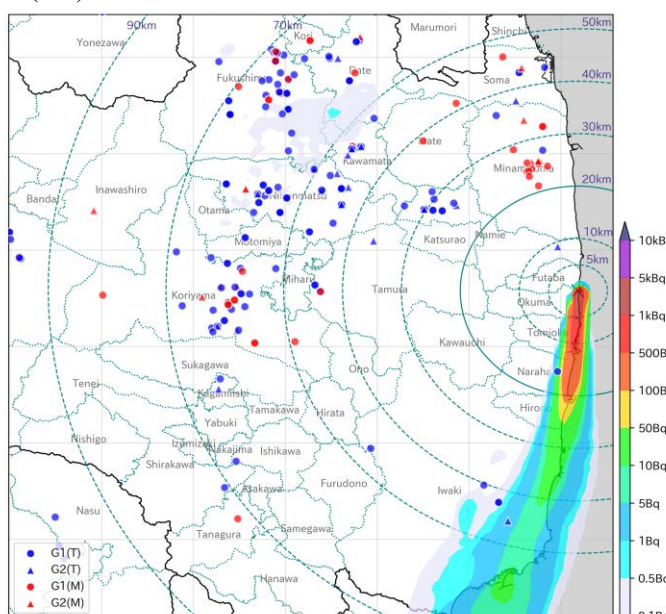
Fig. A13. The locations of individuals on the maps with the ^{137}Cs air concentration at the ground level at 12:00 a.m. on 16 March (1/6), 1:00 a.m. on 16 March (2/6), 2:00 a.m. on 16 March (3/6), 3:00 a.m. on 16 March (4/6), 4:00 a.m. on 16 March (5/6), and 5:00 a.m. on 16 March (6/6).
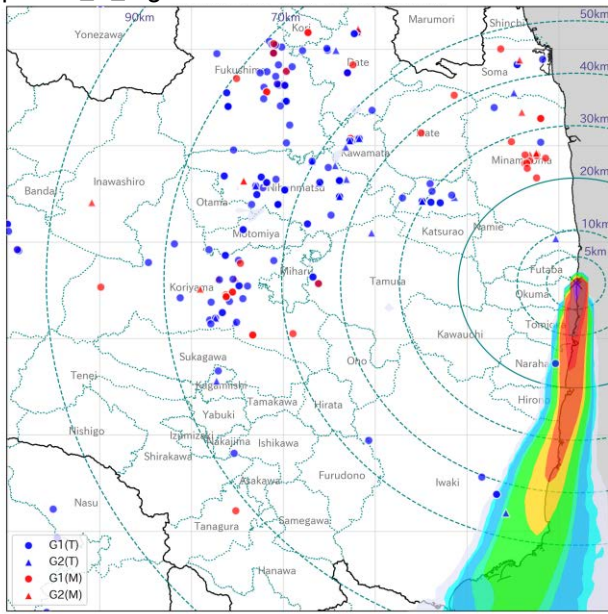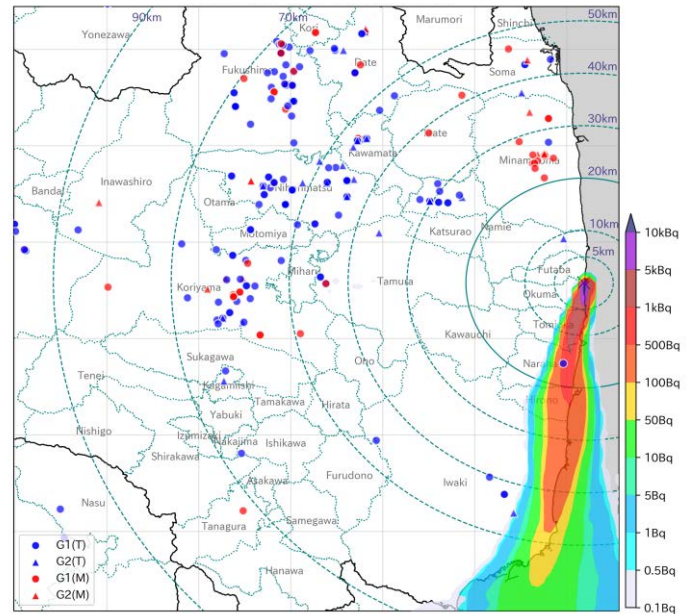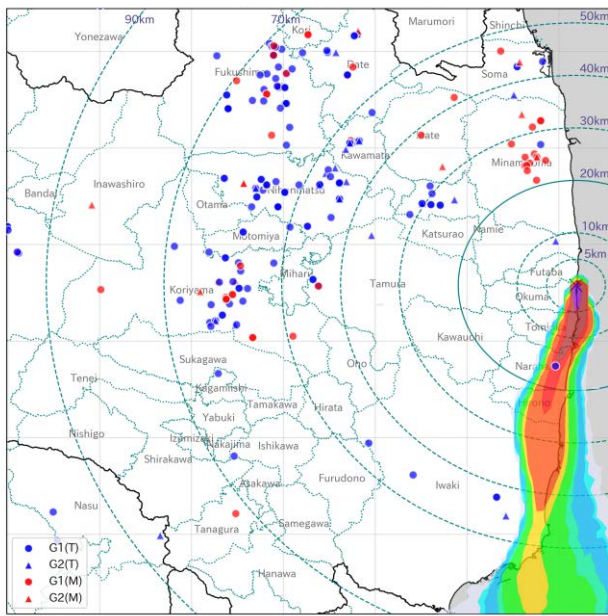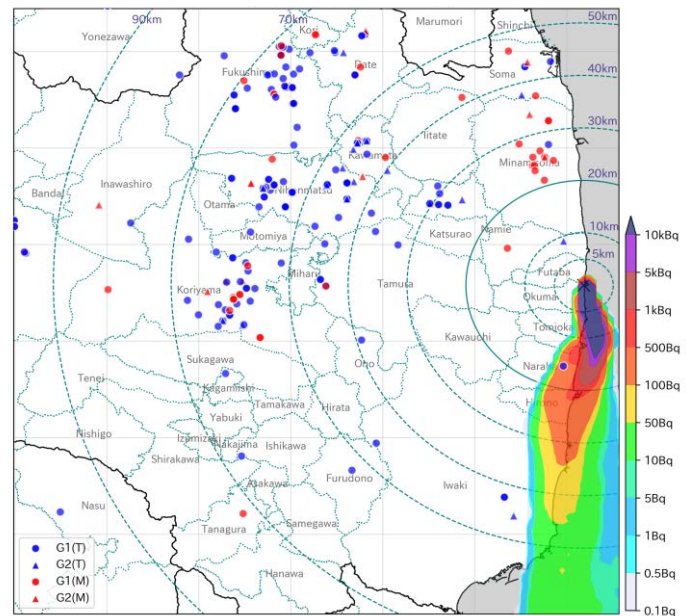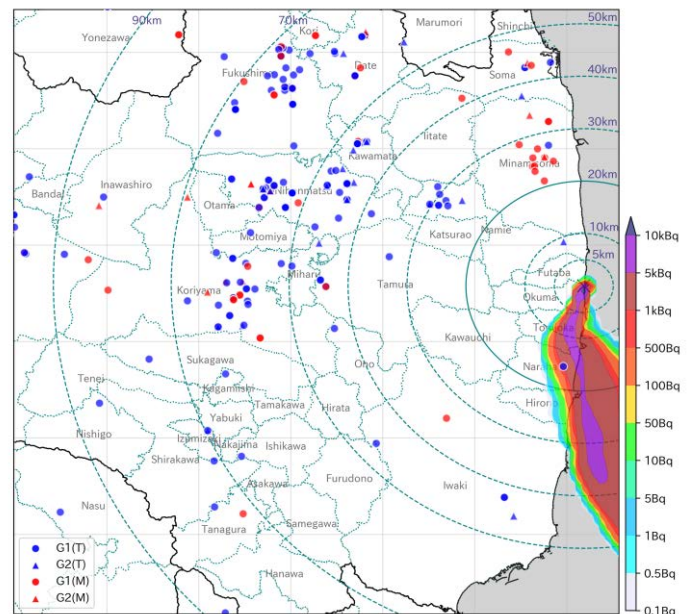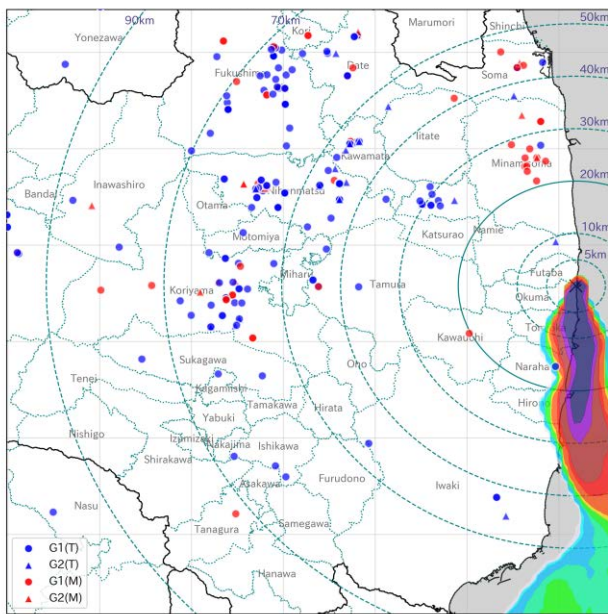
Fig. A14. The locations of individuals on the maps with the ^{137}Cs air concentration at the ground level at 6:00 a.m. on 16 March (1/6), 7:00 a.m. on 16 March (2/6), 8:00 a.m. on 16 March (3/6), 9:00 a.m. on 16 March (4/6), 10:00 a.m. on 16 March (5/6), and 11:00 a.m. on 16 March (6/6).
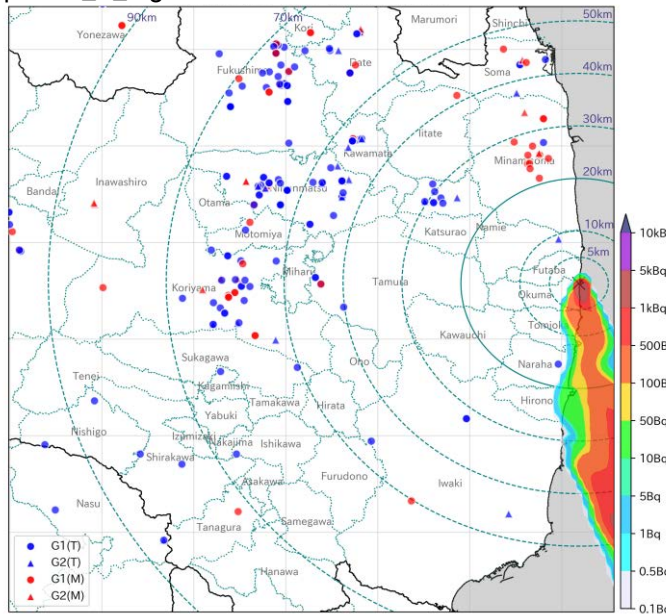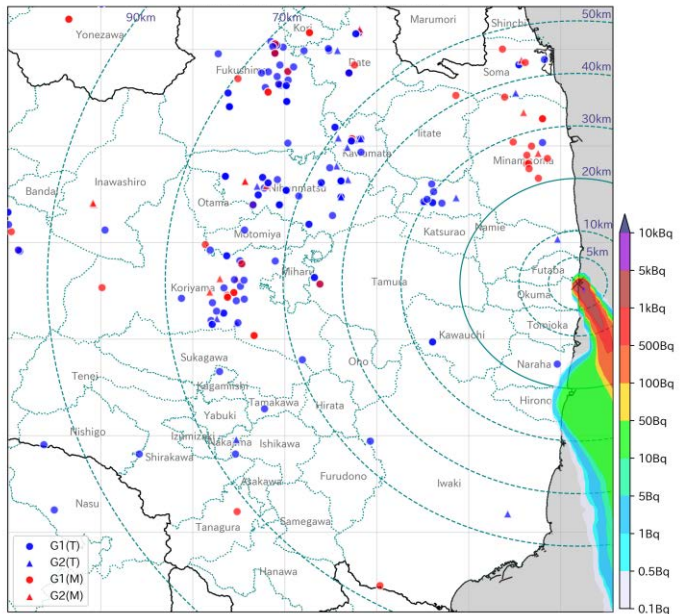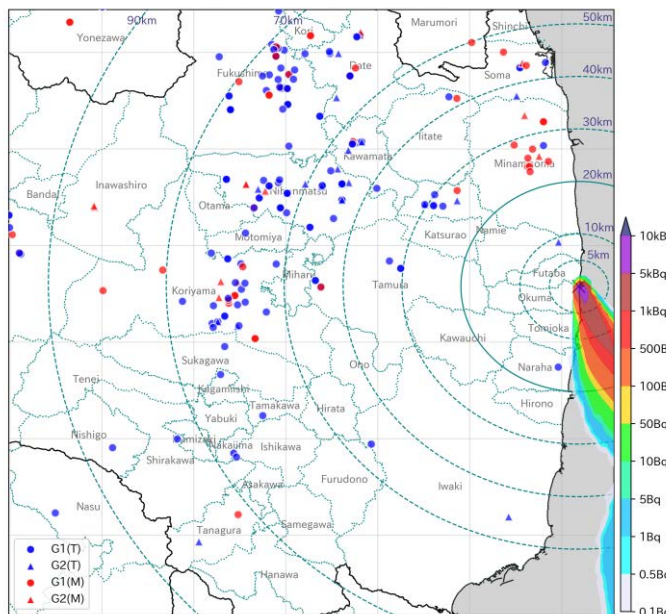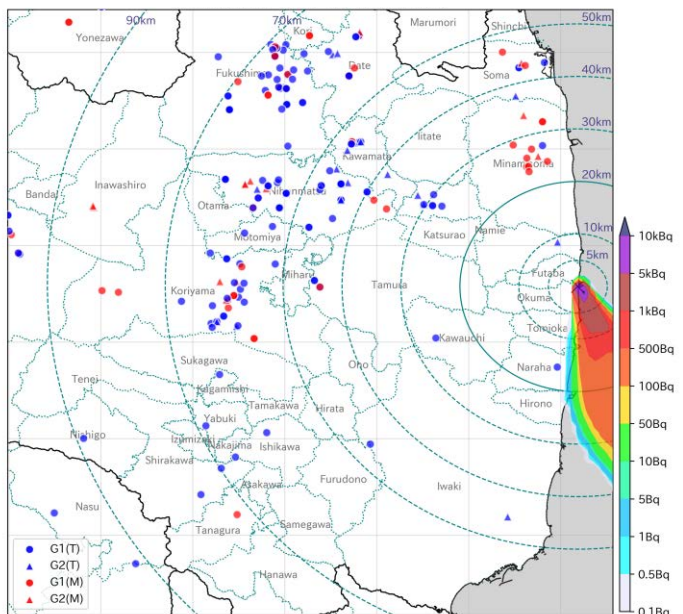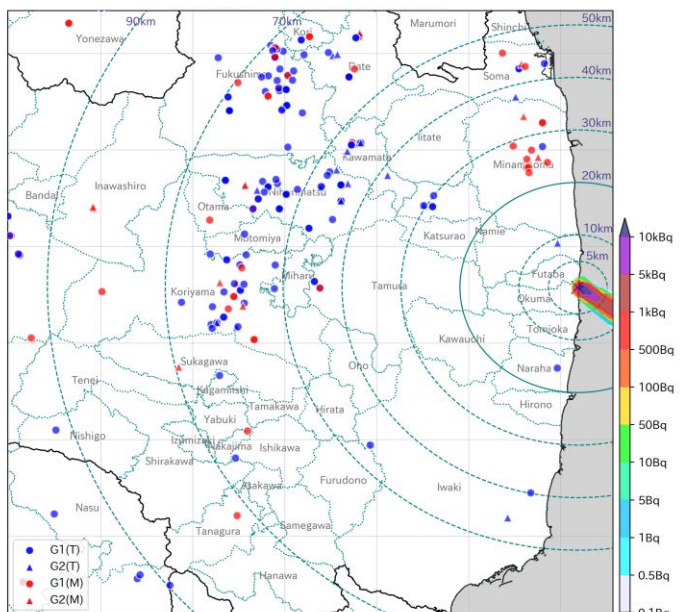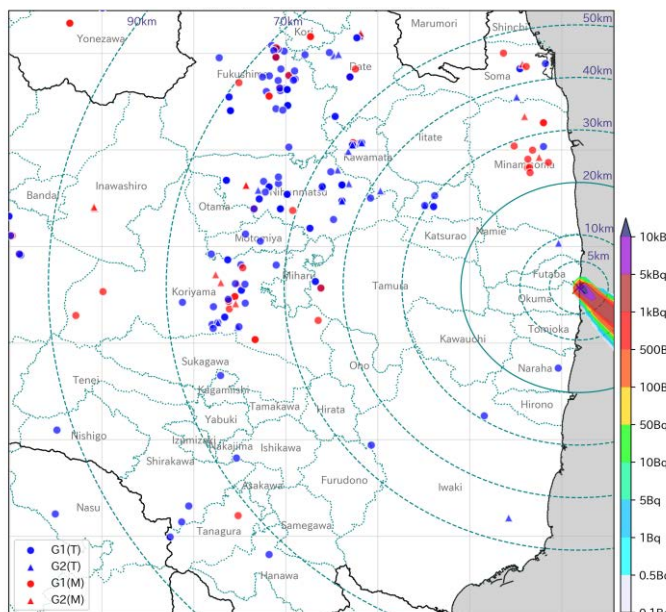
Fig. A15. The locations of individuals on the maps with the ^{137}Cs air concentration at the ground level at 12:00 p.m. on 16 March (1/6), 1:00 p.m. on 16 March (2/6), 2:00 p.m. on 16 March (3/6), 3:00 p.m. on 16 March (4/6), 4:00 p.m. on 16 March (5/6), and 5:00 p.m. on 16 March (6/6).
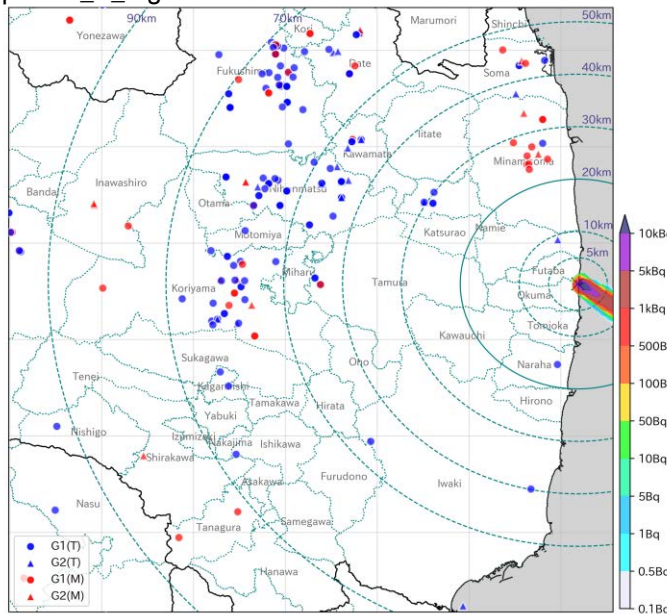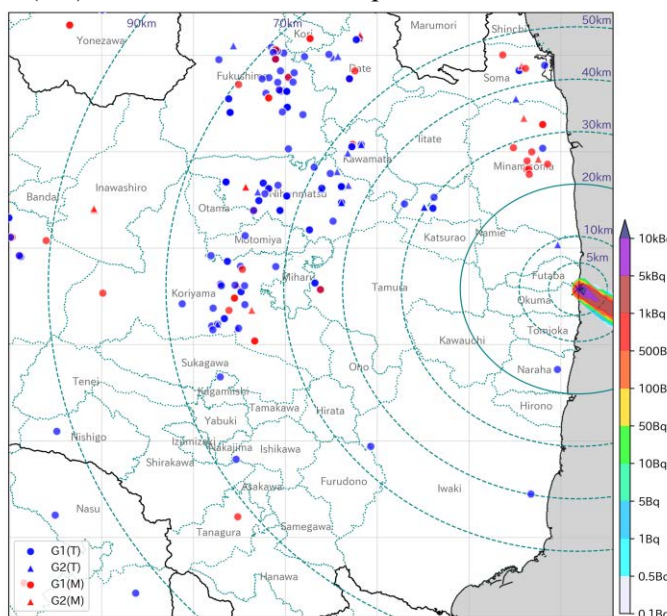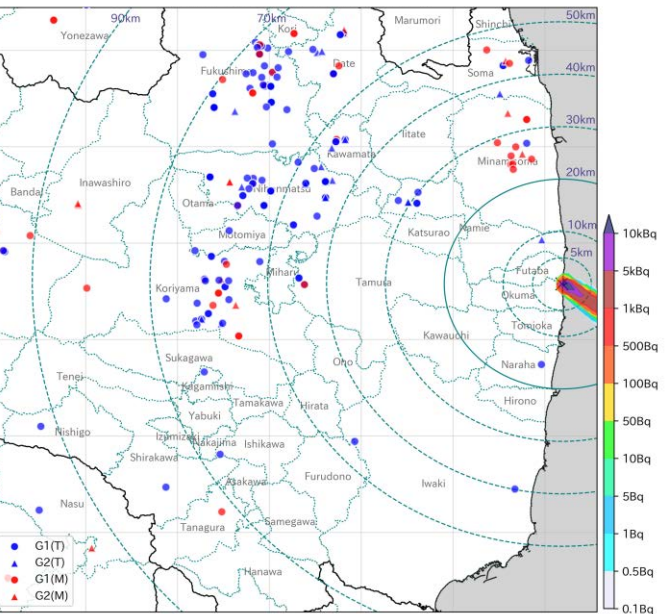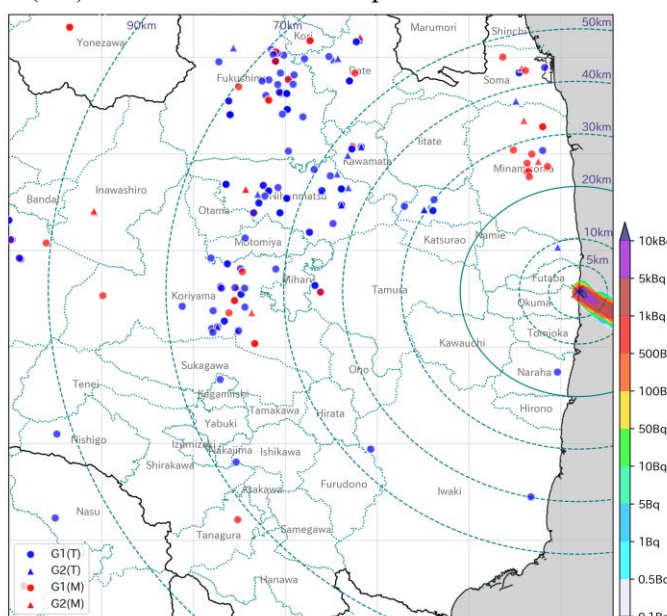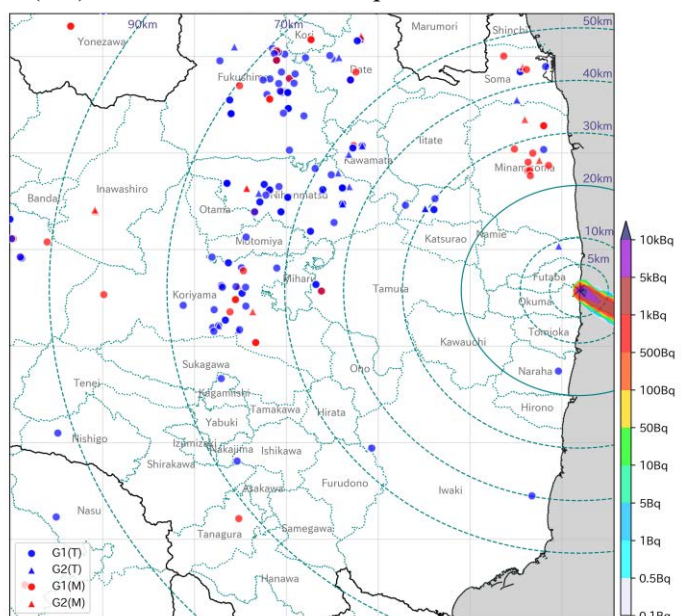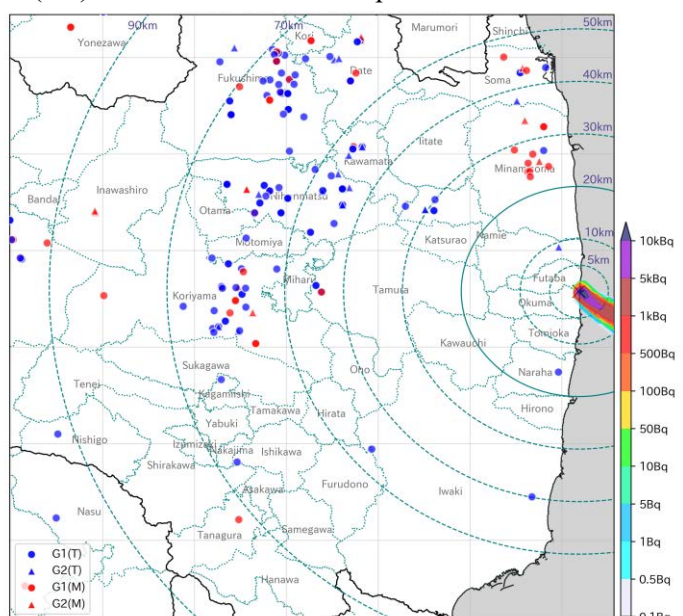
Fig. A16. The locations of individuals on the maps with the ^{137}Cs air concentration at the ground level at 6:00 p.m. on 16 March (1/6), 7:00 p.m. on 16 March (2/6), 8:00 p.m. on 16 March (3/6), 9:00 p.m. on 16 March (4/6), 10:00 p.m. on 16 March (5/6), and 11:00 p.m. on 16 March (6/6).
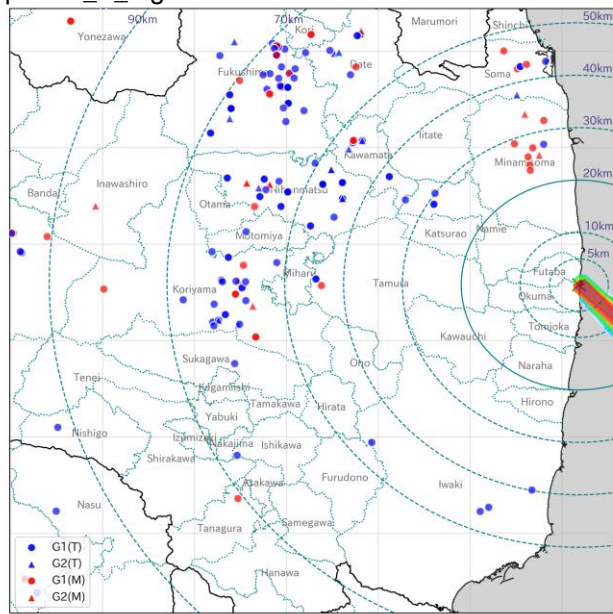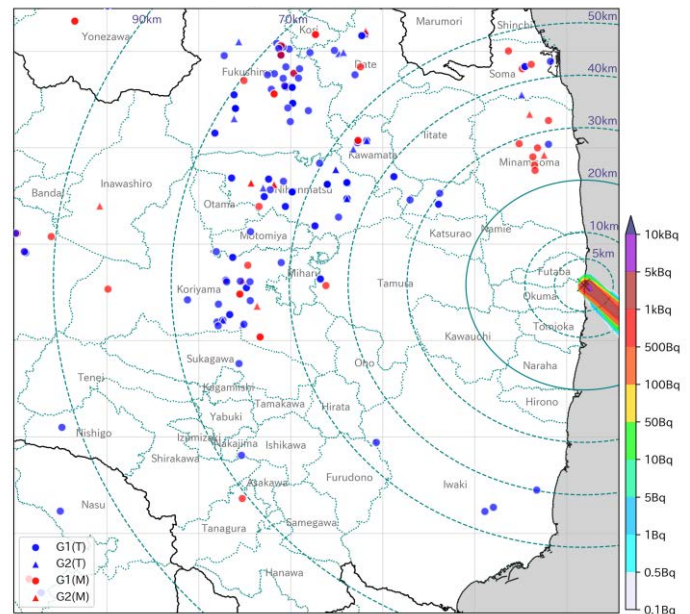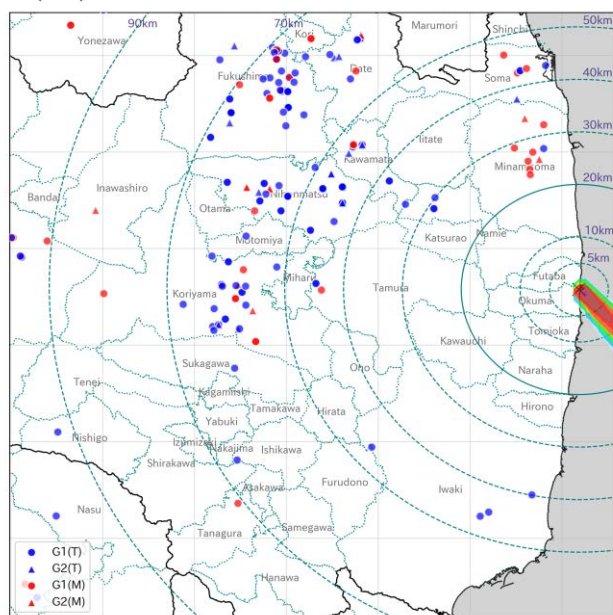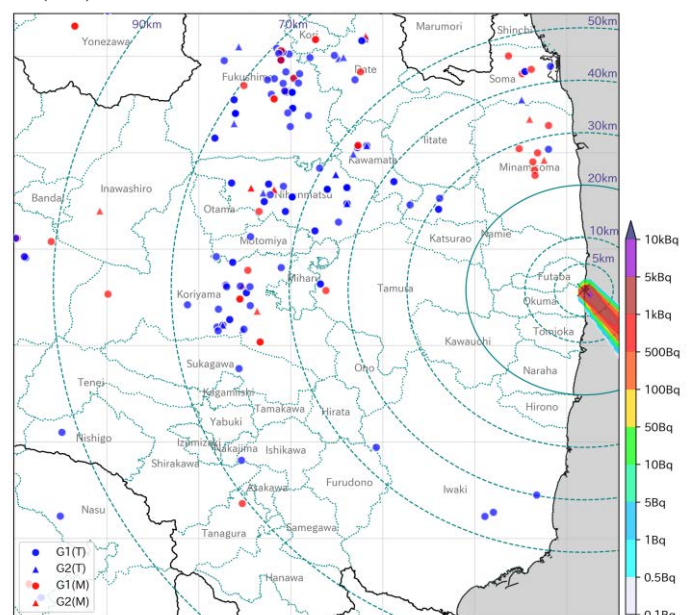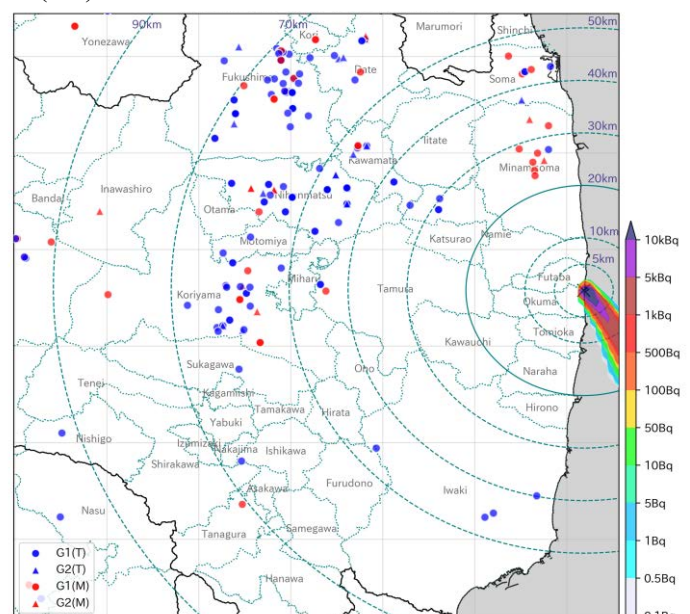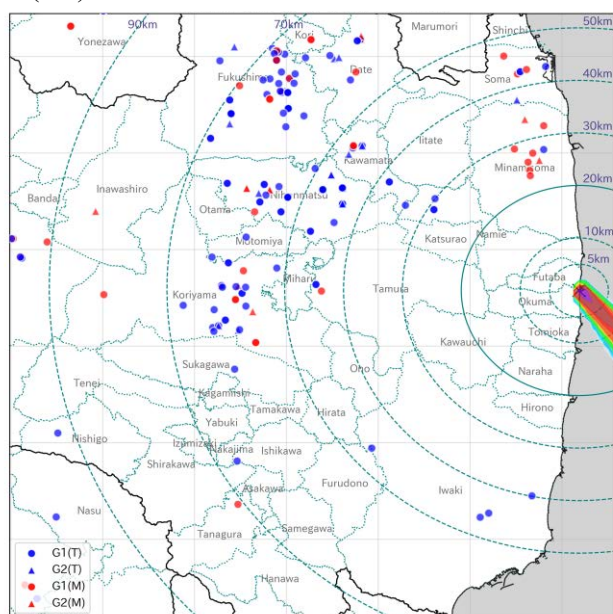
Fig. A17. The locations of individuals on the maps with the ^{137}Cs air concentration at the ground level at 12:00 a.m. on 18 March (1/6), 1:00 a.m. on 18 March (2/6), 2:00 a.m. on 18 March (3/6), 3:00 a.m. on 18 March (4/6), 4:00 a.m. on 18 March (5/6), and 5:00 a.m. on 18 March (6/6).
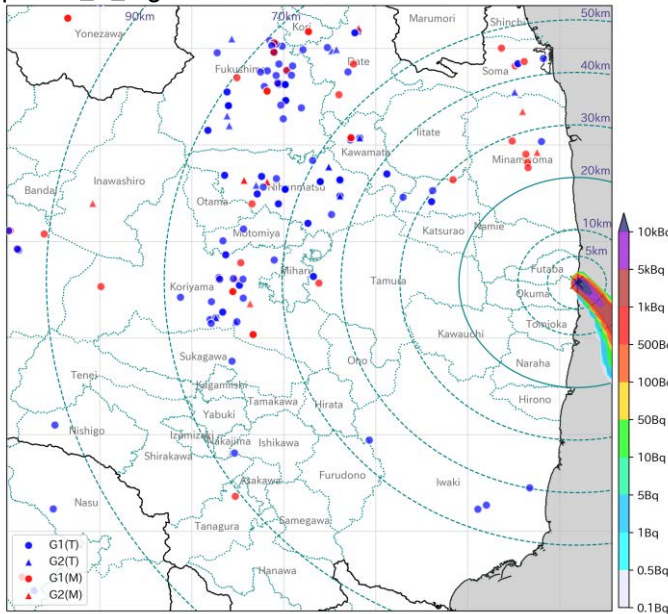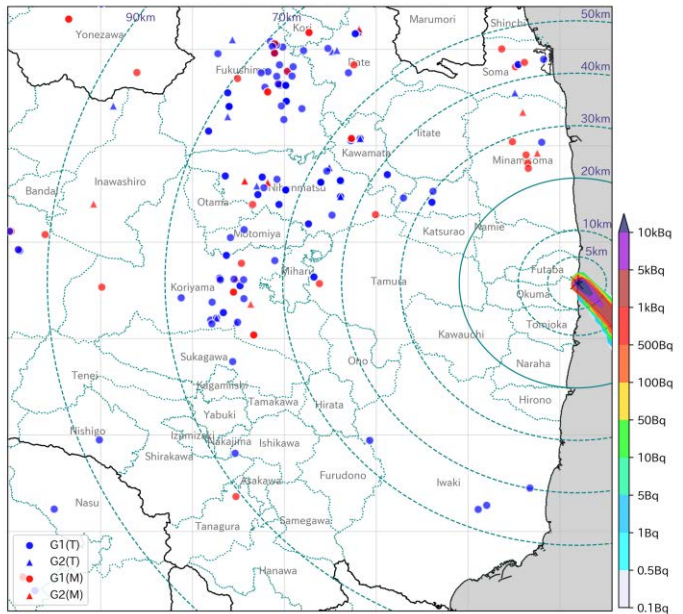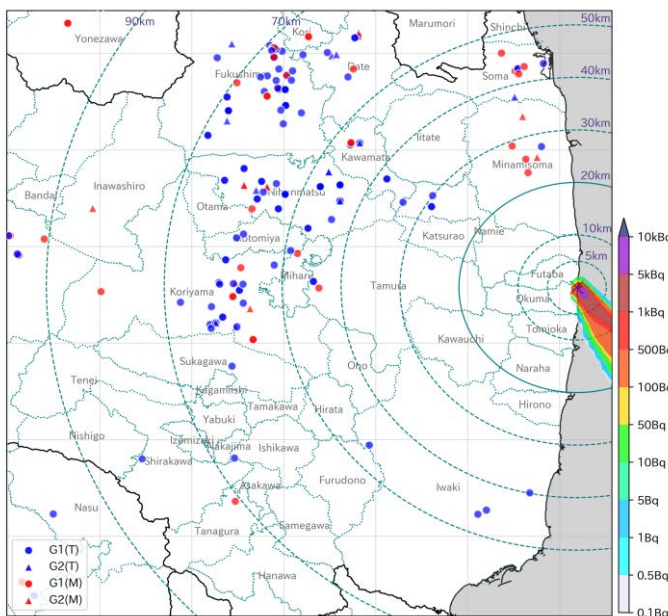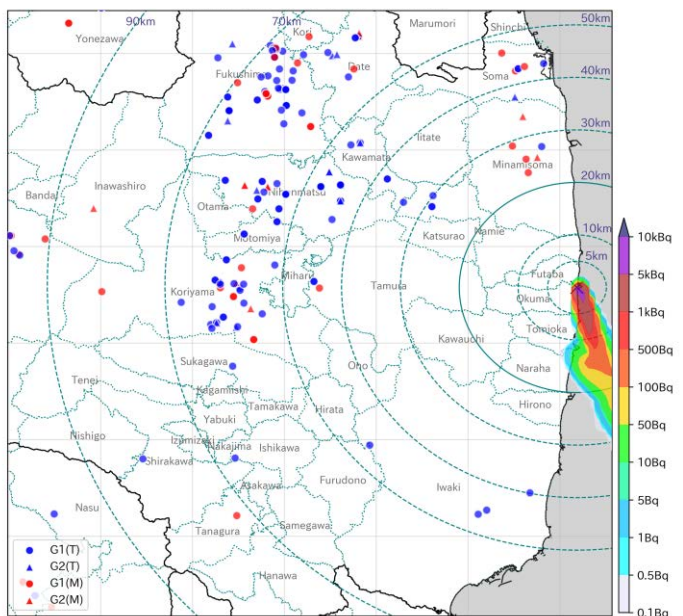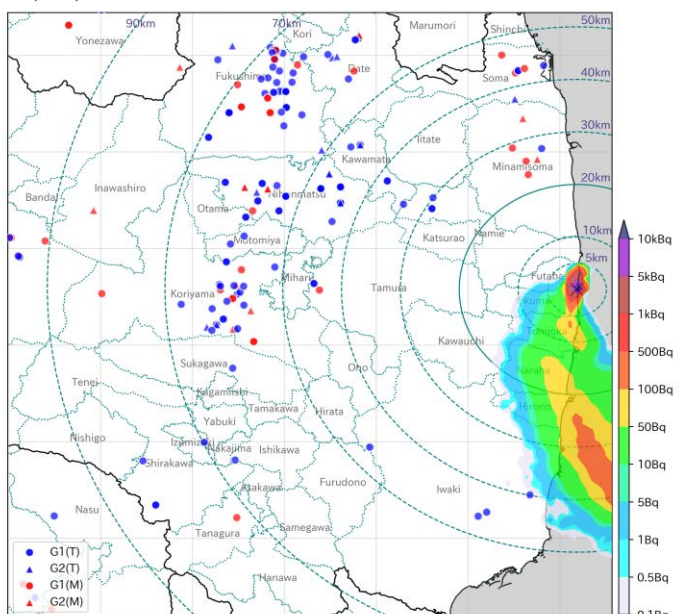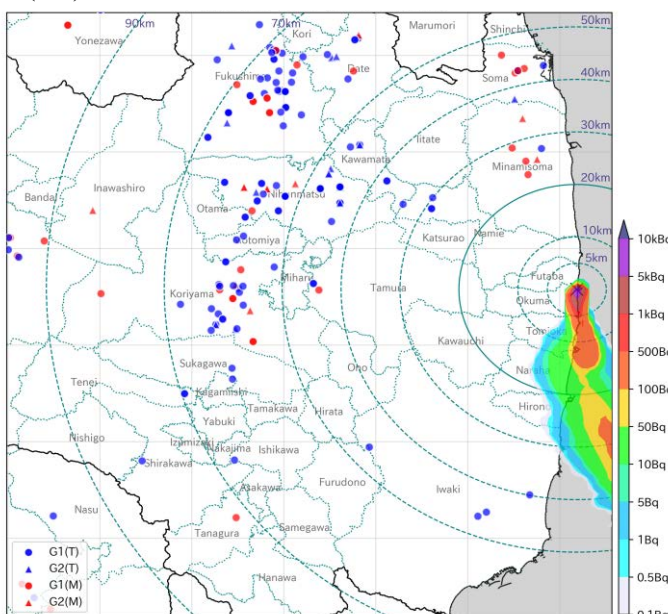
Fig. A18. The locations of individuals on the maps with the ^{137}Cs air concentration at the ground level at 6:00 a.m. on 18 March (1/6), 7:00 a.m. on 18 March (2/6), 8:00 a.m. on 18 March (3/6), 9:00 a.m. on 18 March (4/6), 10:00 a.m. on 18 March (5/6), and 11:00 a.m. on 18 March (6/6).
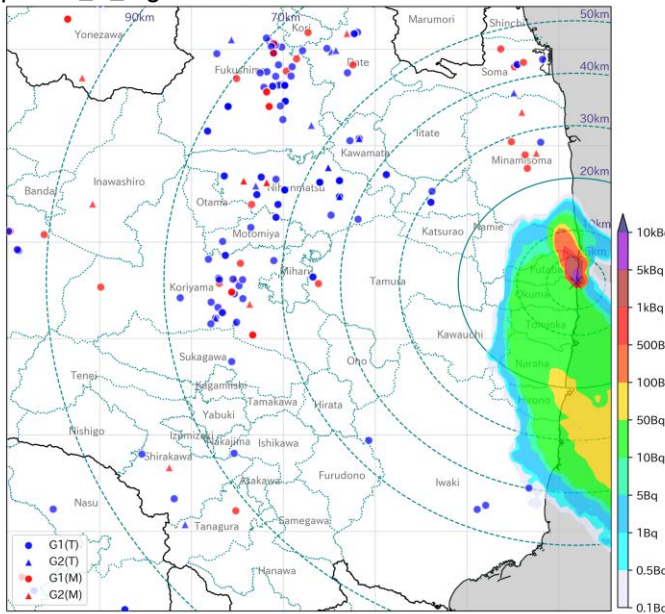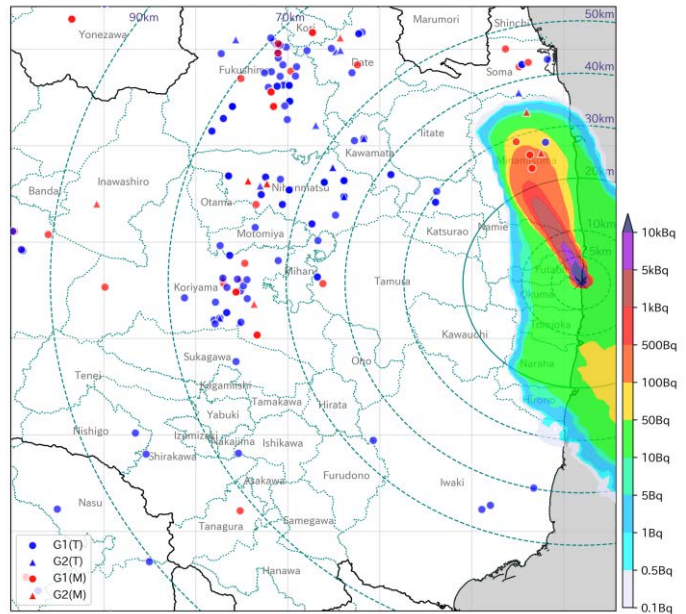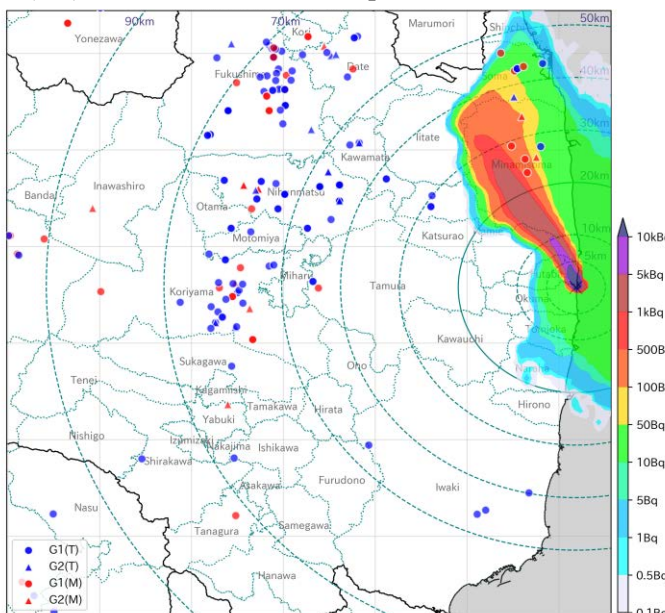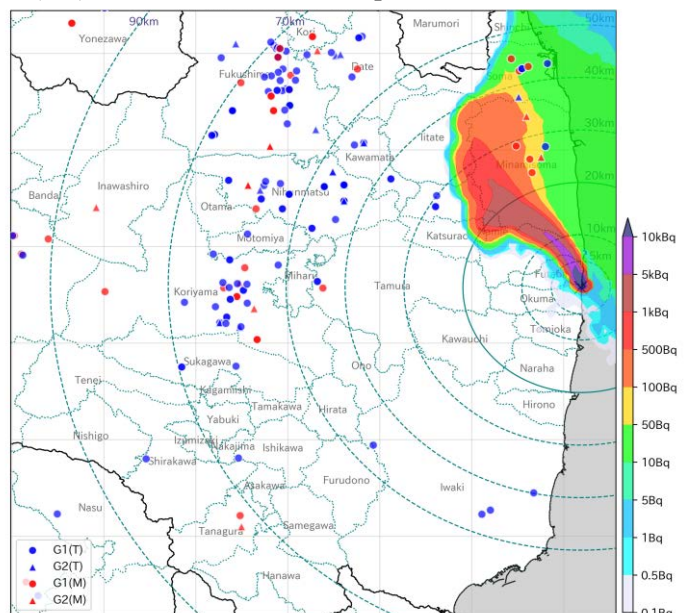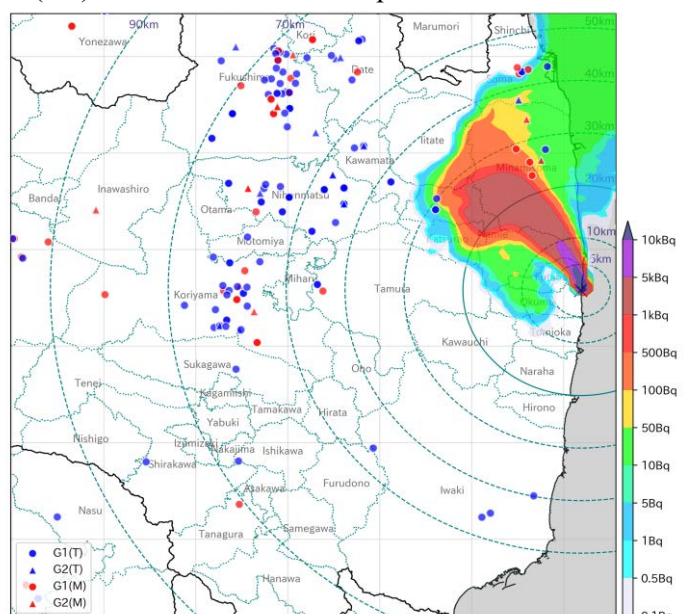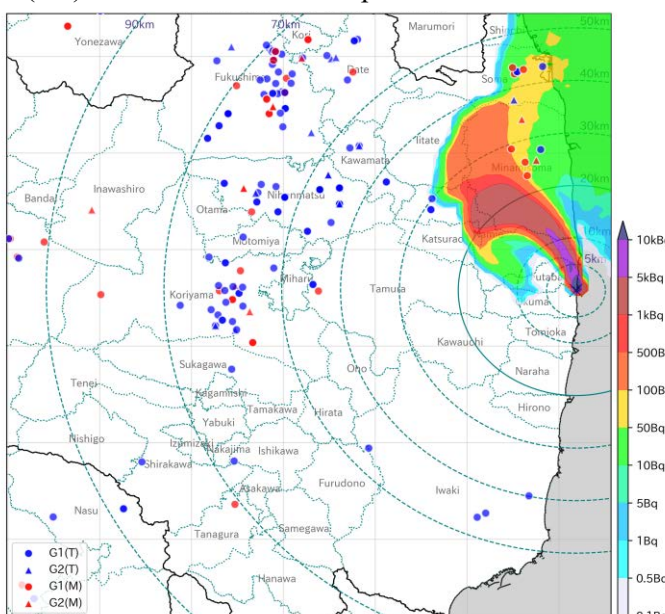
Fig. A19. The locations of individuals on the maps with the ^{137}Cs air concentration at the ground level at 12:00 p.m. on 18 March (1/6), 1:00 p.m. on 18 March (2/6), 2:00 p.m. on 18 March (3/6), 3:00 p.m. on 18 March (4/6), 4:00 p.m. on 18 March (5/6), and 5:00 p.m. on 18 March (6/6).
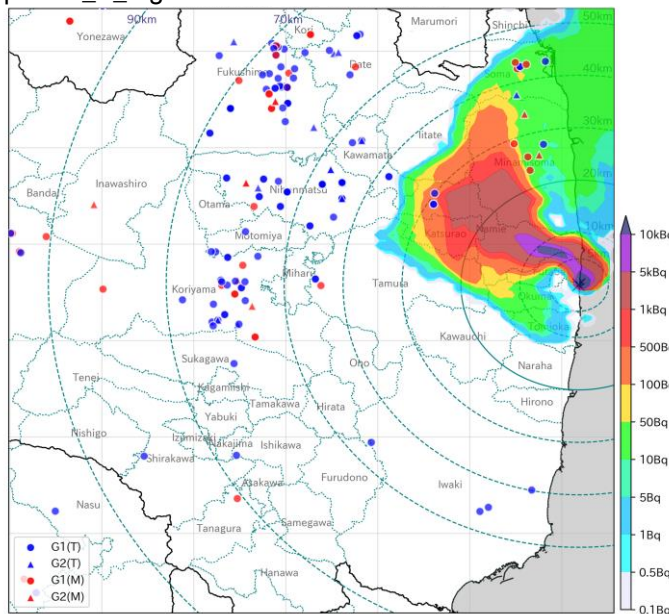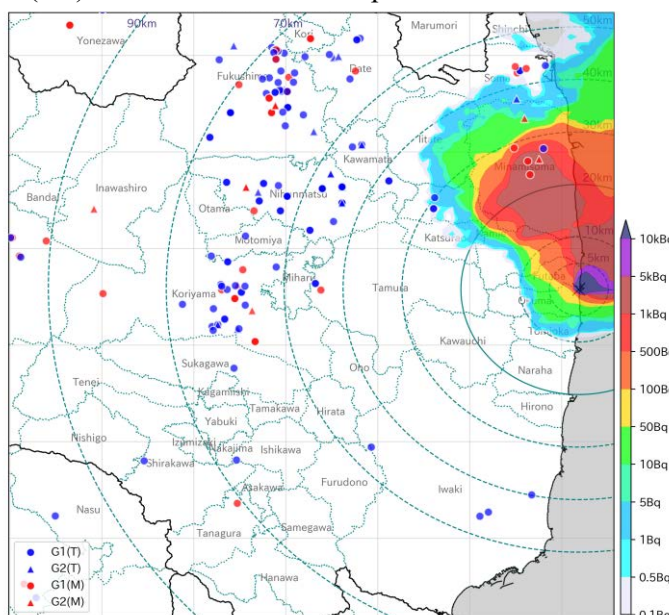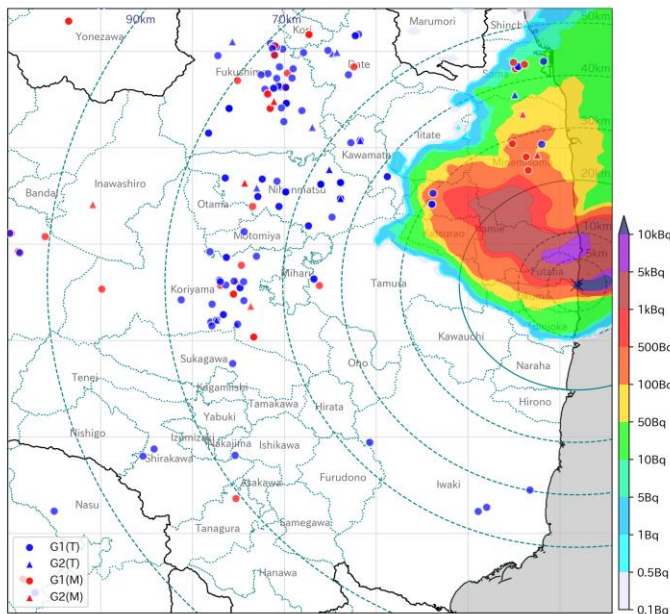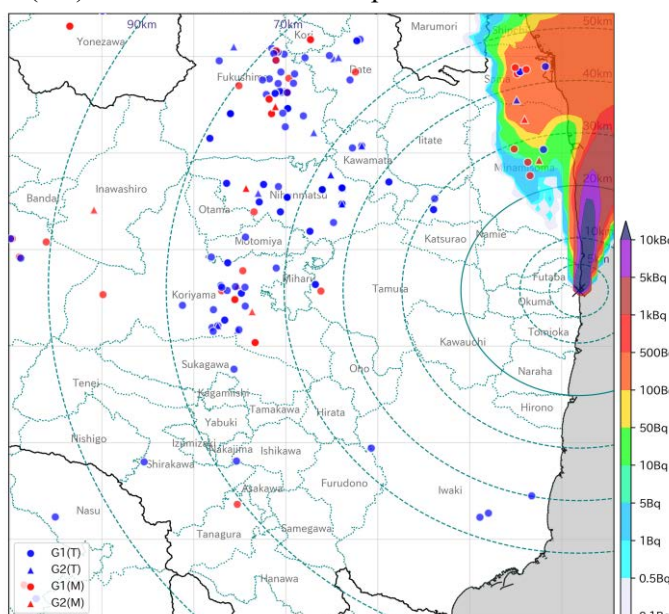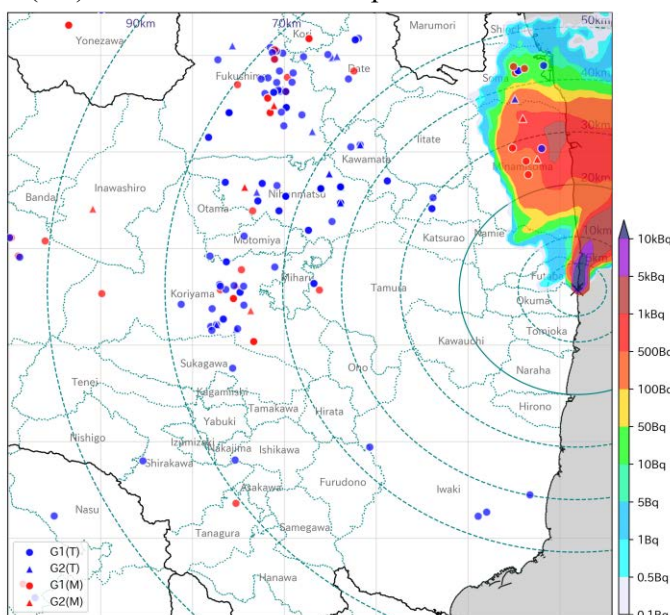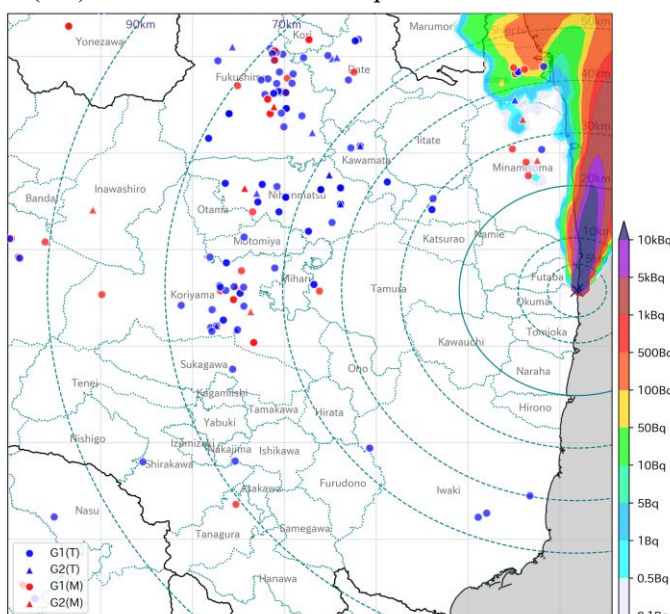
Fig. A20. The locations of individuals on the maps with the ^{137}Cs air concentration at the ground level at 6:00 p.m. on 18 March (1/6), 7:00 p.m. on 18 March (2/6), 8:00 p.m. on 18 March (3/6), 9:00 p.m. on 18 March (4/6), 10:00 p.m. on 18 March (5/6), and 11:00 p.m. on 18 March (6/6).
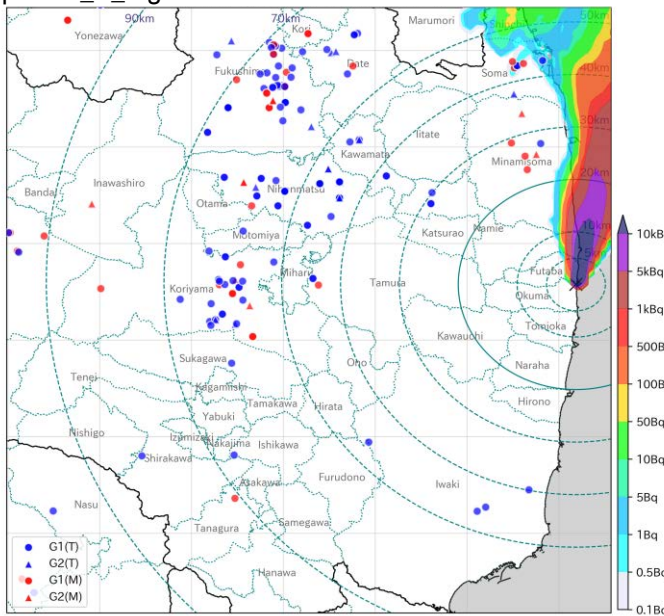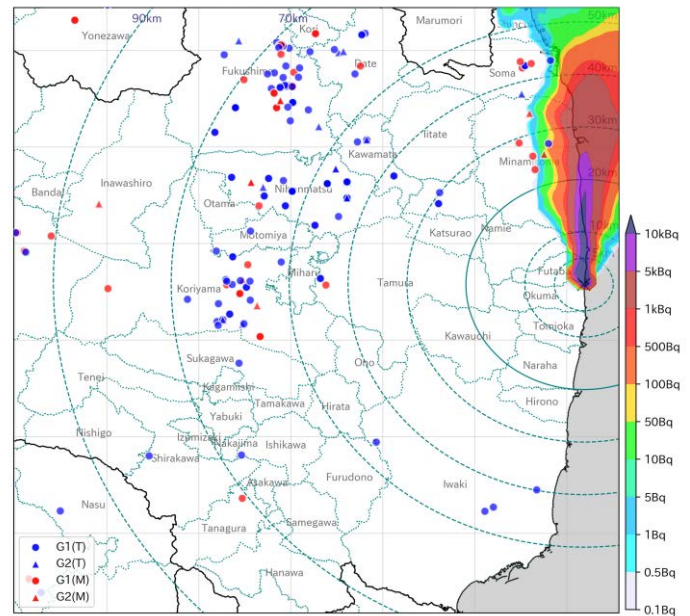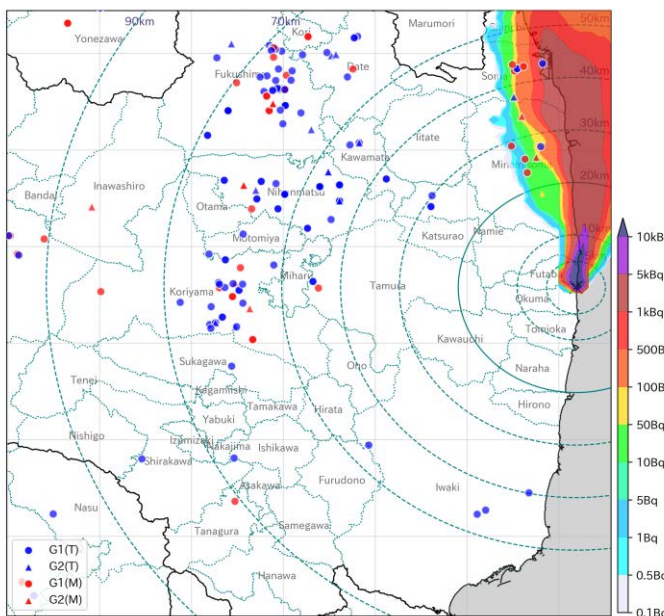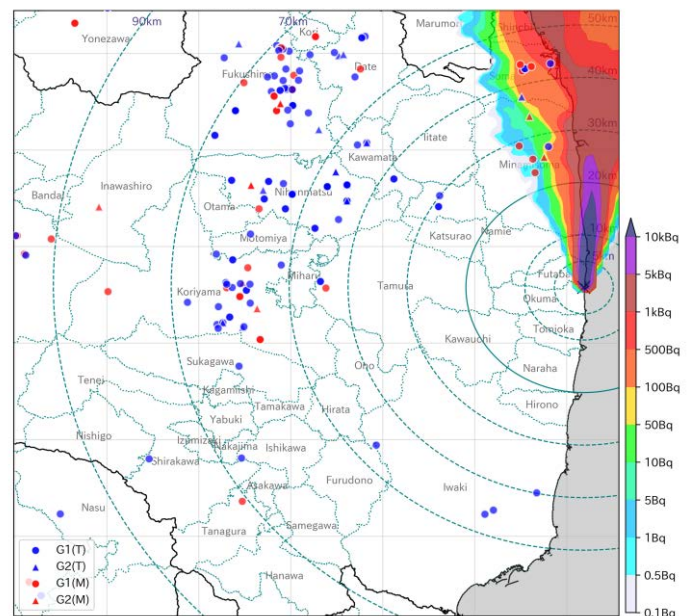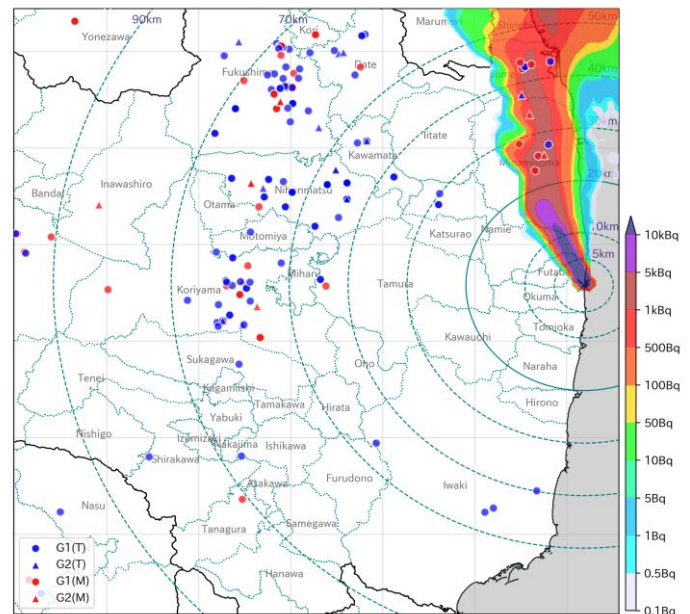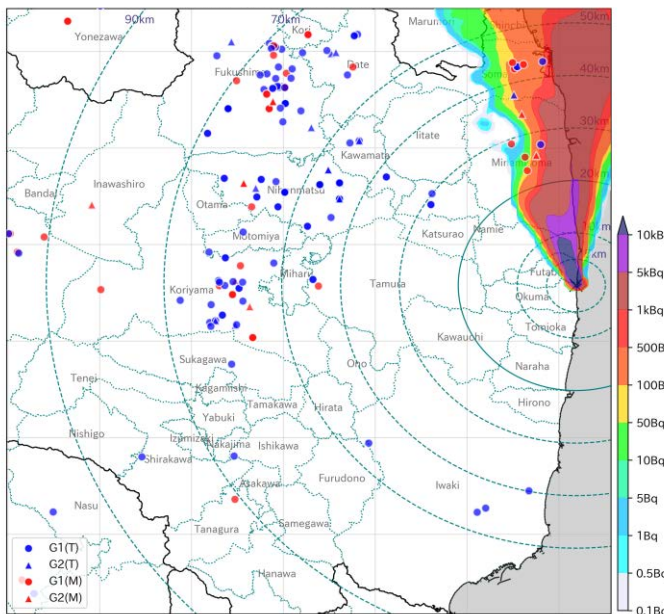
Fig. A21. The locations of individuals on the maps with the ^{137}Cs air concentration at the ground level at 12:00 a.m. on 19 March (1/6), 1:00 a.m. on 19 March (2/6), 2:00 a.m. on 19 March (3/6), 3:00 a.m. on 19 March (4/6), 4:00 a.m. on 19 March (5/6), and 5:00 a.m. on 19 March (6/6).
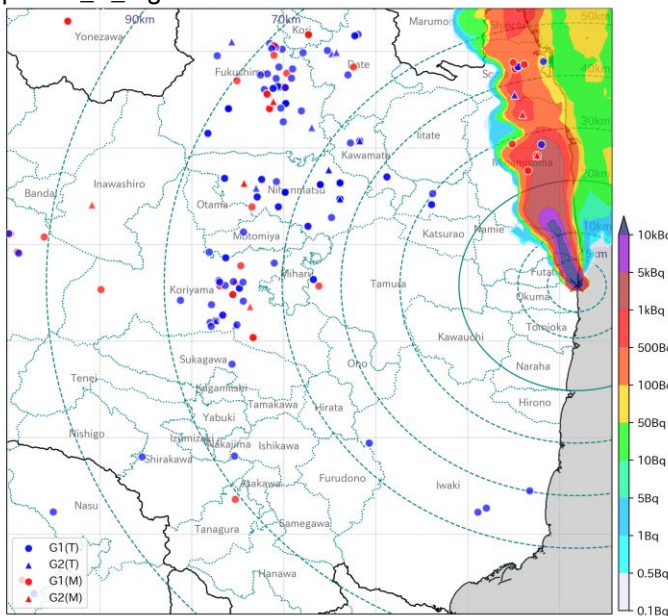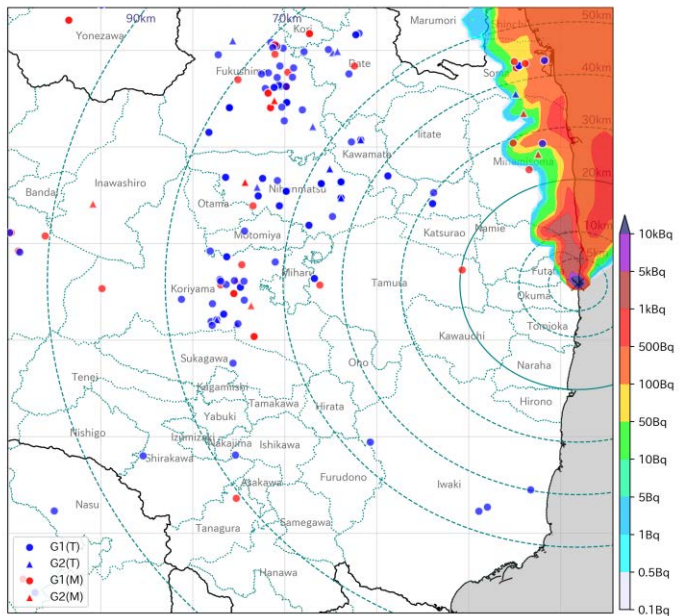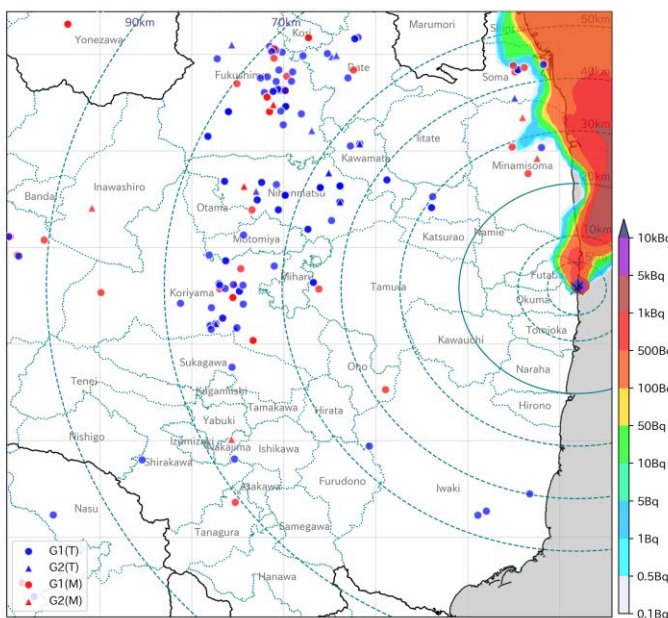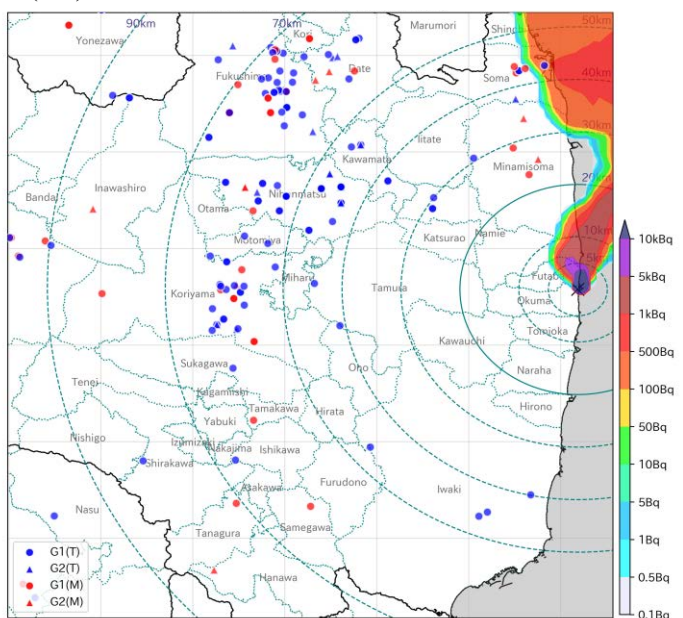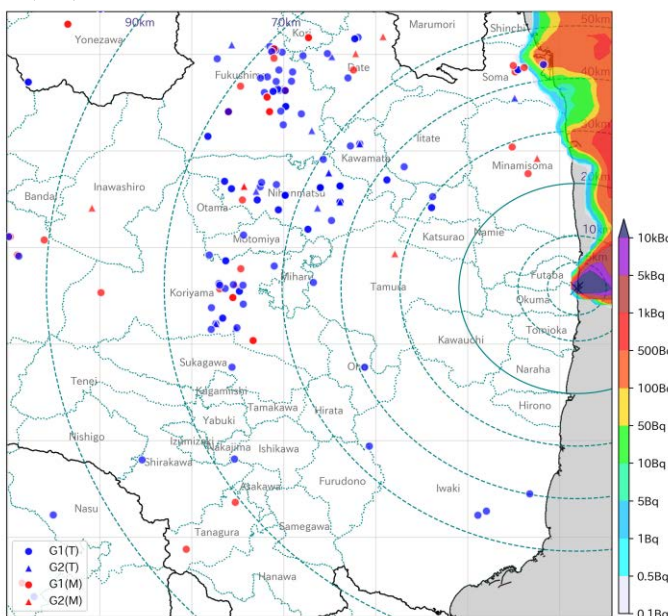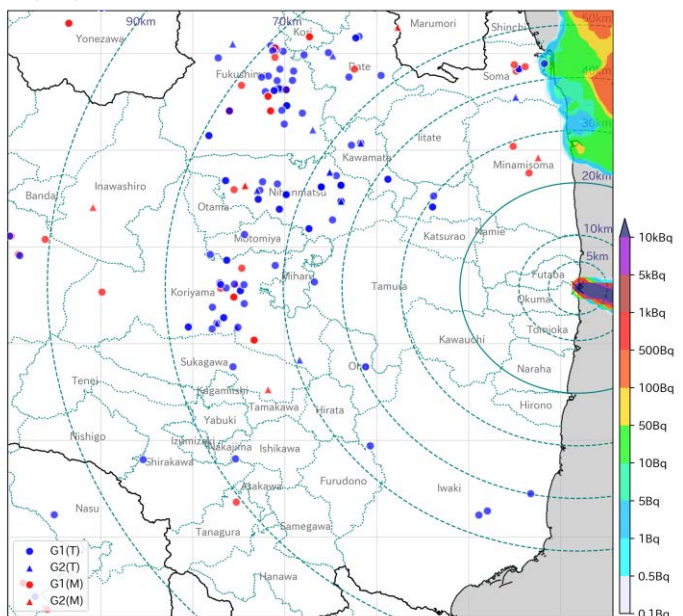
Fig. A22. The locations of individuals on the maps with the ^{137}Cs air concentration at the ground level at 6:00 a.m. on 19 March (1/6), 7:00 a.m. on 19 March (2/6), 8:00 a.m. on 19 March (3/6), 9:00 a.m. on 19 March (4/6), 10:00 a.m. on 19 March (5/6), and 11:00 a.m. on 19 March (6/6).
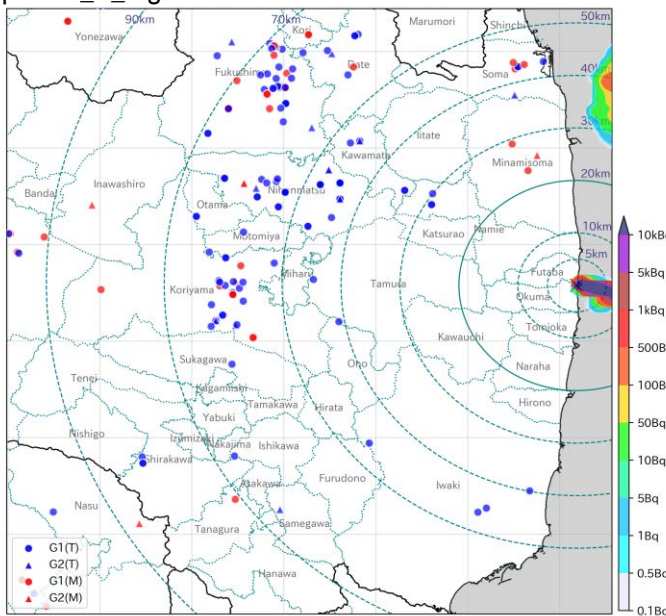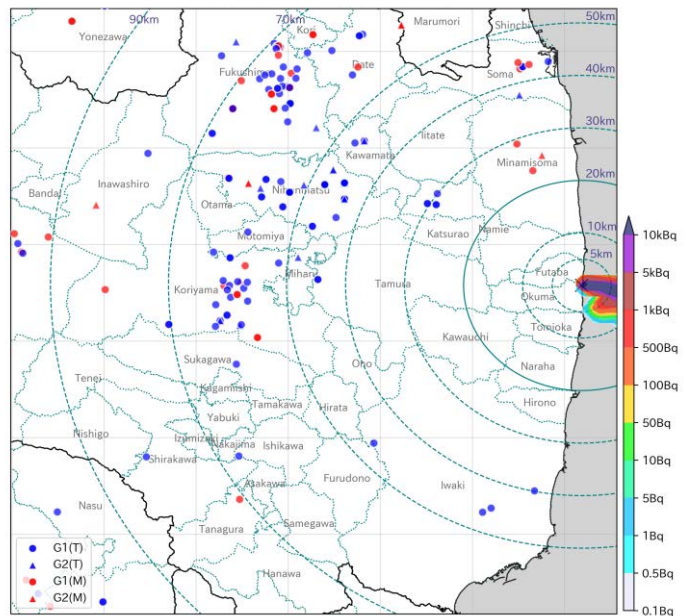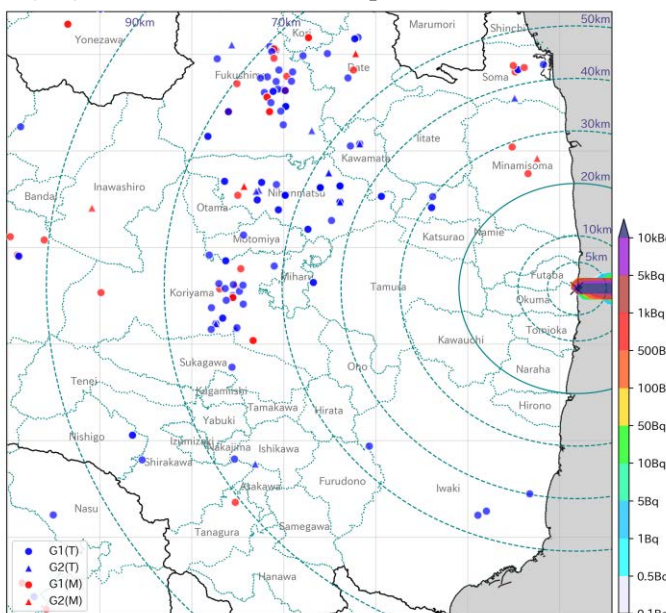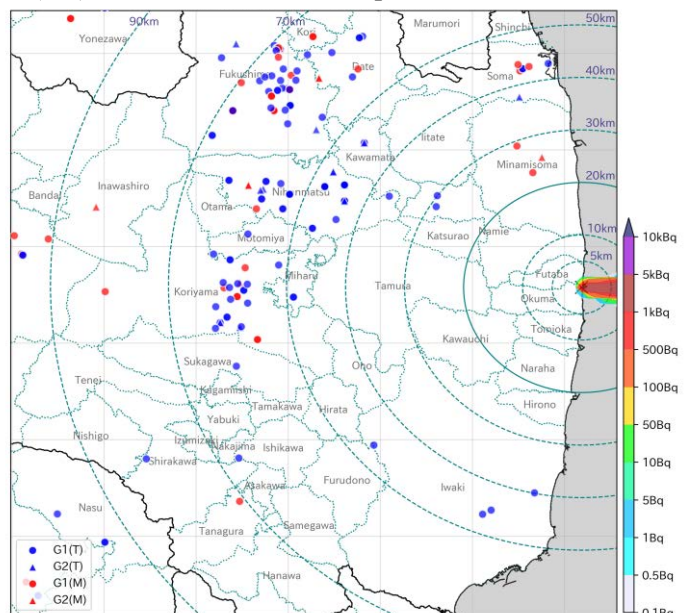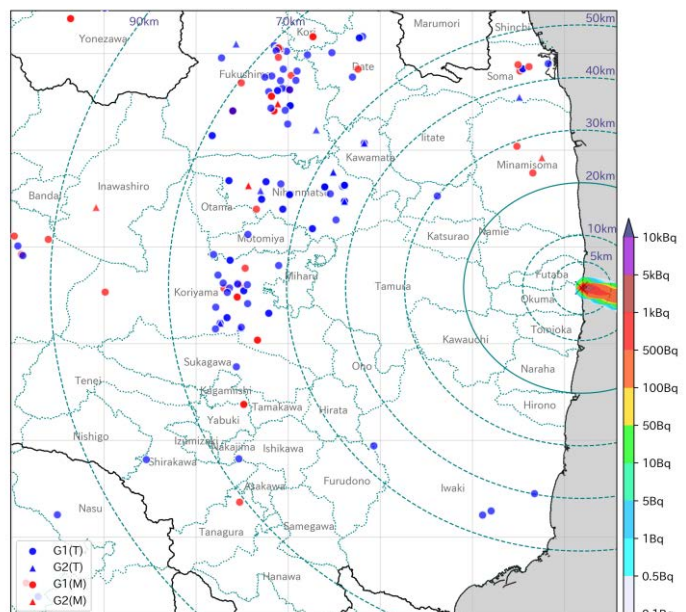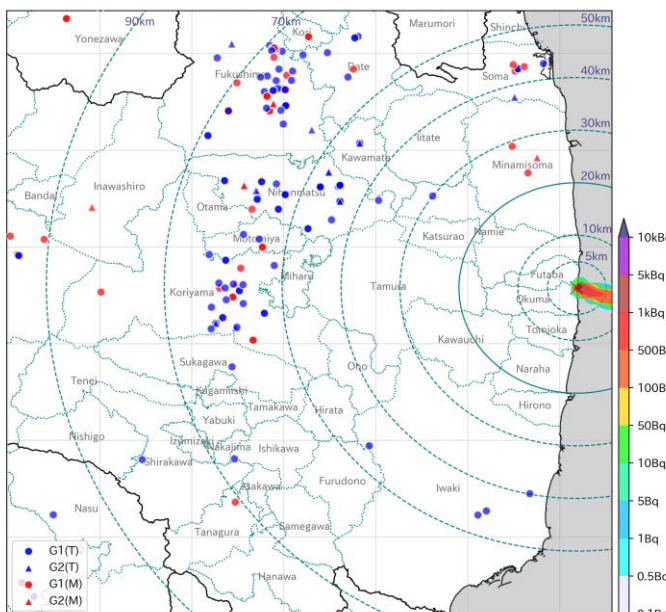
Fig. A23. The locations of individuals on the maps with the ^{137}Cs air concentration at the ground level at 12:00 p.m. on 19 March (1/6), 1:00 p.m. on 19 March (2/6), 2:00 p.m. on 19 March (3/6), 3:00 p.m. on 19 March (4/6), 4:00 p.m. on 19 March (5/6), and 5:00 p.m. on 19 March (6/6).
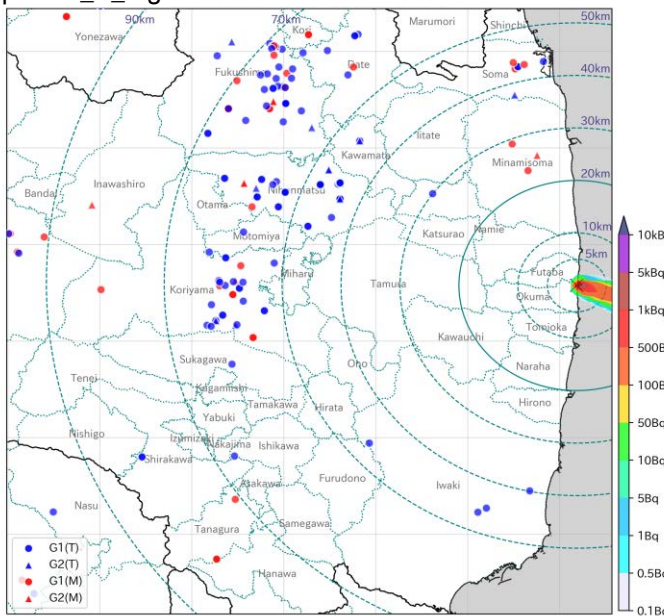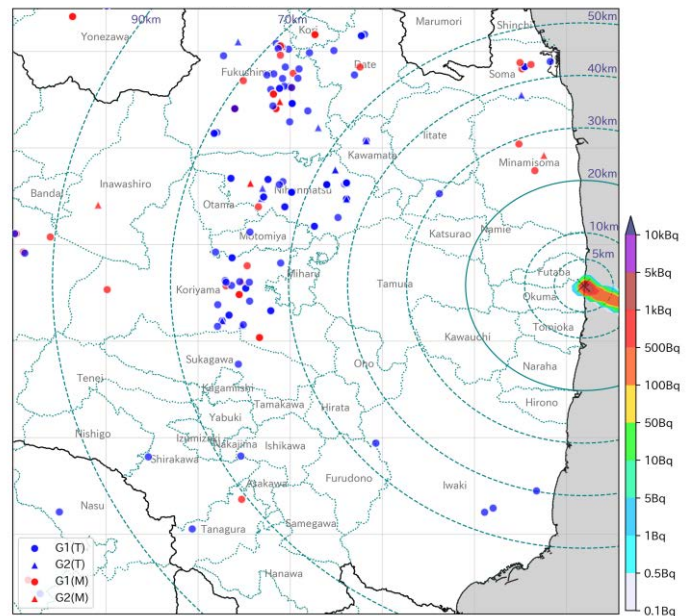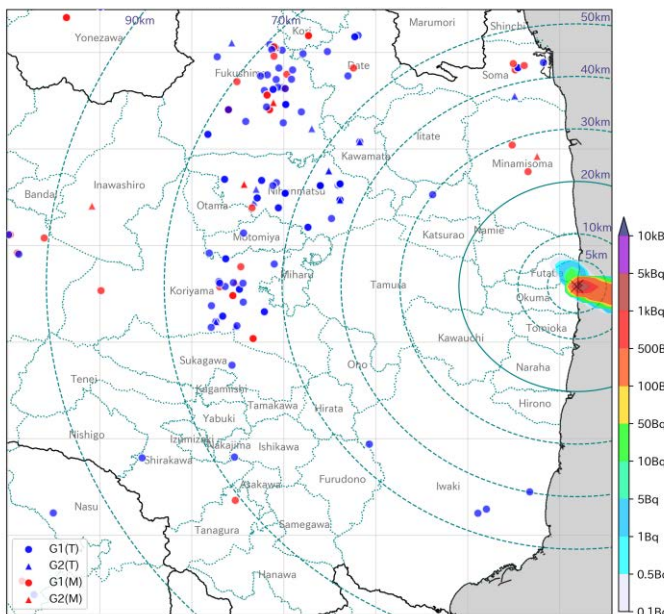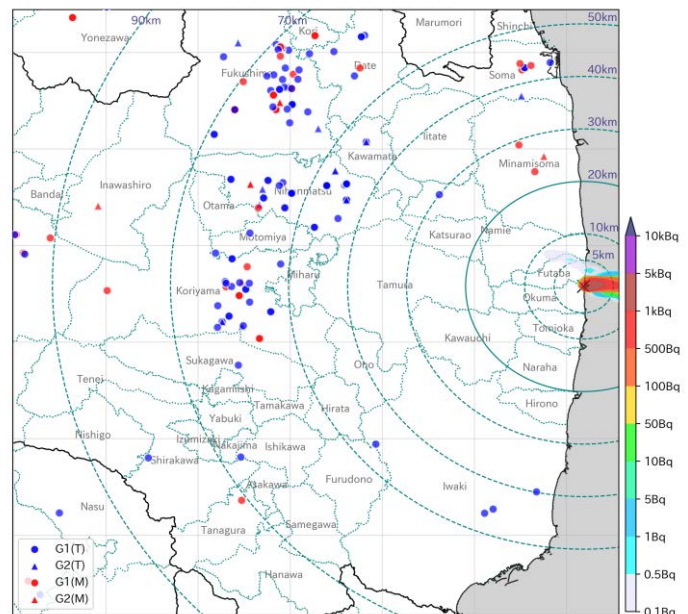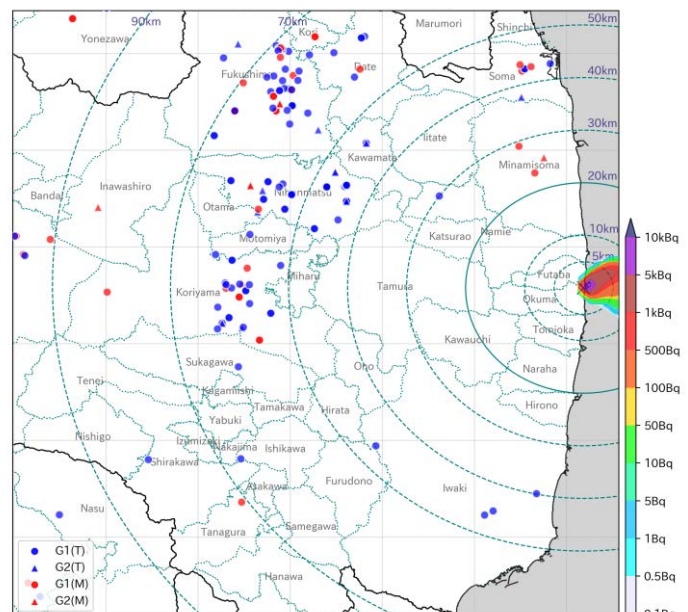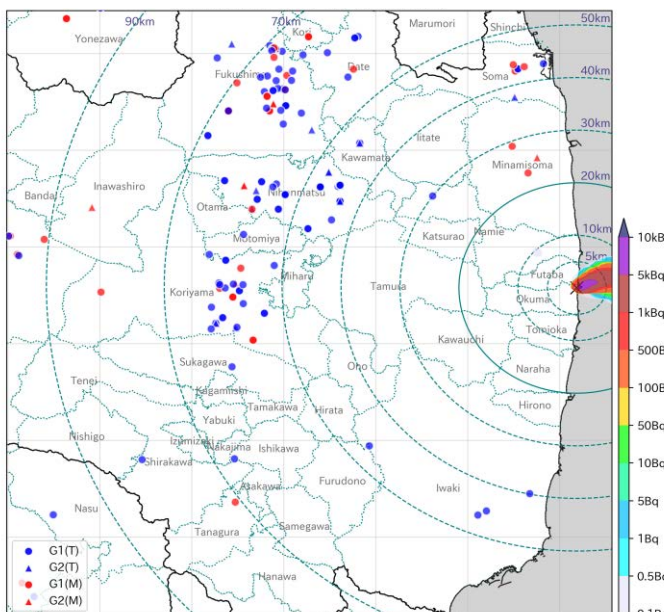
Fig. A24. The locations of individuals on the maps with the ^{137}Cs air concentration at the ground level at 6:00 p.m. on 19 March (1/6), 7:00 p.m. on 19 March (2/6), 8:00 p.m. on 19 March (3/6), 9:00 p.m. on 19 March (4/6), 10:00 p.m. on 19 March (5/6), and 11:00 p.m. on 19 March (6/6).
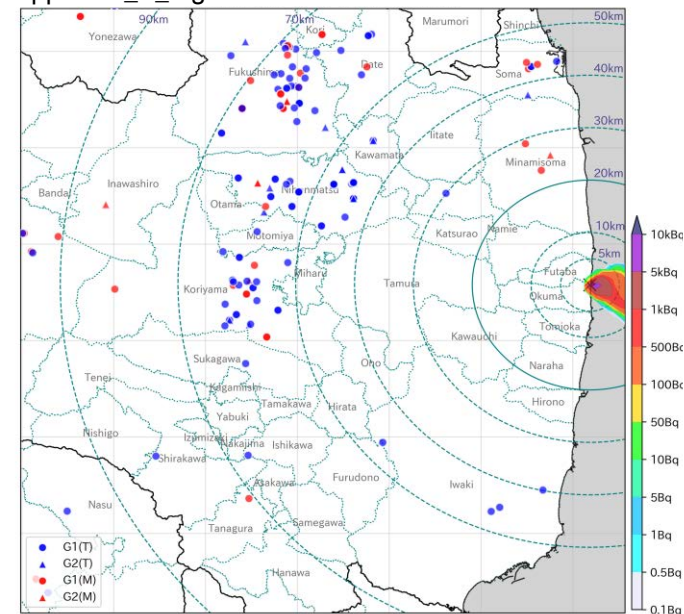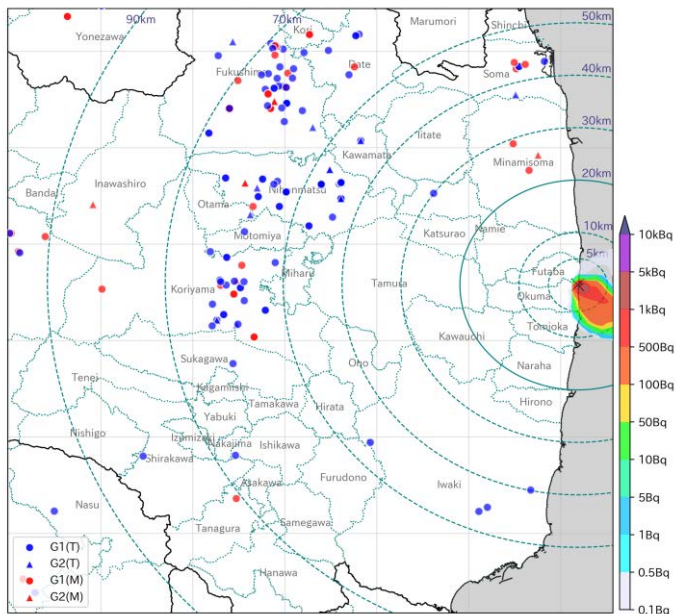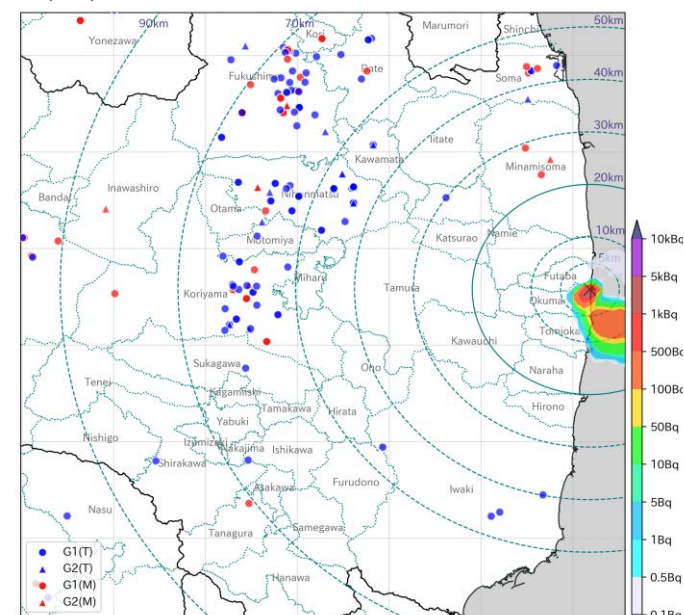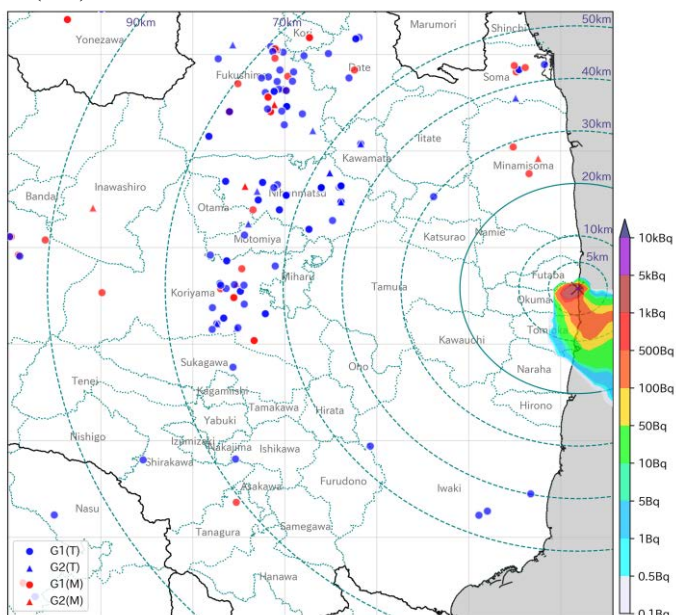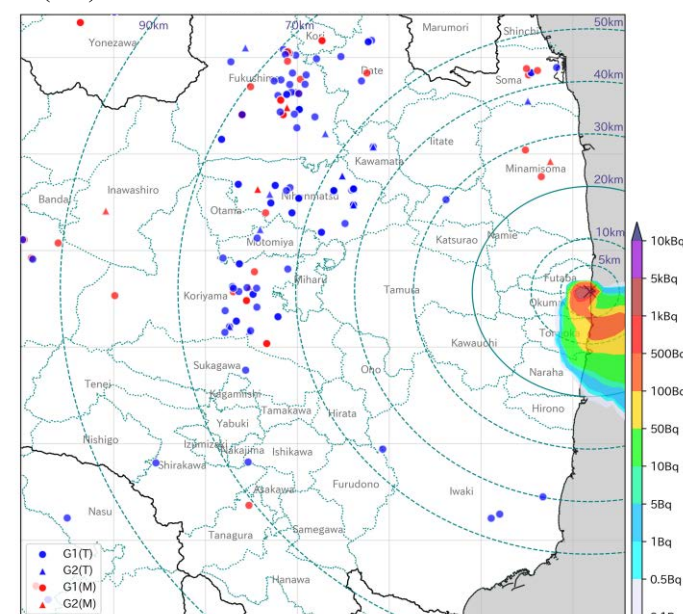
Fig. A25. The locations of individuals on the maps with the ^{137}Cs air concentration at the ground level at 12:00 a.m. on 20 March (1/6), 1:00 a.m. on 20 March (2/6), 2:00 a.m. on 20 March (3/6), 3:00 a.m. on 20 March (4/6), 4:00 a.m. on 20 March (5/6), and 5:00 a.m. on 20 March (6/6).
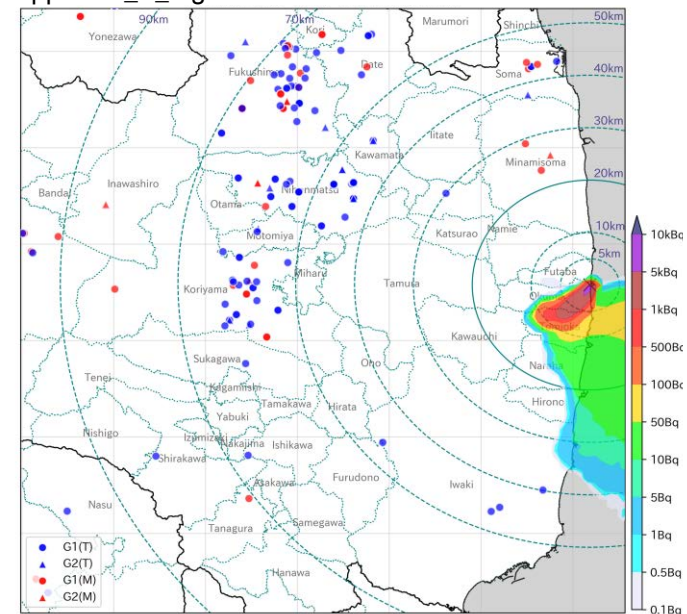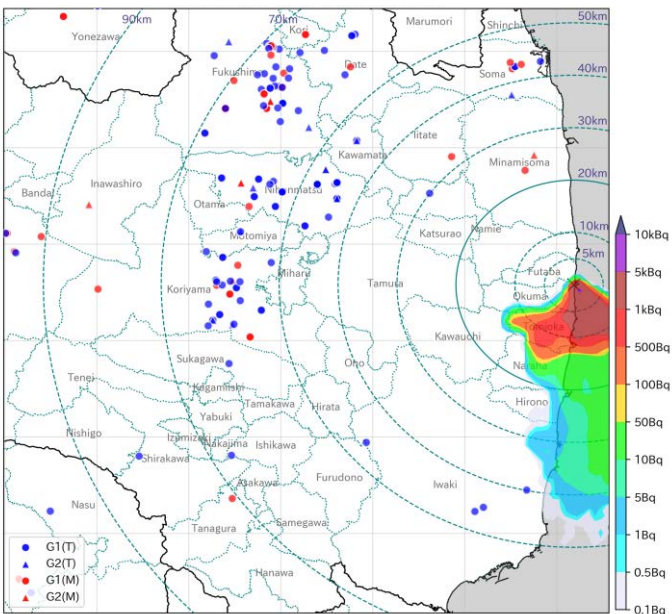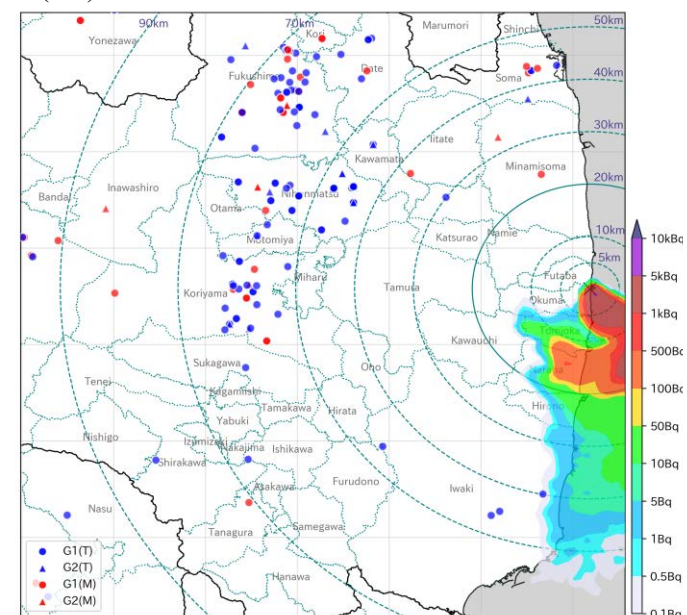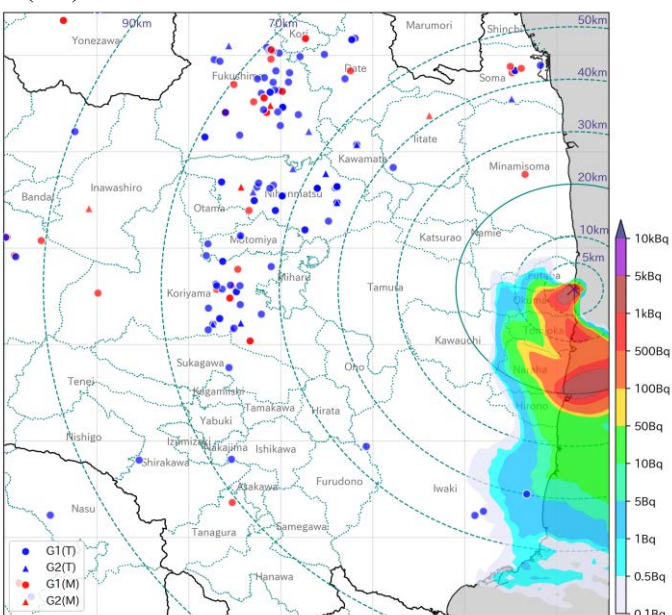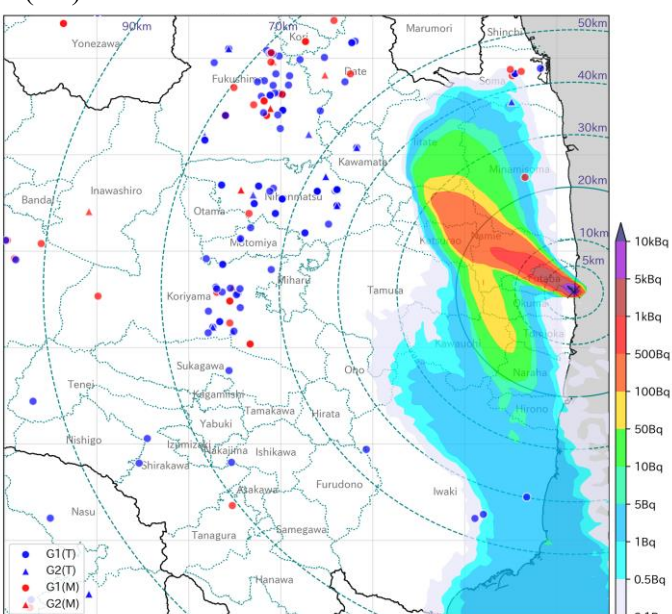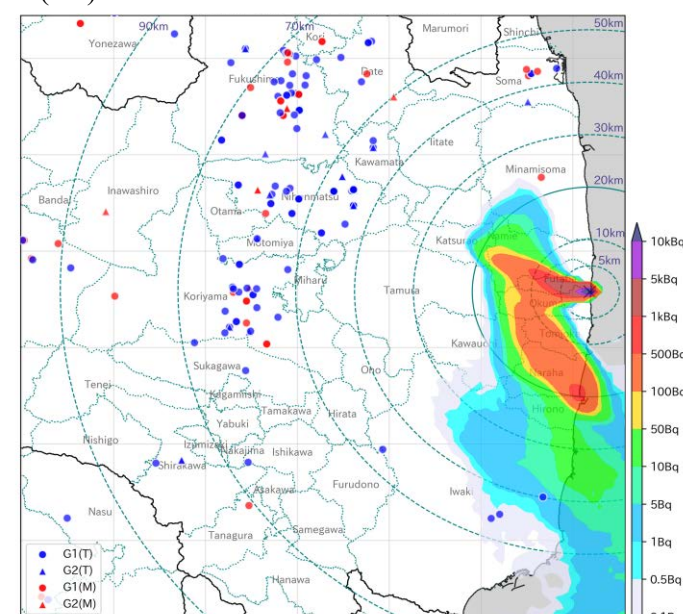
Fig. A26. The locations of individuals on the maps with the ^{137}Cs air concentration at the ground level at 6:00 a.m. on 20 March (1/6), 7:00 a.m. on 20 March (2/6), 8:00 a.m. on 20 March (3/6), 9:00 a.m. on 20 March (4/6), 10:00 a.m. on 20 March (5/6), and 11:00 a.m. on 20 March (6/6).
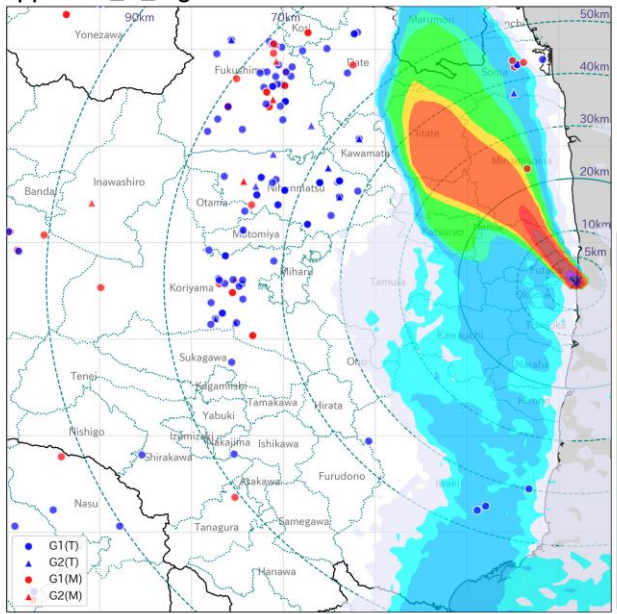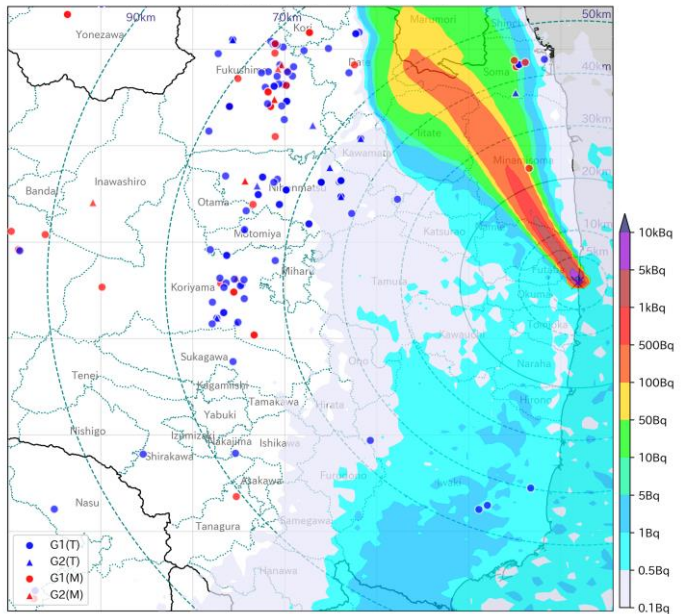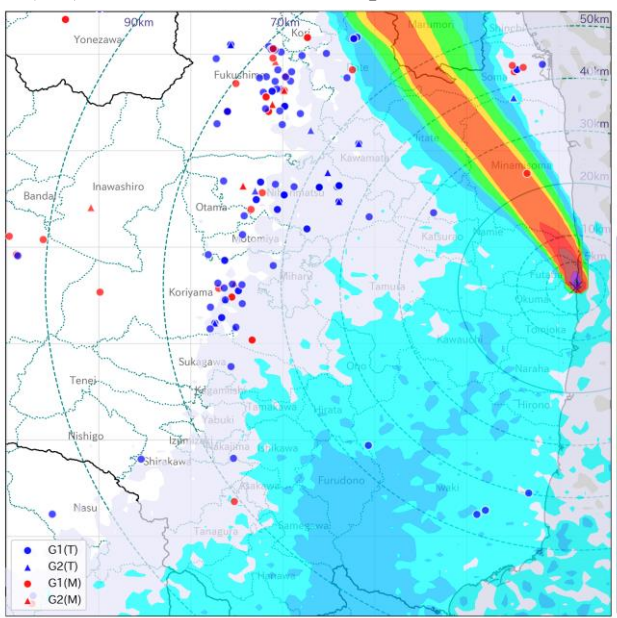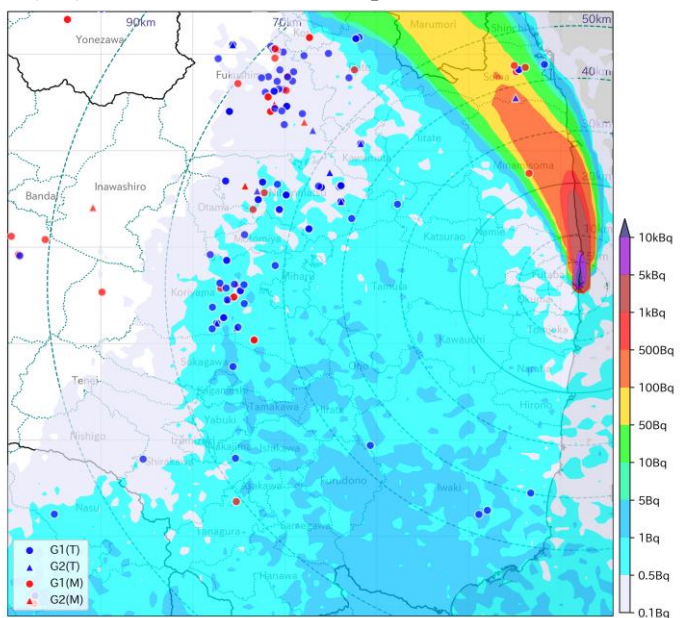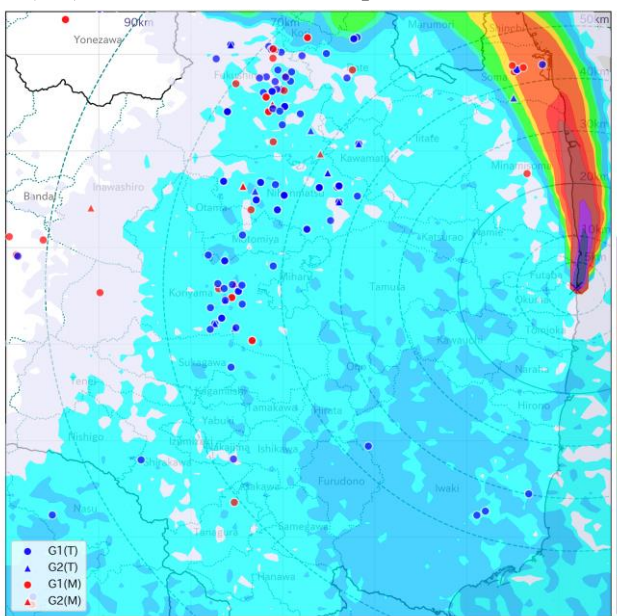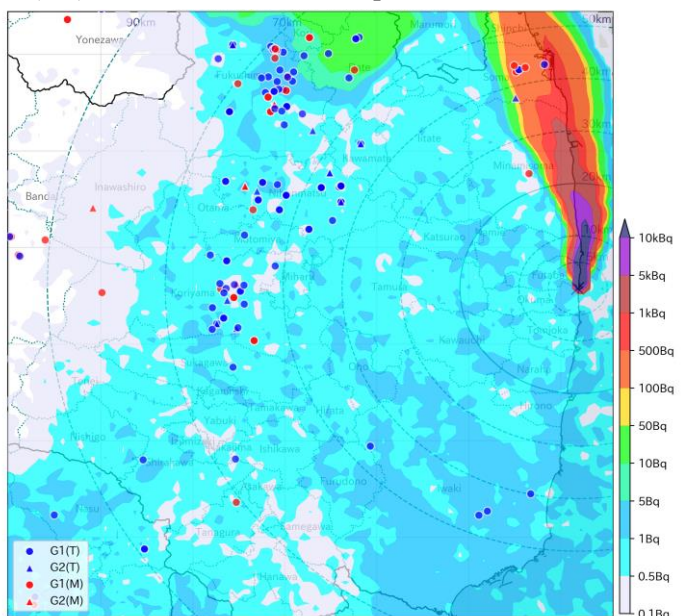
Fig. A27. The locations of individuals on the maps with the ^{137}Cs air concentration at the ground level at 12:00 p.m. on 20 March (1/6), 1:00 p.m. on 20 March (2/6), 2:00 p.m. on 20 March (3/6), 3:00 p.m. on 20 March (4/6), 4:00 p.m. on 20 March (5/6), and 5:00 p.m. on 20 March (6/6).
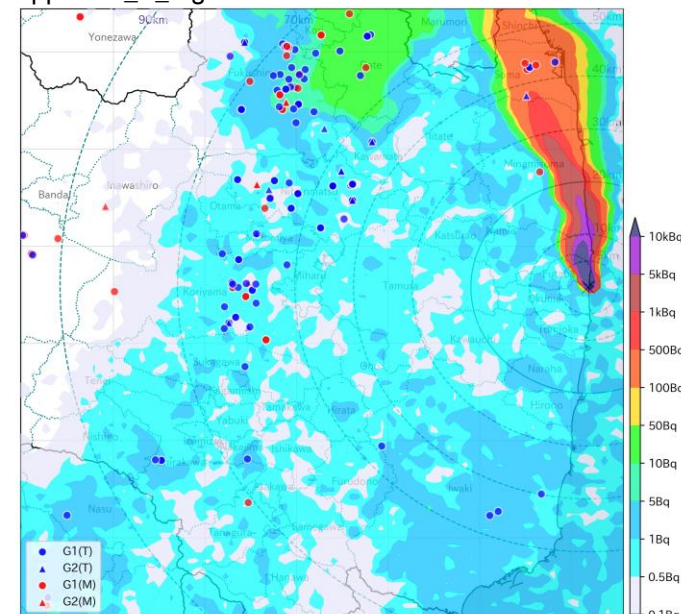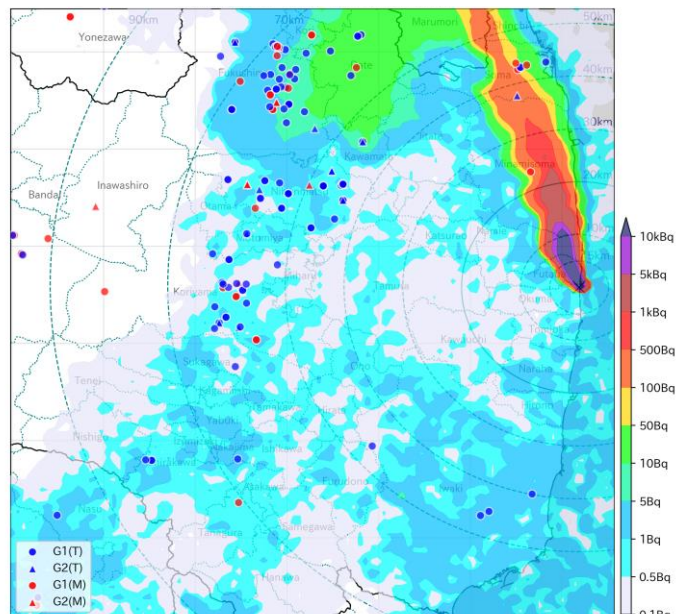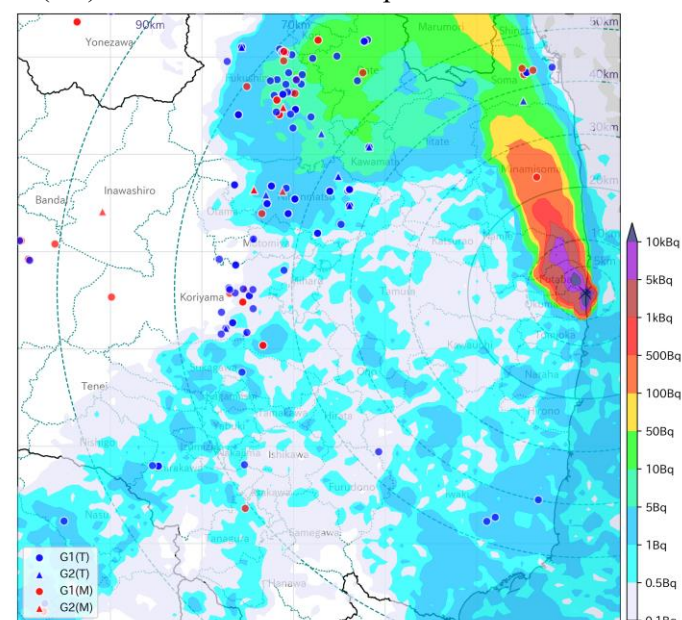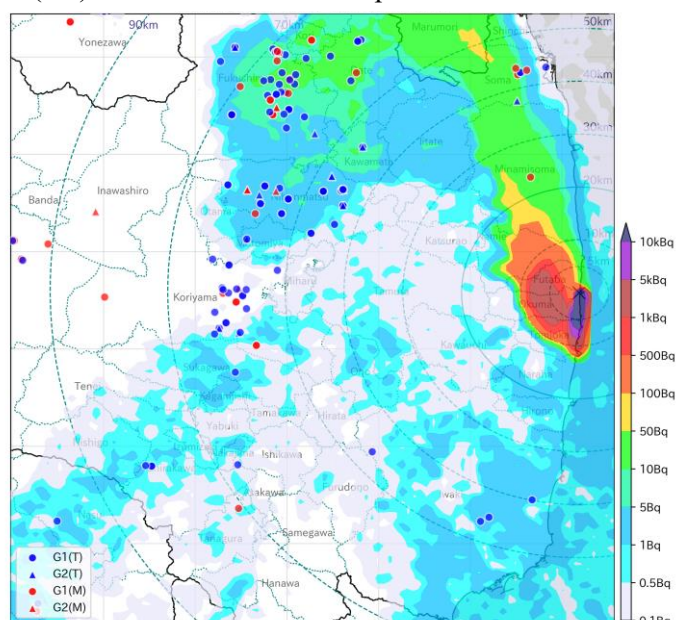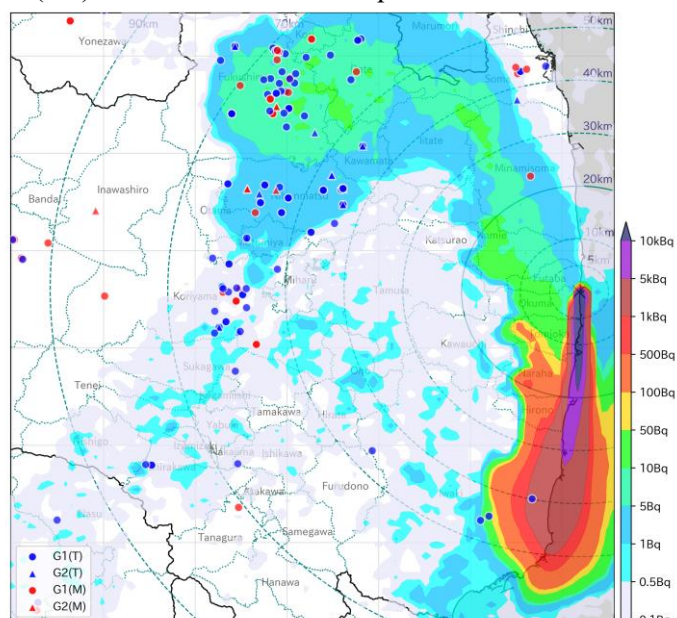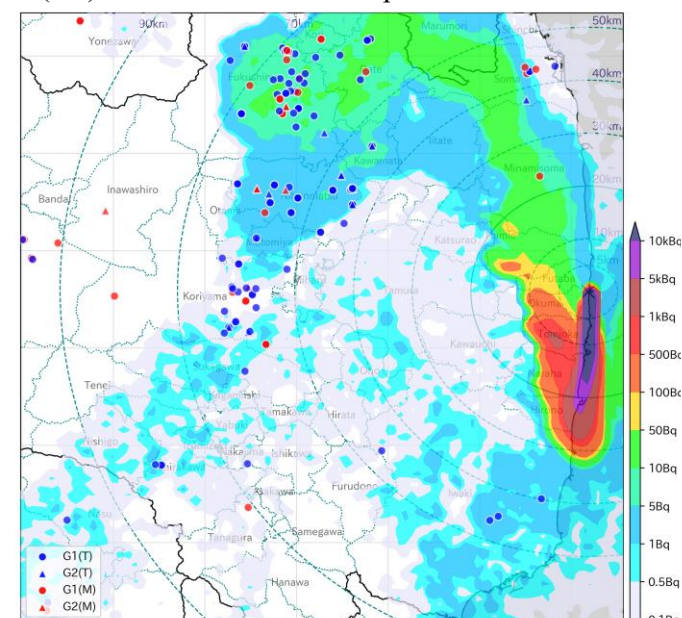
Fig. A28. The locations of individuals on the maps with the ^{137}Cs air concentration at the ground level at 6:00 p.m. on 20 March (1/6), 7:00 p.m. on 20 March (2/6), 8:00 p.m. on 20 March (3/6), 9:00 p.m. on 20 March (4/6), 10:00 p.m. on 20 March (5/6), and 11:00 p.m. on 20 March (6/6).
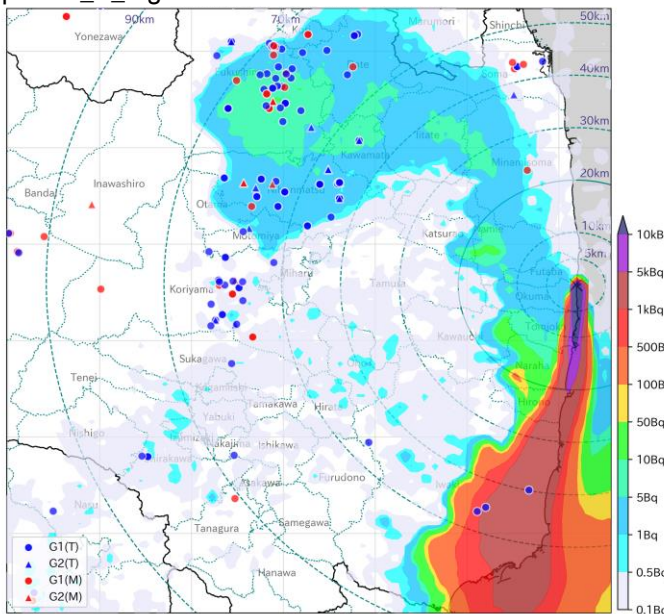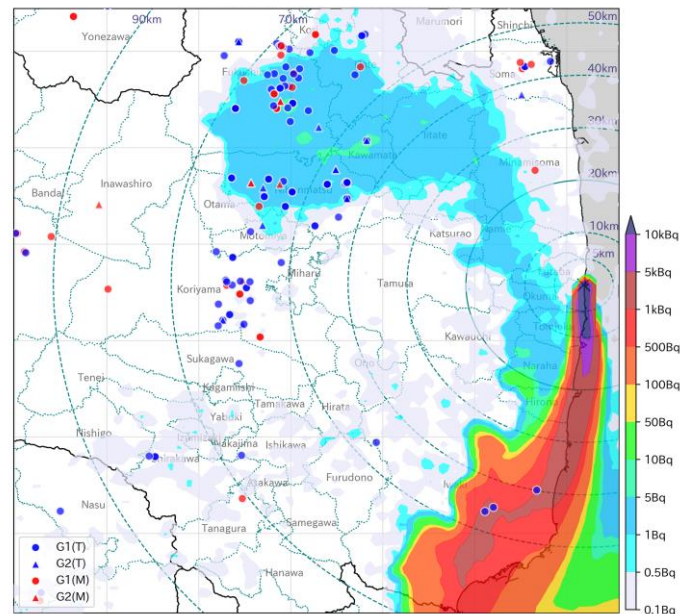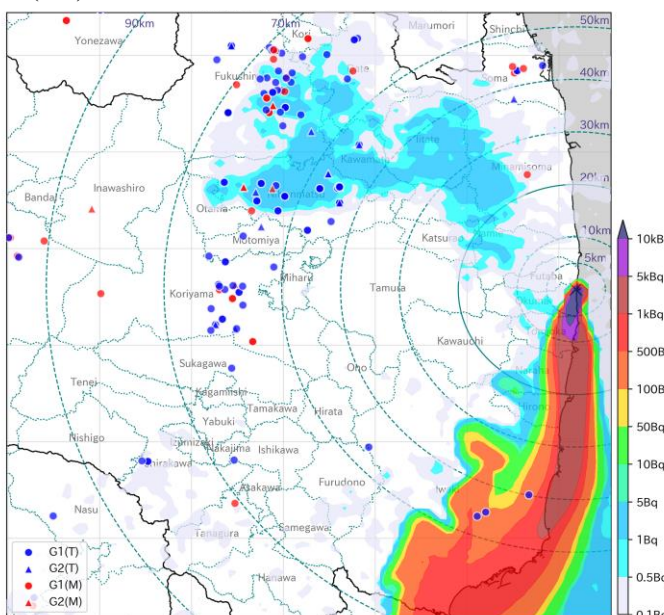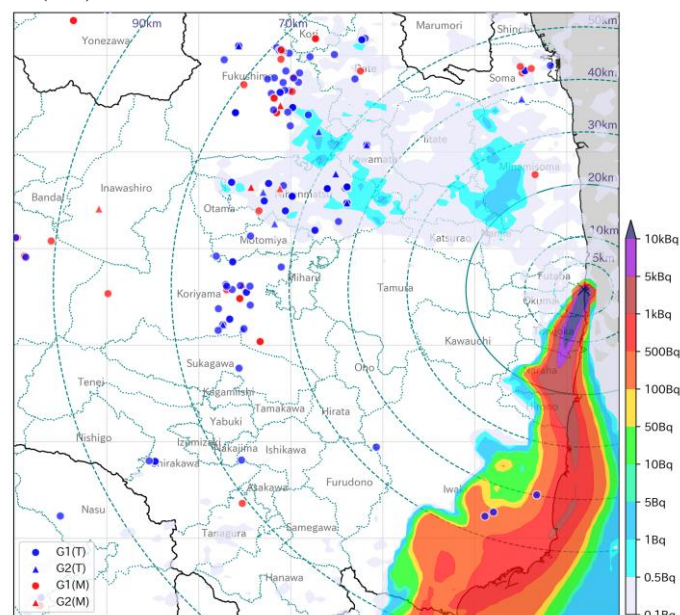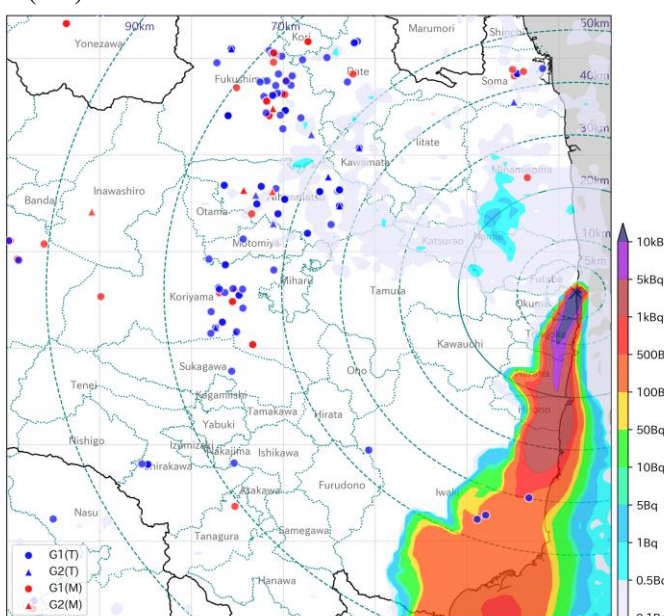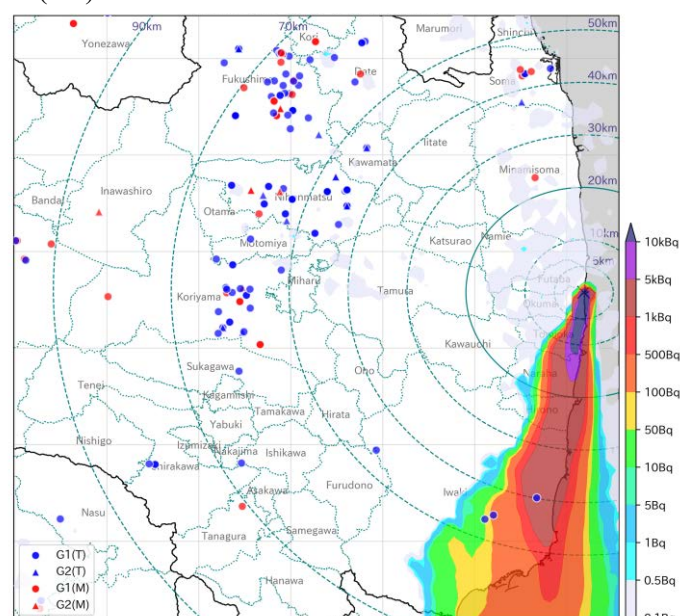
Fig. A29. The locations of individuals on the maps with the ^{137}Cs air concentration at the ground level at 12:00 a.m. on 21 March (1/6), 1:00 a.m. on 21 March (2/6), 2:00 a.m. on 21 March (3/6), 3:00 a.m. on 21 March (4/6), 4:00 a.m. on 21 March (5/6), and 5:00 a.m. on 21 March (6/6).
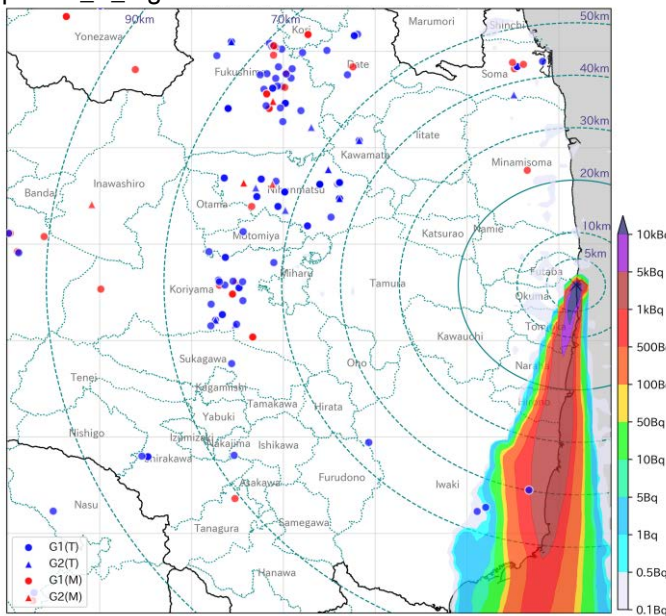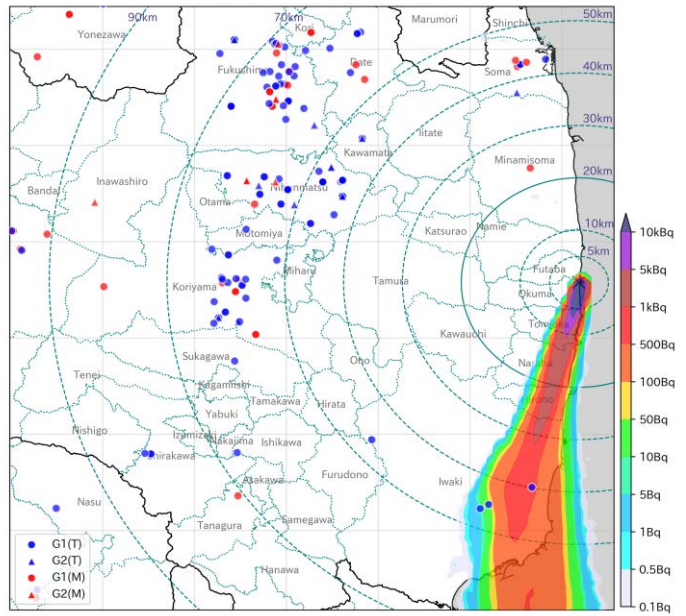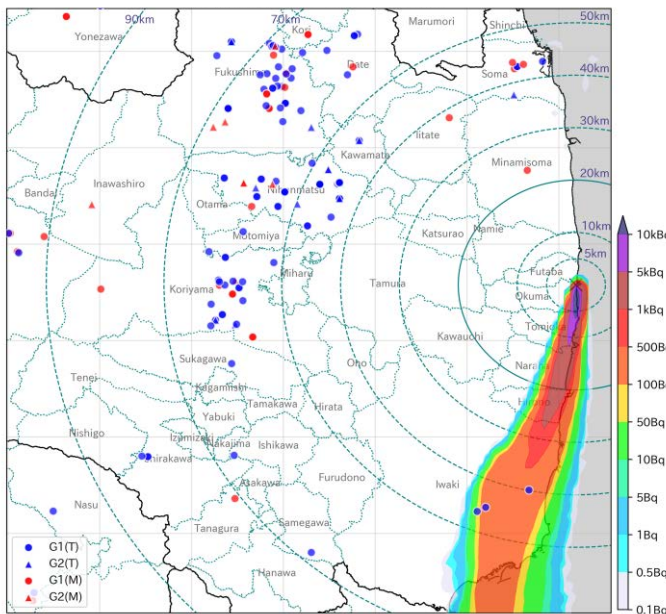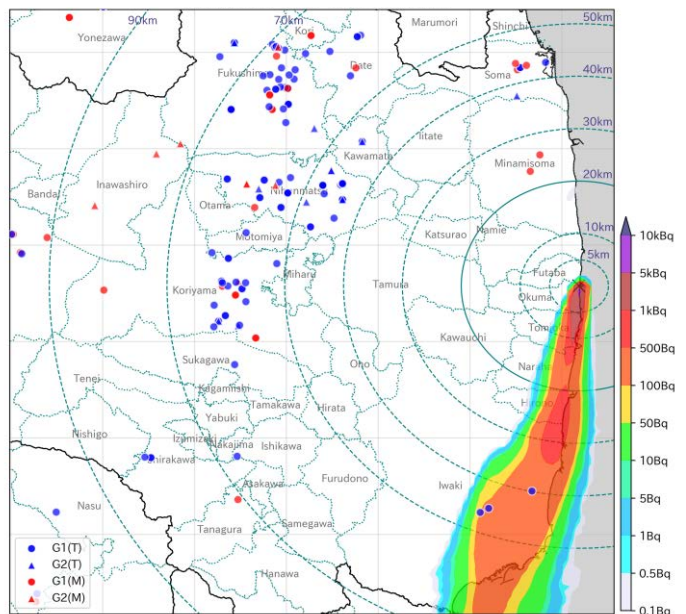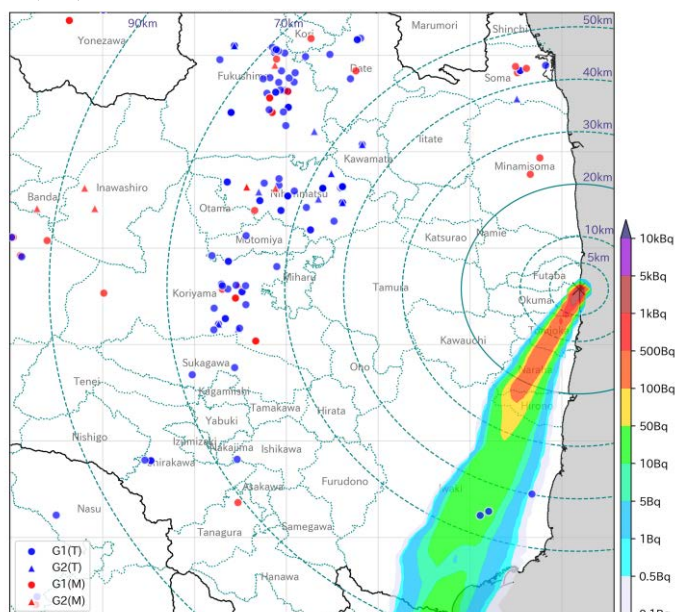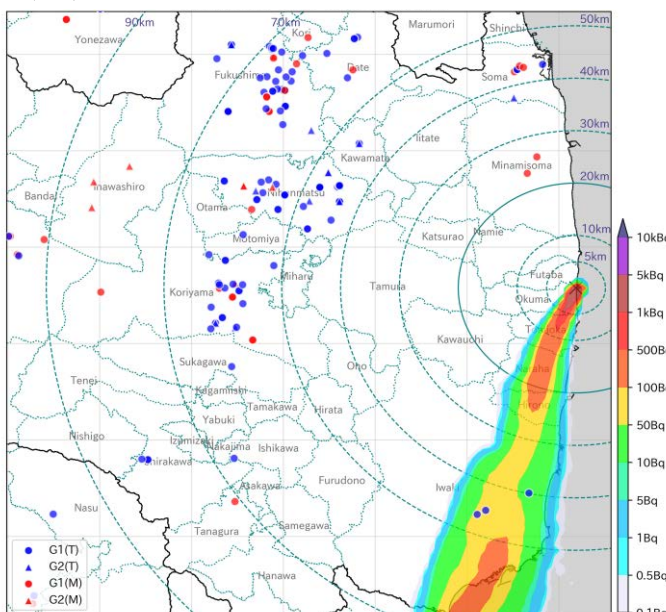
Fig. A30. The locations of individuals on the maps with the ^{137}Cs air concentration at the ground level at 6:00 a.m. on 21 March (1/6), 7:00 a.m. on 21 March (2/6), 8:00 a.m. on 21 March (3/6), 9:00 a.m. on 21 March (4/6), 10:00 a.m. on 21 March (5/6), and 11:00 a.m. on 21 March (6/6).
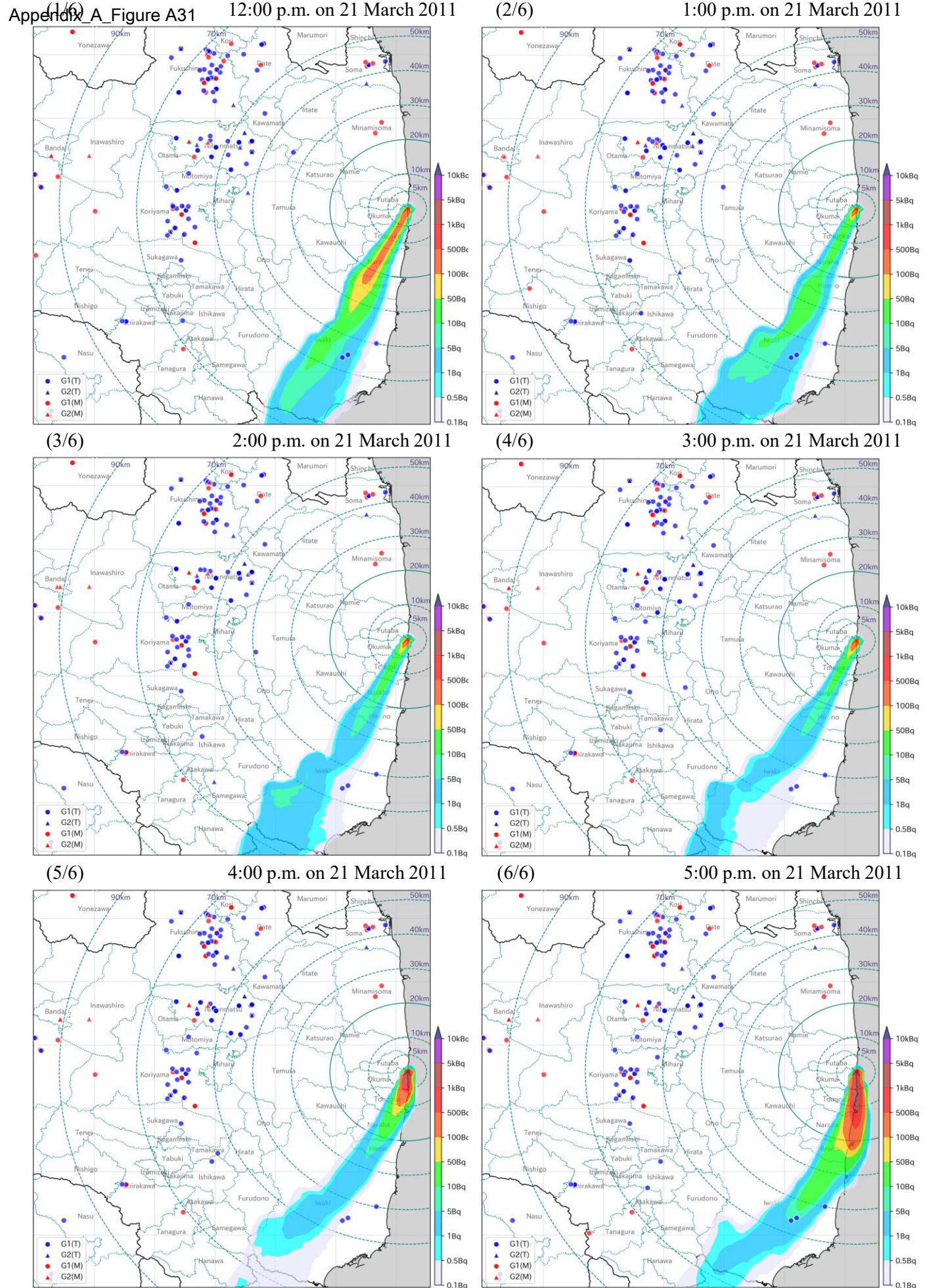
Fig. A31. The locations of individuals on the maps with the ^{137}Cs air concentration at the ground level at 12:00 p.m. on 21 March (1/6), 1:00 p.m. on 21 March (2/6), 2:00 p.m. on 21 March (3/6), 3:00 p.m. on 21 March (4/6), 4:00 p.m. on 21 March (5/6), and 5:00 p.m. on 21 March (6/6).
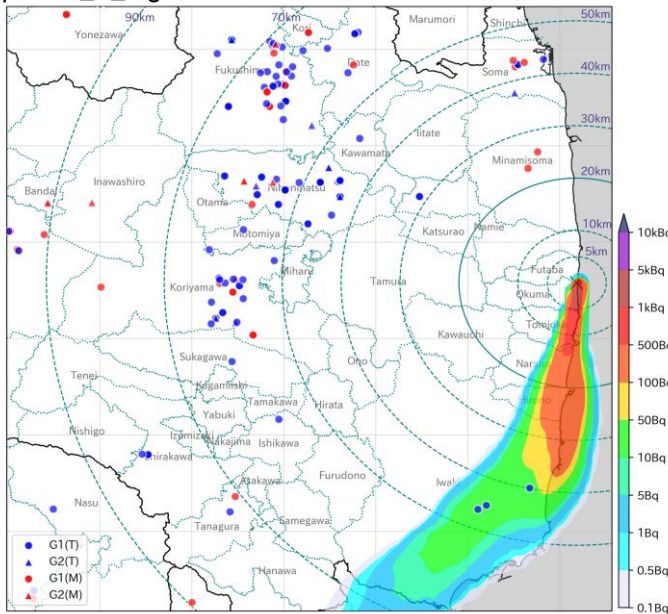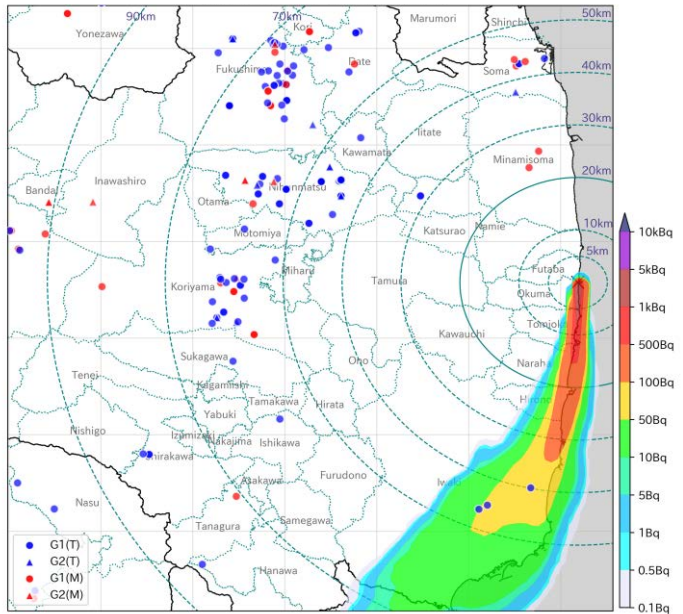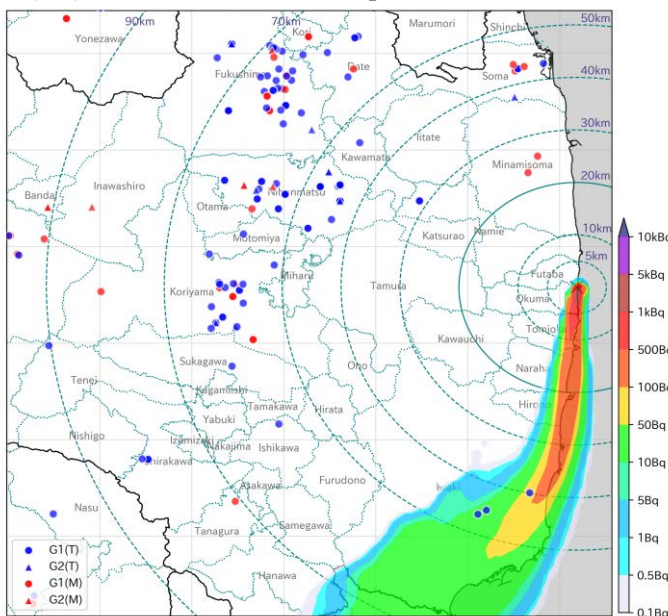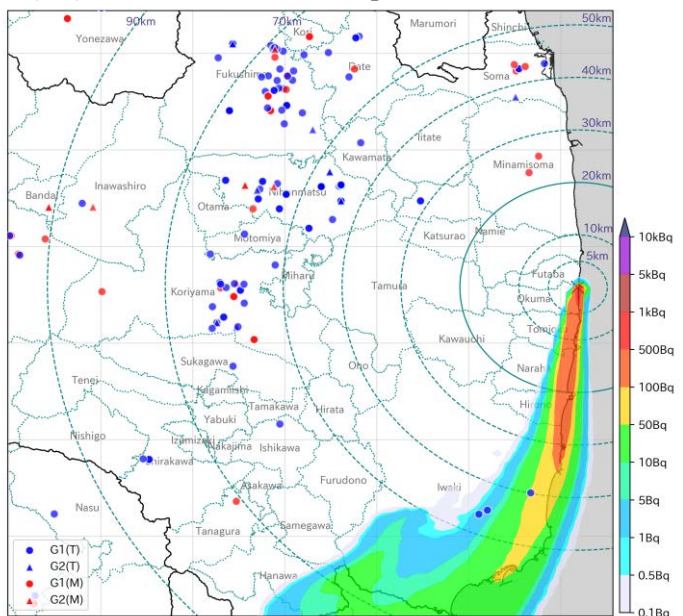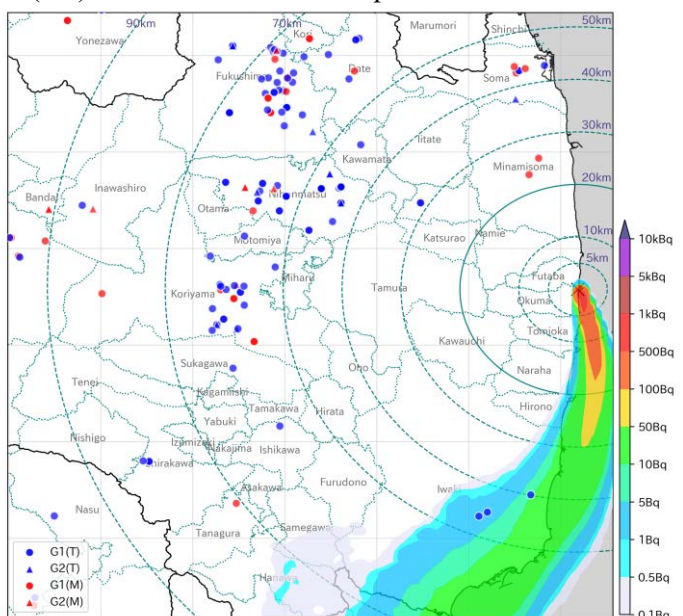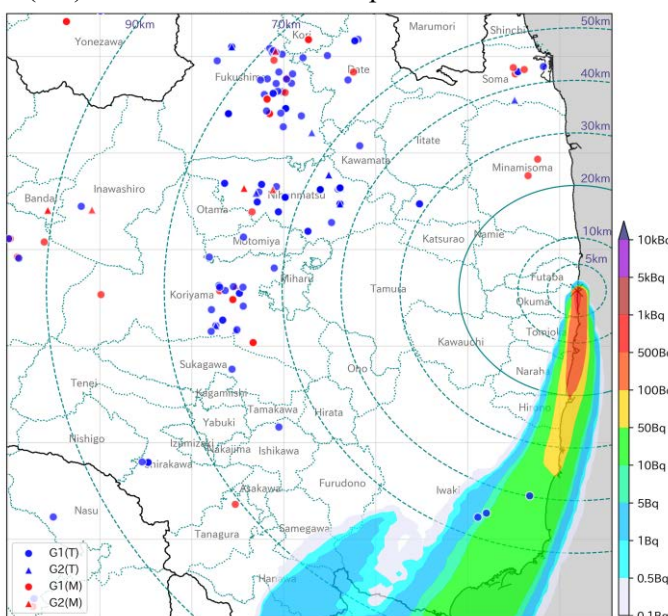
Fig. A32. The locations of individuals on the maps with the ^{137}Cs air concentration at the ground level at 6:00 p.m. on 21 March (1/6), 7:00 p.m. on 21 March (2/6), 8:00 p.m. on 21 March (3/6), 9:00 p.m. on 21 March (4/6), 10:00 p.m. on 21 March (5/6), and 11:00 p.m. on 21 March (6/6).
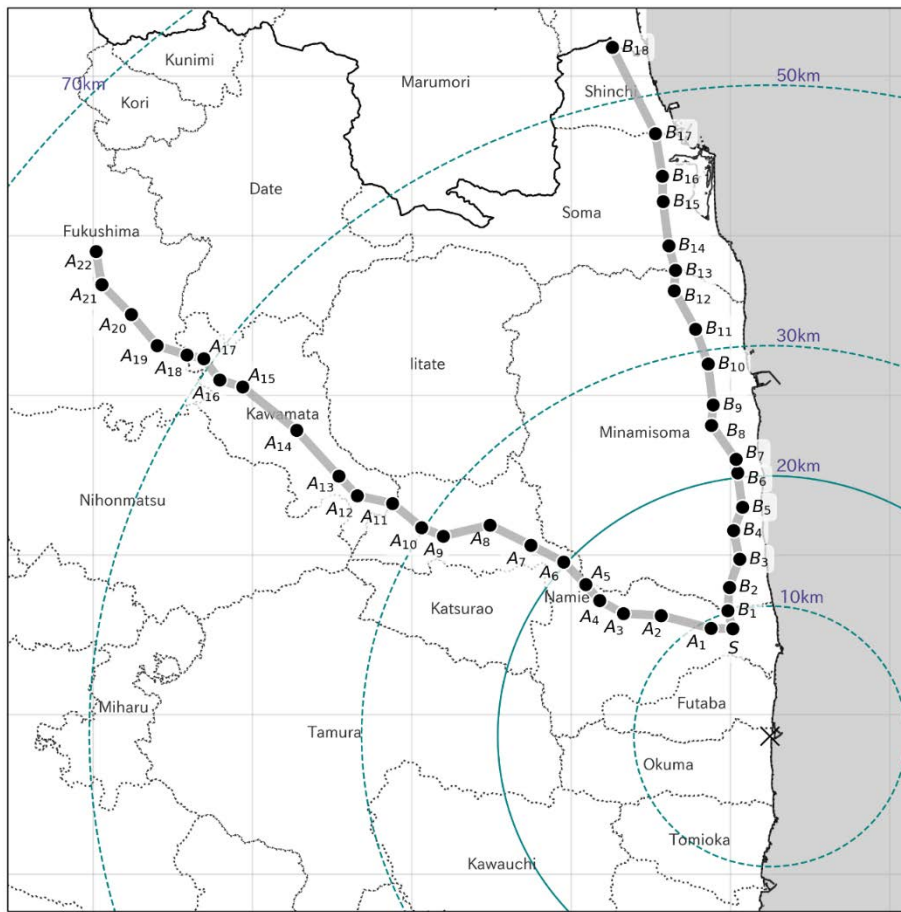
Fig. B1 The locations of the points listed in Tables B2 and B3.